Experimental Investigation of Anisotropic Etching of Silicon in Tetra-Methyl Ammonium Hydroxide

Sasan Naseh

A Thesis

in

the Department

of

Electrical and Computer Engineering

Presented in Partial Fulfillment of the Requirements
for the Degree of Master of Applied Science at
Concordia University
Montreal, Quebec, Canada

August 1995

Abstract

Experimental Investigation of Anisotropic Etching of Silicon in Tetra-Methyl Ammonium Hydroxide

Anisotropic etching of silicon is of such fundamental importance in silicon micromachining that it has been studied and continues to be studied by many researchers. Yet, even with all the attention that it has received, there remain many difficulties, such as toxicity of the most commonly-used etchants. This work is an extensive experimental investigation of anisotropic etching of silicon in the relatively non-toxic tetra-methyl-ammonium hydroxide (TMAH). Using a temperature-controlled etch apparatus, basic etch rate experiments on both Si{100} and Si{110} confirm and extend previous literature results. Extensive underetch experiments shows that the TMAH is qualitatively similar to other more common etchants such as KOH and EDP, but has several quantitative differences. The underetched planes are found to be a sensitive function of etchant composition. Under certain etchant conditions, {110} planes are found to be planes that etch slower than expected. The evolution of hillocks on {100} etched surface is characterized, as a function of etchant parameters. Hillocks are found to occur only at TMAH concentrations less than 20 wt.%. Re-etch experiments show that hillock-producing conditions at the etched surface are disturbed if the etch is interrupted. The effect of externally applied stress on the etch rate is investigated and found to be not significant. However very subtle stress-induced features are observed. The use of TMAH in CMOS-compatible micromachining is explored in certain device geometries.

ACKNOWLEDGEMENTS

I would like to express my sincere gratitude to my thesis supervisor, Dr. Leslie M. Landsberger, for his continued help, guidance and encouragement during the course of this work. The hours of discussion and consultation with him had been the best times during my studies in Concordia university. I am very grateful to Dr. Mojtaba Kahrizi for his advice and guidance during the whole period of my M. A. Sc. studies.

I would like to thank Dr. M. Paranjape for his help during the initial stages of this work.

My sincere thanks goes to my relatives in Canada, and my friend, who helped me to have a good start in my studies at Concordia university.

I express my thanks to my family, who always encouraged me to go for better education.

This work was made possible by the support of the Government of Iran. I am extremely indebted to the Government of Iran for sponsoring me for the Masters program.

Dedicated to my parents

Table of Contents

CHAPTER 5

CHAPTER 6

CHAPTER 7

List of Figures

List of Tables

CHAPTER 1

Introduction

1.1 General

During the last 25 years an increasing amount of research has been done on the fabrication of the sensors on crystalline silicon. There are already many companies around the world which have been producing devices based on silicon microelectromechanical structures for more than 20 years [1]. Also, in research labs all over the world (mostly Japan, United States and Europe), increasing efforts have gone to the area of silicon-based Micro-Electro Mechanical Systems (MEMS). The large number of papers submitted to conferences and workshops about solid state sensors and actuators in recent years is strong evidence of the high rate of growth in this field [2]. According to statistics the market for sensors has had a growth of almost 90% from 1990 to 1995 [3]. Up to now, the automotive industry has been the biggest market for silicon-based microsensors [3]. For example, accelerometers are devices which have applications in the safety systems of cars, and now are often made of silicon-based microelectromechanical sensors. Other industrial sectors, especially biomedical and computer industries are also flourishing markets for MEMS.

1.1.1 Why Silicon?

Crystalline silicon, besides its excellent electrical properties which make it the usual material for fabrication of microelectronics devices, has very attractive mechanical properties, quite similar to those of steel, a material commonly used in mechanical structures. It has a Young's modulus very close to that of steel. Thermal conductivity of silicon is about 50% higher than that of steel and its thermal expansion coefficient is 20% of that of

steel. Silicon is entirely elastic, therefore it does not show any mechanical hysteresis. These properties make it possible to make useful mechanical structures, such as beams and membranes, on the silicon wafers [4]. Because of the high Young's modulus, the resonant frequency of such fabricated structures is high enough for use in sensors such as microphones, and accelerometers.

Also, silicon is highly stress sensitive and shows a significant piezoresistive effect. (Piezoresistivity is the change of the resistivity of a material with respect to external applied stress). In silicon this effect is a function of crystallographic orientation and also of type and amount of doping. This effect has been successfully used to make a variety of micromachined sensors, such as pressure sensors and accelerometers.

Because of these properties, the fabrication of miniaturized mechanical geometries and structures has been accomplished, and such structures can be used in the fabrication of microsensor devices. There are some factors which have played a crucial role in the progress and development of silicon microsensors fabrication [1]:

(1) Crystalline silicon, as the starting material for such fabrication, is easily available and inexpensive, and nowadays the techniques of preparing it with high levels of purity and perfection are well developed.

(2) The microelectronics device fabrication industry is a very mature technology, which is mostly based on thin film deposition and photolithography, both of which have the capability to be miniaturized with high precision and reproducibility. All of these techniques can be applied to microsensors fabrication.

(3) And, most important from an economics point of view is that silicon microelectronics devices are batch fabricated, which makes possible large-scale commercial production of microsensors.

1.2 Bulk and Surface Micromachining

The fabrication of miniaturized mechanical structures on silicon is called micromachining. In general, micromachining can be classified as bulk micromachining or surface micromachining. A brief description of each one is given here.

1.2.1 Bulk Micromachining and Anisotropic Etching

Bulk micromachining technology is based on making mechanical structures by etching single crystal silicon. In this technology, the fabricated parts are made of silicon itself or some other layers which are grown on silicon like thermal oxide, or deposited like LPCVD oxide and silicon nitride. The reason that this technique is called bulk micromachining (as opposed to surface micromachining) is that etching of the bulk of the silicon wafer to a depth of tens of micrometers is quite common. In this way structures like cantilevers, bridges and membranes are made of masking layers such as silicon dioxide or of silicon itself.

The primary tool used in bulk micromachining is wet anisotropic etching. There are many etchants used for this purpose, almost all of which [5] are alkaline solutions. The main property of these solutions is that they etch different orientations of single crystal silicon at different etch rates. {111} planes have the lowest etch rate among all planes with different orientations in all of the anisotropic etchants. So that in many applications it can be considered as a zero etch-rate plane. This effect can be used in the creation of different geometries on a silicon wafer with great accuracy. In Fig.1.1 an oxide cantilever fabricated on a {100} silicon wafer is shown.

Common anisotropic etchants which are used in micromachining are hydrazine-water solution, EDP (ethylenediamine-pyrocathechol-water), potassium hydroxide-water, TMAH (tetra-methyl ammonium hydroxide-water) and cesium hydroxide-water. In the

next chapter anisotropic etching and the properties of these etchants will be explained in detail. In this thesis the major focus will be on the study of bulk micromachining technique, specifically anisotropic etching of silicon in TMAH.

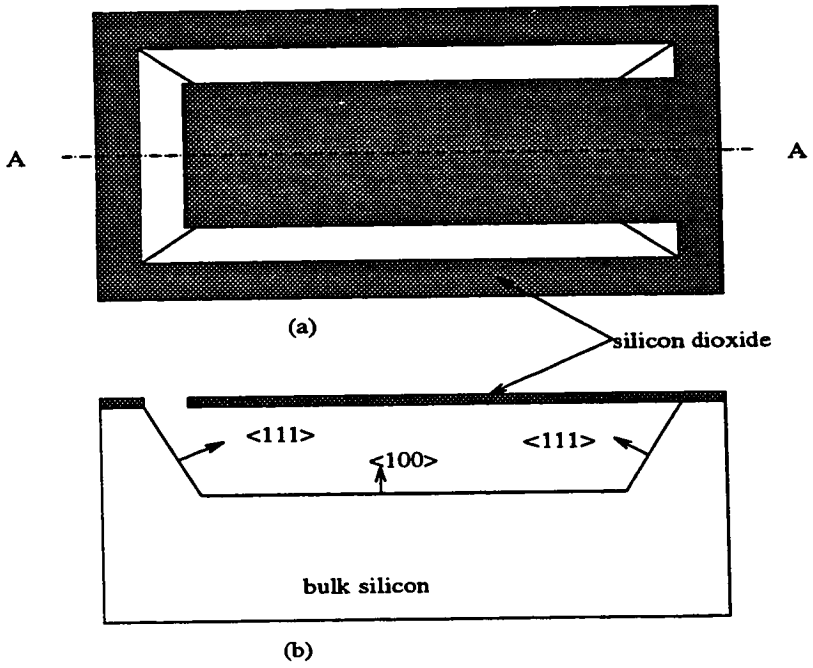

Fig. 1.1: Ideal oxide cantilever made on a {100} wafer. a) Top view. b) A-A cross sectional view.

1.2.2 Surface Micromachining

In surface micromachining, three-dimensional structures are made of deposited thin films on the silicon substrate and they are released by selective etchants. In this technique, the substrate is not affected and the etching is isotropic. Fig.1.2 demonstrates the principal idea of surface micromachining. As can be seen in Fig.1.2 (a) at first, different thin layers are deposited on top of each other (the isolation layer may not be necessary if the etchant does not attack the substrate) on the substrate according to a suitable pattern. Then by using a selective etchant the sacrificial layer which is also called a "spacer" is removed

and the structure will be released. For example, the materials used for this structure can be poly silicon for the body layer and LPCVD oxide for the sacrificial layer.

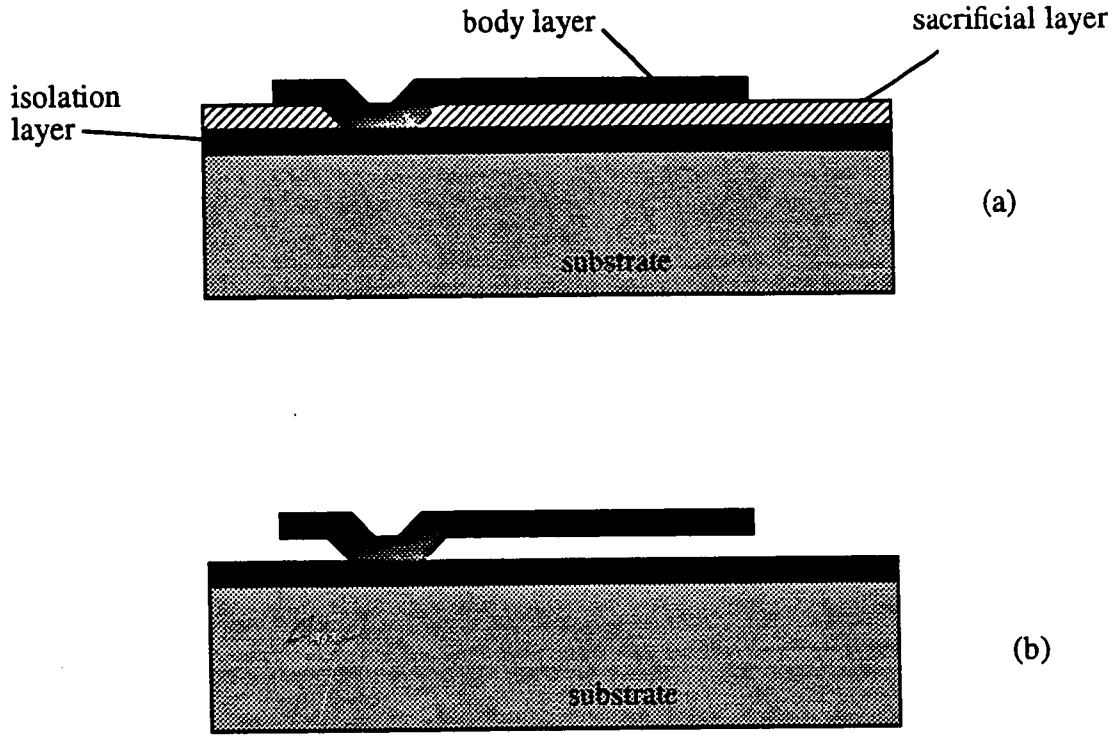

Fig. 1.2: Surface micromachining: a) structural layer before etching; b) released structure after sacrificial layer has been etched.

1.2.3 Motivation for the Study of Anisotropic Etching of Si

Anisotropic etching of silicon is of such fundamental importance in micromachining that it has been studied and continues to be studied by many researchers (see Chapter 2). Yet, even with all the attention that it has received, there remain many difficulties. Some of the popular etchants are toxic or inconvenient to use, or both. Selectivity of etch of various masking layers and other films common to silicon processing varies from etchant to etchant, sometimes inconveniently. While the {111} planes selected are very smooth, they

are often not what the device design calls for. While concave structures bounded by {111} planes are easy to design and achieve, convex structures remain problematic because of the rapid rate of etching convex corners. The evolution of hillocks on an etched surface is a phenomenon which needs to be understood and controlled. Most fundamentally, many problems remain in understanding the fundamental etch mechanism.

For the above reasons, this thesis focuses on an experimental investigation of anisotropic etching of silicon. This thesis studies the new and less toxic TMAH, with the purposes of furthering the characterization of this new etchant for use in MEMS processing, and of obtaining useful data in the quest for understanding the atomic etch mechanism.

1.3 Tetra-Methyl Ammonium Hydroxide as an Anisotropic Etchant of Silicon

In this thesis, the characteristics of tetra-methyl ammonium hydroxide, (TMAH), having the molecular formula $(CH_3)_4NOH$, are investigated. TMAH is not a new material in the semiconductor industry. It has been used as a positive photoresist remover in semiconductor device fabrication. In 1976, it was introduced for the first time as a silicon and silicon dioxide cleaning material and also as a silicon anisotropic etchant [6]. It has some properties which make it a good silicon etchant.

Among the other silicon etchants, KOH[7,8] and NaOH [9,10] have low selectivity with respect to silicon dioxide, and because of metallic ion contamination they are not compatible with VLSI fabrication techniques. Hydrazine [11,12,13] and EDP [14] are poisonous and dangerous to work with (hydrazine is explosive). NH_4OH, which is considered one of the best etchants from the view point of VLSI fabrication compatibility, is volatile and needs additives to obtain stable etching characteristics [15,16].

In contrast with all above mentioned etchants, since TMAH is an organic material it does not cause any metal ion contamination. Also it has a very good Si-SiO_2 selectivity

which makes SiO_2 a good choice for an etching mask. TMAH is relatively nonpoisonous [17] and also safe to work with. It is stable for the range of temperatures usually used, has stable etching characteristics and does not need any additives.

For all of the above reasons TMAH looks to be a very promising material for micromachining applications and is worth being characterized.

1.4 Scope of This Thesis

This thesis is a broad experimental investigation into anisotropic etching of Si using TMAH, ranging from basic experiments to determine etch rates, to the use of TMAH to release micromachined structures. The purposes are on several levels: (a) to confirm and complement existing data available in the literature; (b) to obtain data which can be useful in obtaining a better understanding of the fundamental atomic etch mechanisms at work in anisotropic etching of Si; (c) to use the experimental data to improve techniques for micromachining mechanical device structures on silicon.

The thesis is organized as follows:

In the next chapter (Chapter 2), most of the anisotropic etchants which have been being used in micromachining are reviewed, including KOH, EDP, and hydrazine. Also, a short summary of results of other research about TMAH is included.

Chapter 3 begins by explaining the apparatus and procedures used in most of the experiments reported in the thesis. Then, basic etch rate experiments are presented. Si{100} and Si{110} wafers are etched in TMAH at various concentrations and temperatures, and the results are compared to previous research available in the literature. Also, in the interests of using TMAH for bulk micromachined devices, the etch rates of various masking materials and other typical microelectronics materials such as titanium nitride and spin-on-glass are studied.

Chapter 4 describes an extensive sequence of underetch experiments, for use both in modelling of fundamental etch processes, and for use in creating mechanical structures on Si. The underetch rate variations with mask-edge angle are compiled for both Si{100} under a variety of conditions, and Si{110} under some typical conditions. The resulting underetched planes are observed in detail.

In Chapter 5 the occurrence of etch-induced hillocks is experimentally studied. Individual hillocks created during etching of Si{100} in TMAH are characterized by SEM. Further, an experimental investigation of the evolution of hillocks size, density and shape is conducted.

In Chapter 6, again in the interests of searching for clues about the fundamental atomic mechanisms in anisotropic etching, some effects of bending stress applied to silicon samples during etching in TMAH are observed.

Chapter 7 demonstrates the use of the information found in Chapters 3 and 4 in some applications of TMAH for anisotropic etching in the fabrication of some micromachined devices. Among other issues, release of a cantilever beam is considered.

Finally, Chapter 8 is a conclusion.

CHAPTER 2

Review of Common Silicon Etchant Systems

In this chapter, the most commonly used silicon etchants are reviewed. Anisotropic etching is not only a critical tool in bulk micromachining [18,19,20,21,22] but it also has other applications in the fabrication of various types of integrated circuits [23,24], power MOSFETs [25,26] and some other semiconductor devices [27]. In these kinds of devices, V-grooves and U-grooves are used for isolating different regions from each other, where the grooves are created by using anisotropic etchant. Detection of pinholes in thermal oxide and passivation layers can be considered as another application of anisotropic etching [10]. Most of the etchants which are discussed here are anisotropic, although one isotropic etchant is also discussed.

2.1 Anisotropic Etching of Silicon

As it was mentioned in Chapter 1, a critical tool in bulk micromachining technology is wet anisotropic etching. The anisotropic etchants have some common properties, although to different extents, which make them very useful in micromachining. These properties are:

(1) anisotropy: the etch rate of silicon is strongly dependent on the orientation of the surface to be etched;

(2) selectivity: they are highly selective, with the etch rate of silicon much higher than that of other materials commonly used as etching masks like SiO_2, Si_3N_4 and Au;

(3) the etch rate of highly doped p-type silicon is much lower than that of lightly-doped silicon, making it possible to fabricate thin silicon membranes. These common properties are explained here and the characteristics of each one is explained subsequently.

2.1.1 Anisotropy

In all anisotropic etchants reported so far, the {111} family of surfaces have the minimum etch rate, which in many practical cases can be considered as zero etch rate. For the other two most typically considered orientations, whether {100} etches faster than {110}, or vice versa usually depends on the composition of the etchant used.

Consider a {100} wafer immersed in the etchant, having oxide as a mask and patterned with a square opening as shown in Fig.2.2. The bare {100} silicon surface is attacked by the etchant. Etching proceeds until only {111} surfaces remain, and the etch rate on all such {111} surfaces is very low.

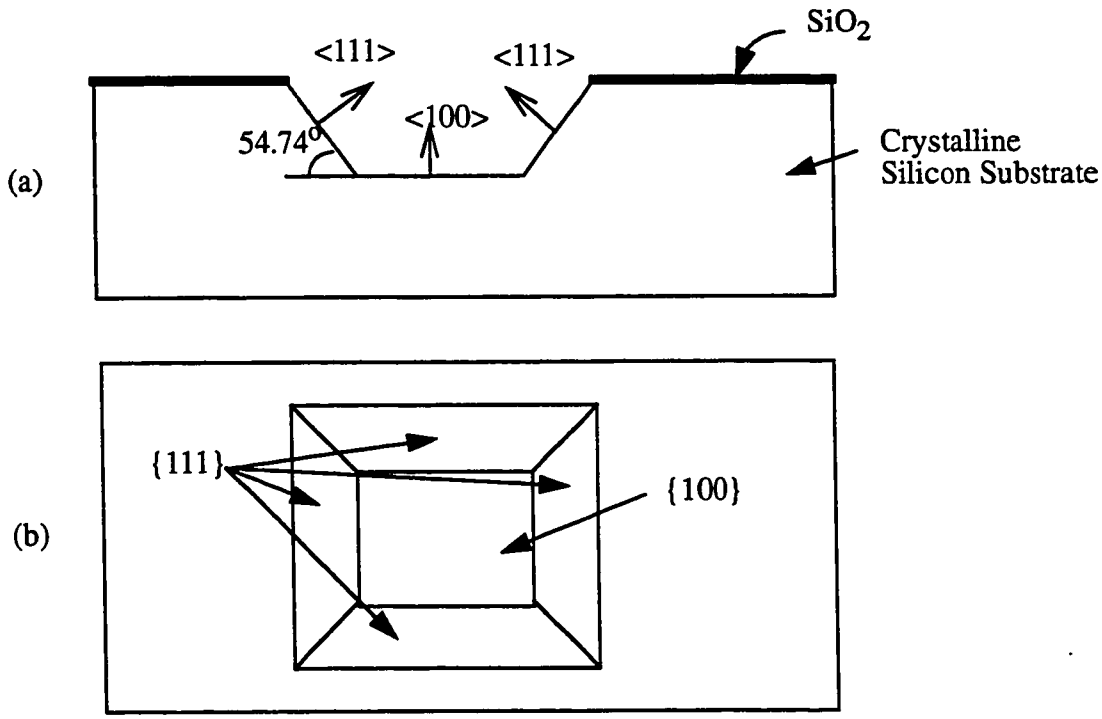

Fig. 2.1: (a) Cross sectional and (b) top view of a cavity etched on a Si {100} wafer anisotropically.

The behavior of convex corners and concave corners are totally different in the etchant. In the case of concave corners, after two {111} planes reach each other, the etching is practically stopped. Concave corners can be said to expose "slow-etching" planes. However, when a convex corner is exposed to an anisotropic etchant, some specific surfaces appear which have the highest etch rates among the different orientations. Different researchers have reported different "fastest etching" surfaces. Some of these surfaces are: {211} [11],{331} [28],{221} [29] and {411}[30]. In Fig.2.2 this situation is shown. After the appearance of these fastest etching surfaces, etching continues until either these surfaces are totally etched away, or until the etch front reaches to a concave corner confined by {111} planes.

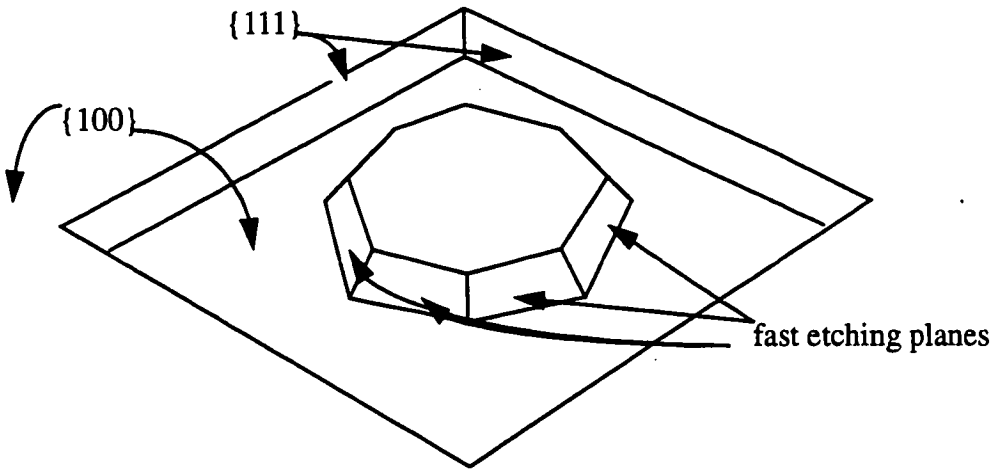

Fig. 2.2: Perspective view of a cavity etched in {100} silicon, with a mesa shape at the middle of the cavity. The etching mask is not shown in this picture.

Overall, etching continues until all surfaces other than {111} orientation are etched and all exposed surfaces are {111}. No matter what is the shape of the mask, the terminal shape of the cavity etched in a {100} silicon wafer is a pit with a rectangular base and a pyramidal shape inside the silicon [1]. This is shown in Fig.2.3.

The edges of the rectangular base of the cavity are aligned with the intersection of the

{111} planes and {100} plane and its dimensions are equal to the dimensions of the smallest rectangle formed this way which contains the opening window. In Fig.2.4 the cross section of the etched sample shown in Fig.2.3 is shown.The maximum depth of the cavity can be determined by using Fig.2.4.

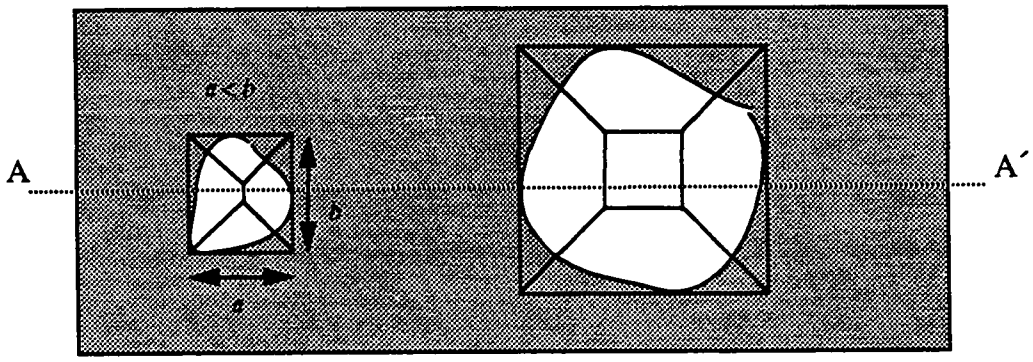

Fig. 2.3: Top view of open window for silicon etching. Outlines of the final cavity confined by {111} planes are shown. The shaded area is covered by the masking material.

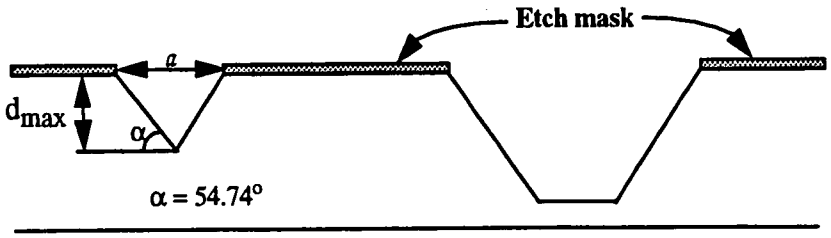

Fig. 2.4: A-A´ cross sectional view of the etched sample shown in Fig.2.3.

Some part of the mask overhanging over the cavity is also shown in Fig.2.4. The size of d_{max} is the maximum depth of the cavity and "a" is the smaller edge of the rectangle in Fig.2.3. It can be seen from Eq.(2.1) that the final depth of the etched cavity is a function of only the smaller edge. In this formula the etch rate of {111} surface is considered to be negligible.

$$d_{max} = \frac{a}{\sqrt{2}} \tag{2.1}$$

If d_{max} is greater than the thickness of the wafer, a hole through the wafer will result.

In a similar way {110} wafers can be discussed, regarding the shape of the etched cavity and etch depth. In this case also, etching continues until etch fronts reach {111} surfaces. The top view of the final etched pit will be always a parallelogram, with angles between edges equal to 70.5^{o} and 109.5^{o}. The edges of this parallelogram are the intersection of {111} with the surface of the wafer, and its dimensions are so that this is the smallest parallelogram which contains the window in the etch mask. In this case the depth of the etching is a function of both edges of the parallelogram which is equal to:

$$D_{max} = \frac{L}{2\sqrt{3}} \tag{2.2}$$

The parameters used in Eq.(2.2) are shown in the Fig.2.5 [31]. In {110} wafers it is possible to create long narrow grooves with vertical walls, which is not possible on {100} wafers.

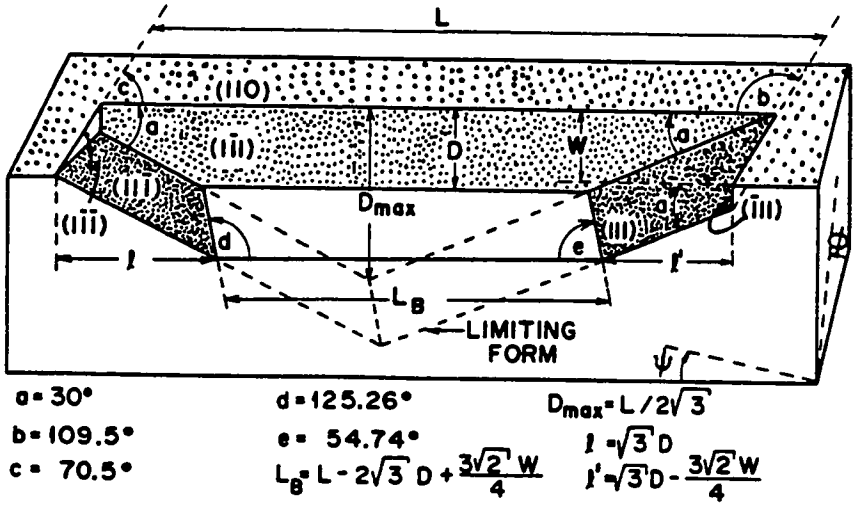

Fig. 2.5: Cross sectional view of a {110} surface etched anisotropically (from ref. [31]).

Although {111} wafers are not usually used for bulk micromachining purposes, the etched surface can be discussed in the same way as the other two major orientations. Fig.2.6 and Fig.2.7 show the cross section and top view of an etched {111} surface [5]:

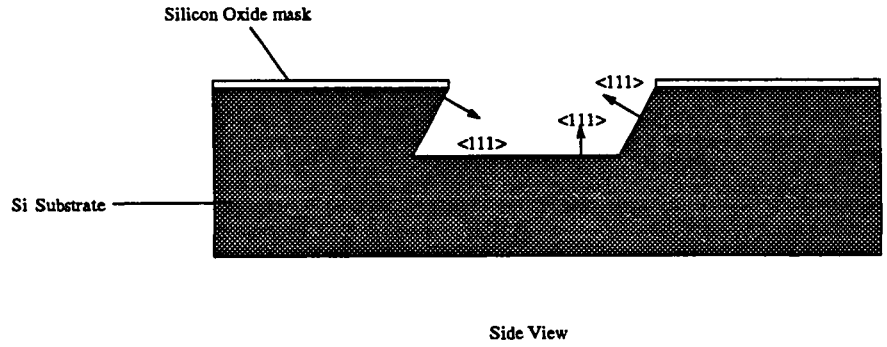

Fig. 2.6: Cross section of a cavity etched anisotropically on a {111} surface (from ref. [5]).

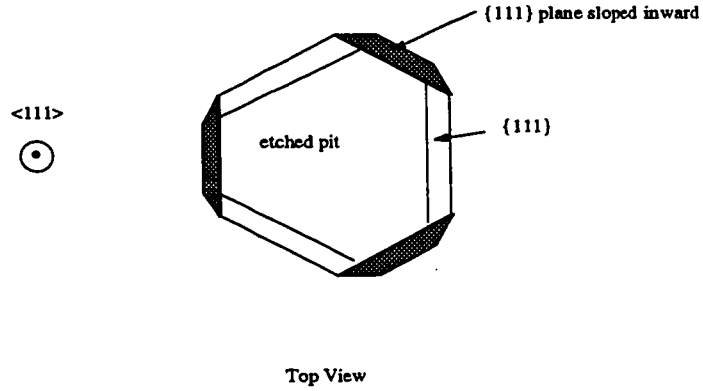

Fig. 2.7: Top view of a cavity which appears on a {111} surface etched anisotropically (from ref. [5]).

As seen in etching of {100} and {110} surfaces, during etching of Si{111} the etch fronts and the periphery of the etched pit are {111} surfaces. The etched cavity is always a hexagon having all six angles equal to 120^0. However, the lengths of the resulting six edges need not be the same, and will depend on the original mask shape. Of course, the evolution of these cavities on {111} surfaces is much slower than pit evolution on wafers

with other orientations, because of the very slow etch rate of the {111} surface. Due to the particulars of the Si crystal structure, the walls inside the pit, which must be {111} walls, are alternatively sloped inward and outward.

2.1.2 Selectivity of Anisotropic Etchant

In the process of creation of different structures on the silicon wafers some thin films are always used as a mask. The best examples of these materials are SiO_2 and Si_3N_4. The etch rates of these materials are much smaller than that of the silicon substrate. The ratio of silicon etch rate to film etch rate is called selectivity and its value is usually between a few hundreds to a few thousands. In the next sections, the selectivity of each etchant will be discussed in more detail.

2.1.3 Etch Stop Property of Highly Boron-Doped Silicon

The first observation of an etch stop phenomenon for p-type silicon when etched in the EDP was reported by Greenwood in 1969 [32]. He attributed this phenomenon to the presence of a p-n junction. Another report about etch stop in boron doped silicon by Bogh [33], explained that the etch stop was the result of the level of doping of the silicon, rather than the presence of a p-n junction. According to his reasoning this happens at boron concentration of higher than $C_b = 7 \times 10^{19}$ cm^{-3} and does not have anything to do with a p-n junction. It should be mentioned that in fact this is not a complete stop of etching and that even at higher boron concentrations a finite nonzero etch rate is observed.

The etch stop phenomenon has been studied by different researchers [34,35,36,37]. The real mechanism of decrease in the etch rate has not been determined yet and all present theories have some limitations. In some papers the effect of stress has been considered as the cause of this but there is also some evidence [34] which shows that stress is not the cause of the etch decrease. Another theory states that etch rate decrease is a "Fermi

level effect" and can be explained electrochemically [37]. Electrochemical reactions are reactions in which free carriers are involved [38]. Another theory says that since n-type dopant phosphorus also acts as an etch stop at very high concentrations [35] it is not a Fermi level effect and it is because of formation of a passivation film which causes decrease in the etch rate. But it should be mentioned that the reduction of the etch rate in silicon doped with germanium or phosphorus is much smaller and should follow another mechanism [37]. Here specific characteristics of some of the commonly used anisotropic etchants are reviewed.

2.2 Some Common Etchant Systems.

2.2.1 System of Hydrazine-Water Solution.

This system (mixtures of NH_2-NH_2 and H_2O) was introduced for the first time in 1969 by Lee [11]. The main advantage of hydrazine with respect to the other anisotropic etchants is that it does not attack aluminium [11,12,13] which can be very important in some applications. In the first report [11] the results of examination of a ternary solution of hydrazine-water-isopropyl alcohol at boiling temperature of the solution are explained. Some of the mixtures only stained the surface of the silicon without any etching and some other mixtures oxidized the surface of the silicon without etching it.

Lee [11] reported that the boiling point of hydrazine-water-isopropyl alcohol varies sensitively with the proportions of the 3 components. The highest etch rate was reported to be >120 μm/hr, at the highest boiling point of ~120^{o} C.

In this system of etch isopropyl alcohol is a moderator and does not have a complexing role (that is, a role of making the reaction by-products soluble in the etch solution) or oxidizing role in the reaction. The quality of the etched surface depending on the composi-

tion of the solution can change between very smooth surface to a very faceted surface covered with lots of pyramidal shape hillocks. Concave corners, as with the other anisotropic etchants, finally will terminate in {111} surfaces. At convex corners the emerging planes are {112}.

In another report about hydrazine [13] the system of mixture of only hydrazine and water was studied in terms of etch rate of {100} plane, quality of the etched {100} surface, quality of {111} walls and the corners. In Fig.2.8 [12] the etch rates of hydrazine-water mixture are shown in terms of hydrazine concentration for several temperatures.

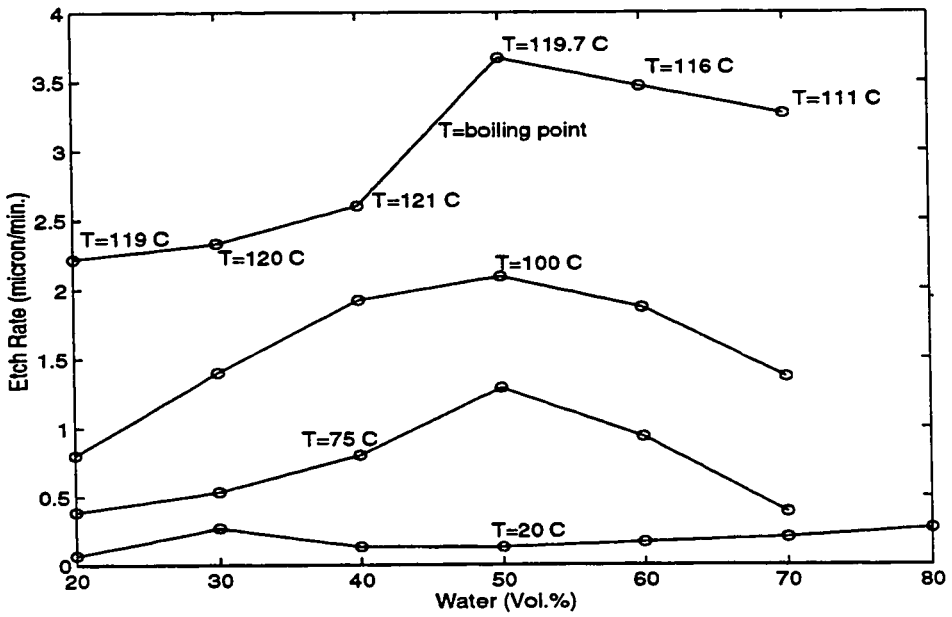

Fig. 2.8: Etch rate of Si {100} plane in hydrazine solution vs. water content for some different temperatures (from ref. [12]).

In general the quality of the surface was found a function of both temperature and composition of the solution and it has been observed that the quality of the surface may be affected in two ways: by the formation of the pyramidal hillocks and by the formation of waveshape structures, which are shown in Fig.2.9 [12].

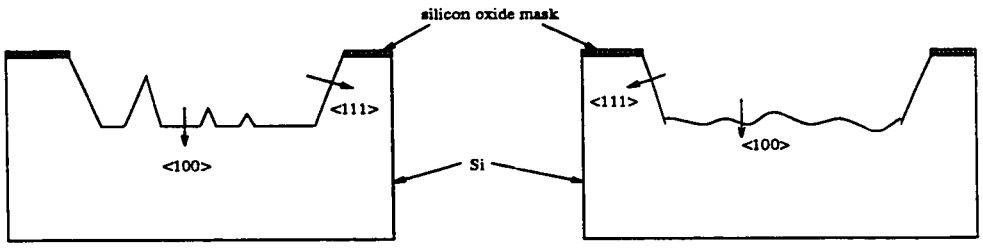

Fig. 2.9: Typical defects in bottom surface of an etched {100} wafer [12]

In this report [12] the effect of adding catechol to the solution of hydrazine water was tested. The result shows that catechol has a worsening effect on the surface quality and increases the density of hillocks. Also, it was observed that sometimes wave-type defects can be caused by insufficient cleaning of the surface. This usually happens when the wafer is not carefully dried before immersed in the etching solution, or when the solution is not well stirred. The major points of this study are as follows:

1. The optimal temperature for the hydrazine-water anisotropic etch is 100^{o} C for different compositions.

2. The composition of the mixture should be chosen according to the particular use of the anisotropic etching;

- For V-groove rings like those used for bipolar transistors isolation [39], or VMOS devices where {111} walls quality is the only important parameter, the solution which gives the best wall quality, low undercutting, and an acceptable yield at the same time should contain about 65 vol.% (percentage of hydrazine by volume) hydrazine.

- For use in two-level structures where both good walls and high quality bottom surface are required, the best concentration range is between 70 and 80 vol.% hydrazine. The same ratio is recommended for the etching of the surfaces where high degree of smoothness is required.

3. Wafers should be carefully cleaned and dried before etching.

4. To keep the solution concentration and therefore etch characteristics constant, a reflux system should be used to avoid excessive evaporation.

From two reports [11,12] about etch characteristics of hydrazine it becomes clear that there are not many compositions of hydrazine-water which have acceptable quality for silicon etching and micromachining. In a more recent report about hydrazine [13] only one specific composition of hydrazine water is considered and characterized. A solution of 50 mole% of hydrazine-water (percentage of hydrazine by mole) is possibly the most practical composition for this system of etch. The result of this study is shown in Fig.2.10.

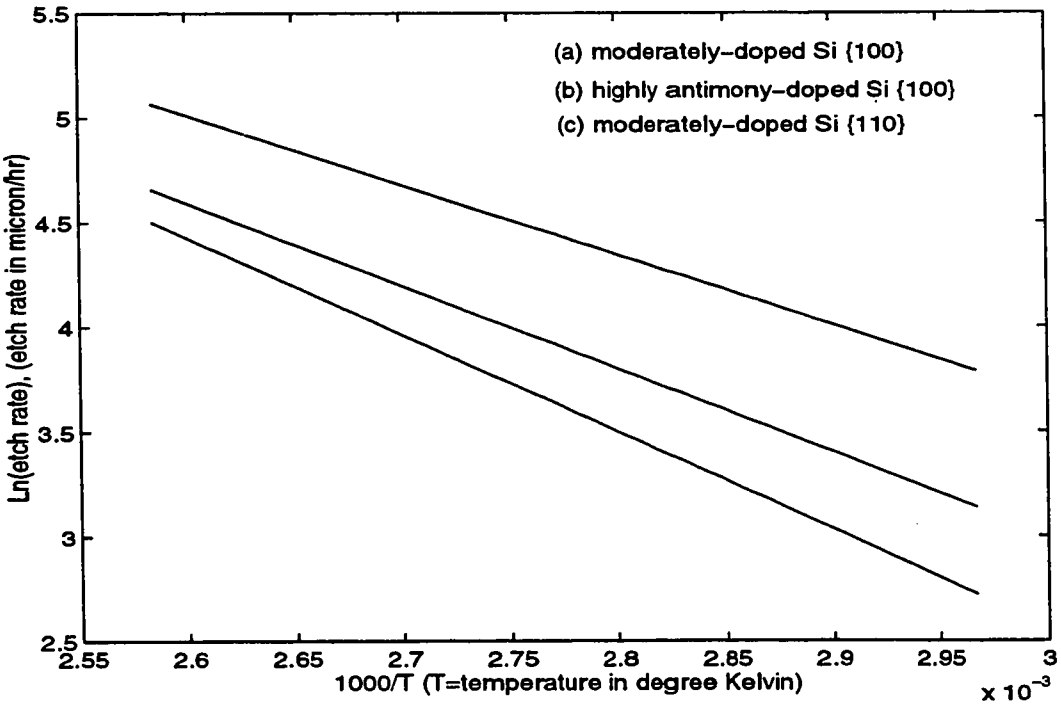

Fig. 2.10: Etch rate of a solution with 1:1 molar ratio of hydrazine and water (from ref.[13]).

The differential etch rate ratio of {100}/{111} and {110}/{111} in the equimolar mixture of hydrazine-water is considered low among the anisotropic etchants. These values are 16 and 9 respectively for a moderately doped wafer at an etchant temperature of 118^{o}

C, which is the boiling point of solution. The etch rate of {111} moderately doped silicon at this temperature is reported to be [13] 11 ± 0.5 μm/hr.

Etch-stop effect of heavy boron-doping-In hydrazine an effect of etch rate reduction at high p-type doping is observed. For boron concentration of 1.5×10^{20} cm^{-3}[13] the etch rate drops significantly and can be considered as zero for many practical cases. The effect of doping on etch rate has been also observed for highly antimony-doped silicon (n-type), etched in hydrazine [13] but this was not found to be as significant an effect as that of heavy boron-doping.

Passivation layer as etching mask- For masking the etching of silicon, SiO_2 and Si_3N_4 layers can be used. Etch rate of thermal SiO_2 in equimolar hydrazine-water solution at 118^o C is close to 100 Å/hr. The etch rate of Si_3N_4 is even smaller but it could not be measured accurately.

Also, it has been observed that the solution of hydrazine-water if exposed to air will be aged and will be oxidized and the result of etching will not be repeatable [13]. To get a repeatable result the etching reactor should be flushed with nitrogen to keep hydrazine from oxidation.

The main disadvantage of this etch system is that hydrazine is highly poisonous material and also at high concentration it can be highly explosive [13]. When working with hydrazine, gloves should be used and the etch reactor should be placed in a fumehood to ventilate the hydrazine fumes.

2.2.2 System of KOH-Water Solution

This system is one of the most common etch system for anisotropic etching. In 1967, the use of a mixture of KOH-water-isopropyl alcohol was reported for the first time [40]. According to this report a mixture of 4.5 g KOH, 15 ml water and 25 ml isopropyl alcohol

gives an etch rate in <100> direction 25 times faster than that of <111> direction. In 1970 a simpler mixture of 50 wt.% KOH (percentage of KOH in the solution by weight) and water was reported [41] which was used for etching vertical wall grooves on a {110} wafer and etch rate in <110> direction was 25 times faster than etch rate in <111> direction. A systematic study of KOH-water-isopropyl alcohol was reported in 1973 [7]. In the experiments described in that report, binary solutions of KOH-water with different wt.% of water were tested. For testing the ternary solutions of KOH-water-isopropyl alcohol, to a solution of KOH-water, isopropyl alcohol was added dropwise to such an extent that no more isopropyl alcohol could be dissolved in KOH-water solution and a thin layer of alcohol formed on top of the solution. In Fig.2.11 [7] the solubility of alcohol in KOH-water solutions in terms of composition is shown. According to this report the etch rate is a function of surface orientation, temperature, KOH concentration, boron doping of silicon and concentration of solvent, which is alcohol. In the Fig.2.12 [7] some results of this experiments are shown.

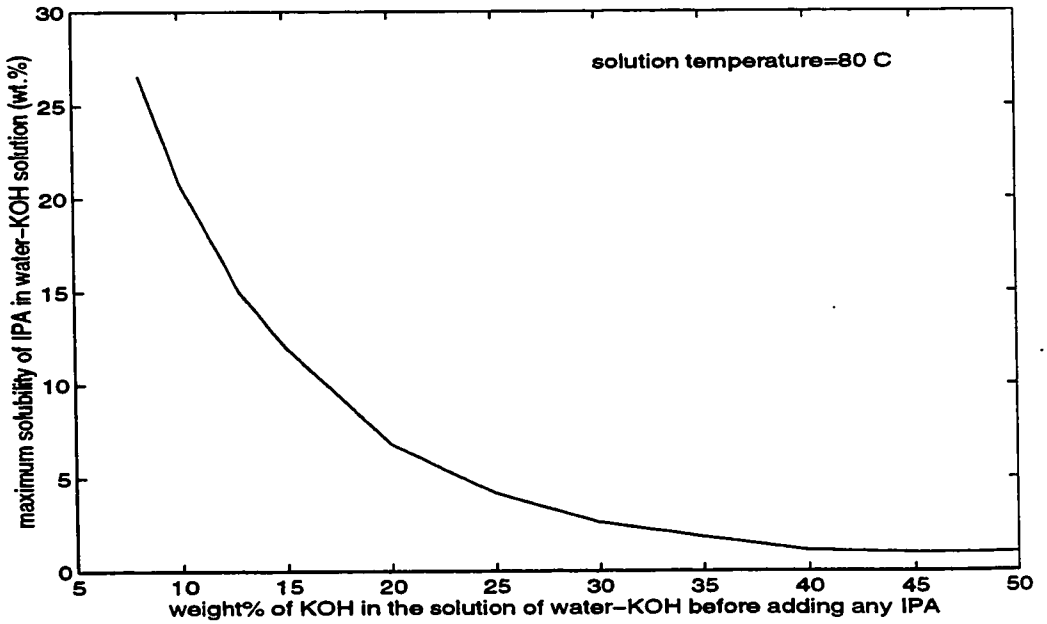

Fig. 2.11: Solubility of isopropyl alcohol in KOH -water solution (from ref. [7]).

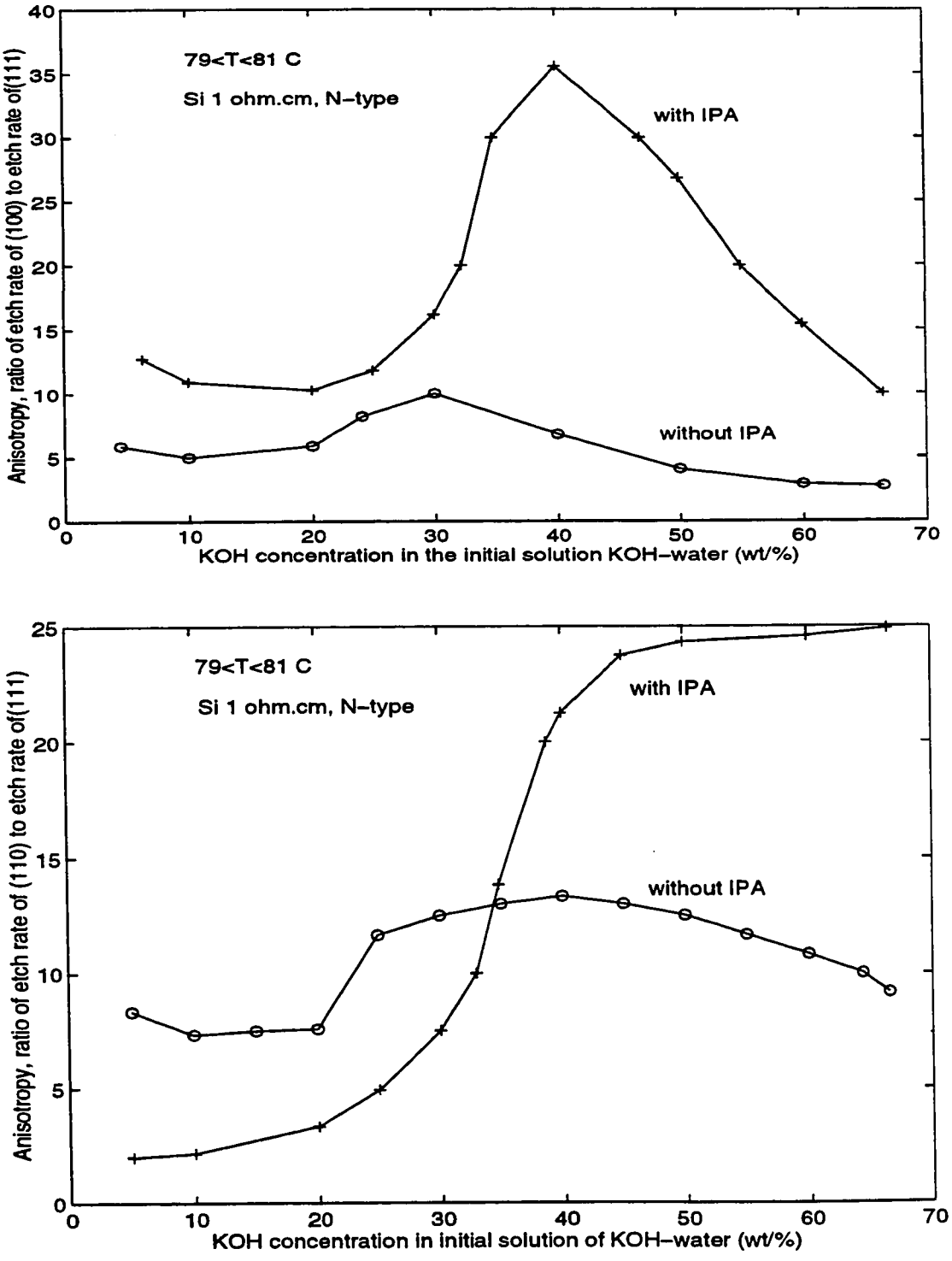

Fig. 2.12: Anisotropy of Silicon etch rate in KOH-IPA water solution (from ref.[7]).

One important point about this system of etch is that anisotropy is a function of solution composition and not a function of temperature. Under optimum conditions an etch rate ratio of 35 for {100}/{111} has been found [7]. Also, in this report it has been remarked that stirring does not have any effect on the etch rate of the <100> direction, which means that the etch process is not a diffusion controlled reaction. Although it is said [7] that addition of isopropyl alcohol results in a higher anisotropy (here, anisotropy is defined as ratio of etch rates of {100} and {110} surfaces to the etch rate of {111} surface.) but in some more recent papers [31] a much higher anisotropy was reported for a mixture of only KOH and water (for a solution of 44 wt.% KOH-water at 120^0 C a ratio of 300:600:1 was measured for the etch rates in the directions of <100>, <110> and <111>, respectively). Also it has been shown [7] that addition of isopropyl alcohol reduces the etch rate. For these reasons the binary solution of KOH-water (without iso-propyl alcohol) is used very often.The reason for large differences among different results can be explained by inaccuracy in mask alignment [42,43,44]. The tolerances (a) the alignment in the patterning of the masks, and (b) the orientation of the flat edge of {110} wafers [31] used in the experiments, should be in the range of 0.1^0 or better. A deviation of 1^0 from exact alignment can lead to large error in measurement of anisotropy. For example, an erroneous value such as 35 for the ratio of etch rates of {110} and {111} planes may be obtained [42].

Fig.2.13 summarizes more recent results[45] for the etch rate of Si {100} in KOH-water solutions as a function of concentration, at 72^0C. The graph shows that the etch rate increases as a function of concentration until a maximum at about 20 wt.%, and then decreases. The etch rate at 60 wt.% is almost 4 times lower than the etch rate at maximum. Reference [45] implies that this type of variation with concentration occurs at other temperatures in the range of 40^0 C to 90^0 C.

It has been observed that the quality of etched {100} silicon surface can be affected

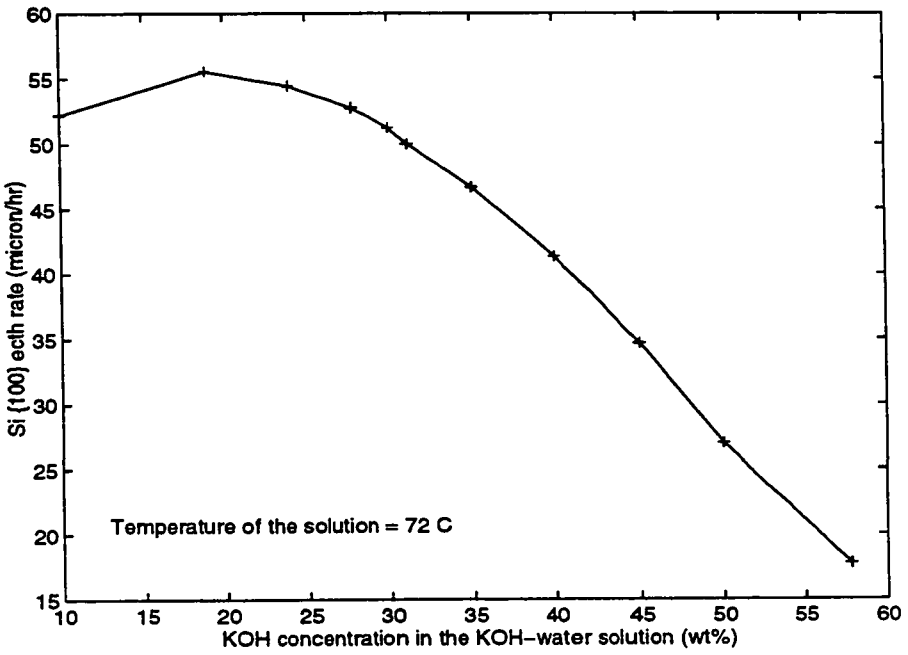

Fig. 2.13: Etch rate of KOH-water solution vs. KOH concentration (from ref.[45]).

by appearance of pyramidal hillocks [46,47]. This type of etch-induced defect can be important in some kinds of devices made on silicon. For example in creating the V-shape and U-shape grooves on the silicon wafers for holding the fiber optic waveguides it is necessary to have a very smooth surface otherwise the fiber will be damaged. There are different parameters which can affect the appearance and density of hillocks. Some of them are:

- KOH concentration in etchant,
- etch temperature,
- etch solution agitation and
- presence and absence of surfactants.

It has been reported [46] that in the KOH-water system at higher temperatures the density of hillocks is more than that of lower temperatures. Also by increasing the concentration of KOH in the solution the hillocks density can be reduced and can even be removed completely. For example at temperature 60^{o} C, concentrations of KOH higher

than 30 wt.% gives a surface without any hillocks [46]. State of agitation of the etchant also affects the density of hillocks in KOH etch system. By stirring the etchant, a decrease of one order of magnitude in the density of hillocks has been observed [46].

When etching a structure defined by a concave mask pattern, the etch proceeds laterally until {111} planes emerge, which have a very smooth surface. When such {111} planes are reached, the etch rate at the concave corners finally decreases to a very low value [45].

Etching of convex corners creates planes which etch the fastest in this system. The planes {331}[28], {411}[30] and {212}[48] have been reported as the fastest etched planes, by different researchers.

Highly boron-doped etch stop effect-The etch stop effect of highly p-doped silicon has been observed in this system [37]. In Fig.2.14 [37] the etch rate of silicon as a function of boron concentration is shown. Average boron concentrations above 7×10^{19} cm^{-3} can be

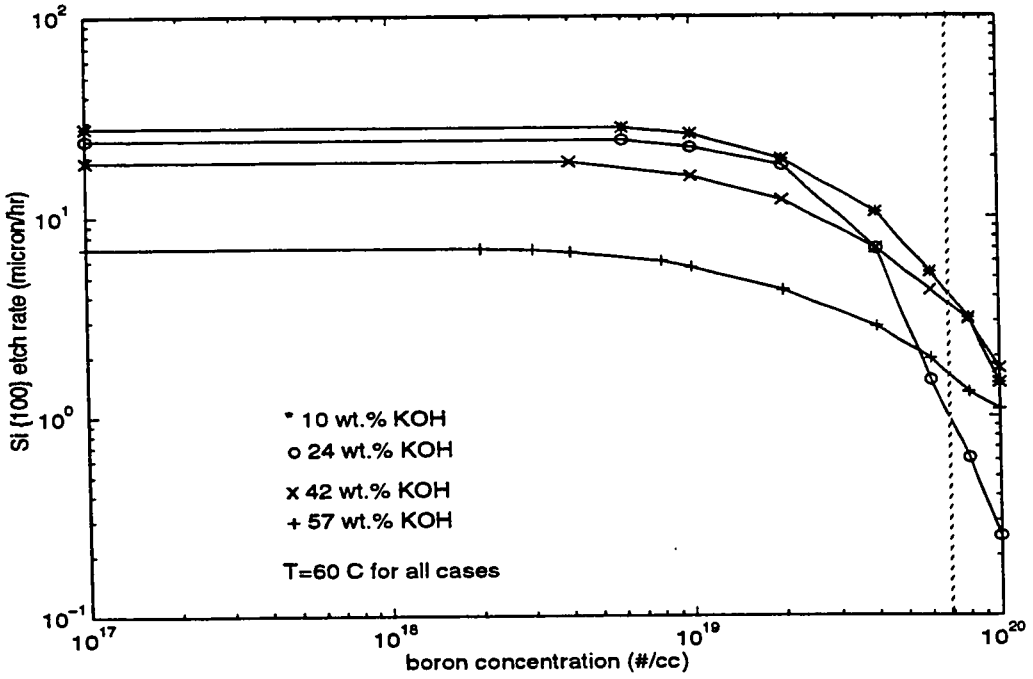

Fig. 2.14: Etch rate of KOH-water solution vs. boron concentration[37].

considered as suitable doping levels to severely reduce the etch rate of Si (at which the etch stop property can be seen).

Passivation layers as etching mask- Similar to the case of other anisotropic etchants, Si_3N_4 and SiO_2 are the mask of practical interest. The silicon nitride layer has been observed to have such a low etch rate that its etch rate can not be measured easily [45]. SiO_2, however, has a nonzero etch rate. In Fig.2.15 [45] the etch rate of SiO_2 is shown as a function of temperature for some concentrations of KOH. It can be remarked here that among common anisotropic etchants, the system of KOH-water has a relatively low selectivity for oxide and for {110} and {100} silicon.

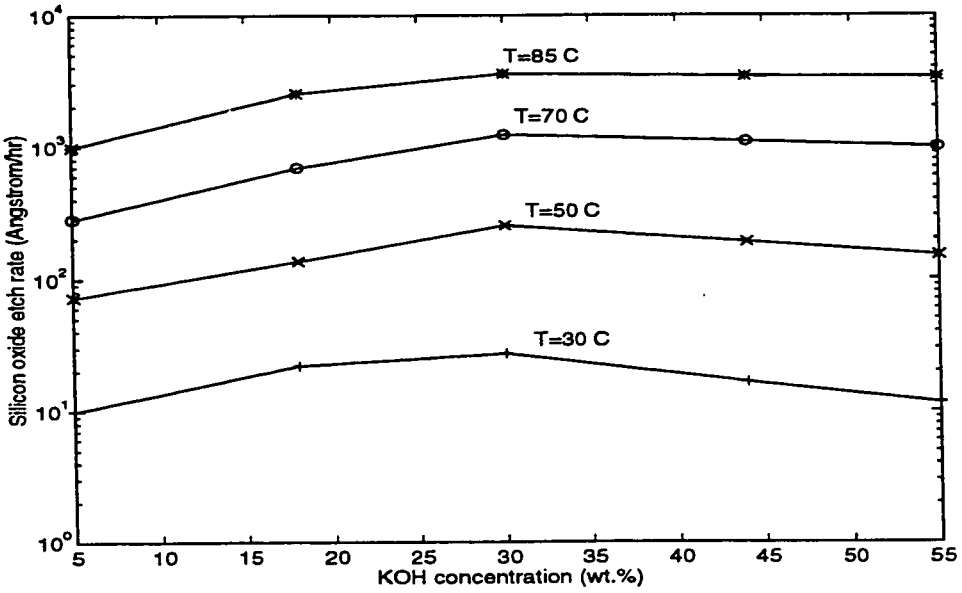

Fig. 2.15: SiO_2 etch rate vs. KOH concentration for some different temperatures (from ref. [44]).

The main advantages of the KOH-water system are that this solution can be prepared very easily and also working with this system is very safe (as opposed to hydrazine-water and EDP systems, KOH does not have poisonous vapor, however, it should not touch skin.). The anisotropy in this system is higher than other etch systems [31]. Disadvantages of this system are relatively high etch rate of oxide (Fig.2.15) and also the presence of K^+

ion in this solution, does not allow it to be used in the applications in which metallic ion contamination may cause a problem, like CMOS compatible micromachining.

2.2.3 System Ethylenediamine-Pyrocatechol-Water(EDP)

For the first time this etchant, EDP (also called EPW), was introduced at 1967 [14]. In that report, solutions with different compositions were examined and a reaction mechanism was proposed for this etch solution. According to this reaction ethylenediamine with molecular formula NH_2-CH_2-CH_2-NH_2 and water, oxidize the silicon surface to hydrated silica, and pyrocatechol with molecular formula $C_6H_4(OH)_2$ plays the role of a complexing agent, which makes the hydrated silica soluble in water. The overall reaction is as follows:

$$2NH_2(CH_2)_2NH_2 + Si + 3C_6H_4(OH)_2 \rightarrow 2NH_2(CH)_2NH_3^+ + [Si(C_6H_4O_2)_3]^= + 2H_2$$

The optimum composition suggested in [14] is following proportion: (Ethylenediamine(liquid): water(liquid): pyrocatechol(solid) -- 17 ml: 8 ml: 3 gr) which gives an etch rate close to maximum etch rate. This composition of etch is called EDP type "T" [45].

A more comprehensive study of this etching system was carried out by some other researchers [49]. The motivation for this study was to find an etchant which can be used for removing thin layers of polysilicon (in the range of 0.5 μm) in integrated circuit fabrication in a way that etch rate can be controlled easily. For having good control on the etch rate, lower temperatures should be used, which using EDP solution type "T" given in [14] causes developing of residues on the surface of chip, although development of residue has been observed at higher temperature as well [49]. Also, this solution is very sensitive to the aging so that during time the etch rate increases in an uncontrolled way [49]. For solving these problems a new composition of EDP was devised by E. Bassous which is called

EDP type "B" solution. The proportion of different component of this solution is (E:P:W - 7.5 ml: 1.2 gr: 2.4 ml). During this study researchers realized that small amounts of a fourth component has major effect on the etch rate characteristics of the solution. This component is pyrazine with molecular formula $C_4N_2H_4$, which small amount of it can be found in the ethylenediamne supplied by some companies. Since small values of this material (below 2 gr/liter ethylenediamine) changes the etch rate drastically and etch rate reaches to a kind of saturation for the amount of pyrazine above 2 gr/liter, for obtaining a repeatable result in using EDP it is suggested to intentionally add some amount of pyrazine (2-4 gr/liter ethylenediamine) to the EDP solution before use in order to minimize the perturbation of etch rate. An advantage of adding pyrazine to the solution is that etch rate of {100} direction increases more than etch rate of {111} direction, which causes an increase in anisotropy from13.5 for EDP without pyrazine to an anisotropy of 18 for EDP with pyrazine [49]. Also, aging effect in "B" type EDP is not as critical as EDP suggested in [14]. Boiling "B" type solution for 2 weeks freely in a well sealed etch reactor (so that no oxygen contacts EDP) did not have any effect on the etch rate of the solution. Bubbling oxygen in this solution at room temperature did not change the characteristics of the etchant. However if oxygen bubbling is done at high temperatures, for instance 95^{o} C and higher, the etch rate changes to higher values (sometimes twice) and remains at that value.

By increasing the concentration of pyrazine two effect have been observed [49], first a tendency for residue formation at 115^{o} C was observed and second, the EDP type "B" with a concentration of pyrazine of 6 gr/liter of ethylenediamine has a much less sensitivity to oxygen exposure. This raises the idea of changing the composition of the solution, to a new composition with higher amount of pyrocatechol and with a pyrazine concentration of 6 gr/liter of ethylenediamine. This new composition is (E: P: W -7.5 ml: 2.4 gr: 2.4 ml) which is called EDP type "F". This solution is an excellent etch in terms of enhancing the

etch rate at 115^{o} C without incurring the undesirable side effect of the residue formation. Also it shows significant resistance to oxygen exposure [49].

Although etch type "F" is residue formation resistant at higher temperature, but at lower temperature residue has been seen. A new etch composition called type "S" can be useful for the purpose of solving this problem [49]. The composition of type "S" etch is (E: P: W- 7.5 ml: 1.2 gr: 1 ml) with pyrazine concentration of 6 gr/liter of ethylenediamine. This etchant has a lower etch rate of silicon but does not show any evidence of residue formation to temperatures as low as 50^{o} C. An application of this etch is etching thin films of poly silicon in integrated circuit fabrication, because etch rate can be controlled with good accuracy at low temperature and does not leave any residues [49].

About effect of agitation of solution on the etch rate of silicon it has been reported that the reaction of etching silicon should not be a diffusion limited reaction [14]. However in a latter report it has been remarked that stirring of the solution can have considerable effect on the etch rate [50]. In Fig.2.16 [45] a curve for the etch rate of EDP type "S"

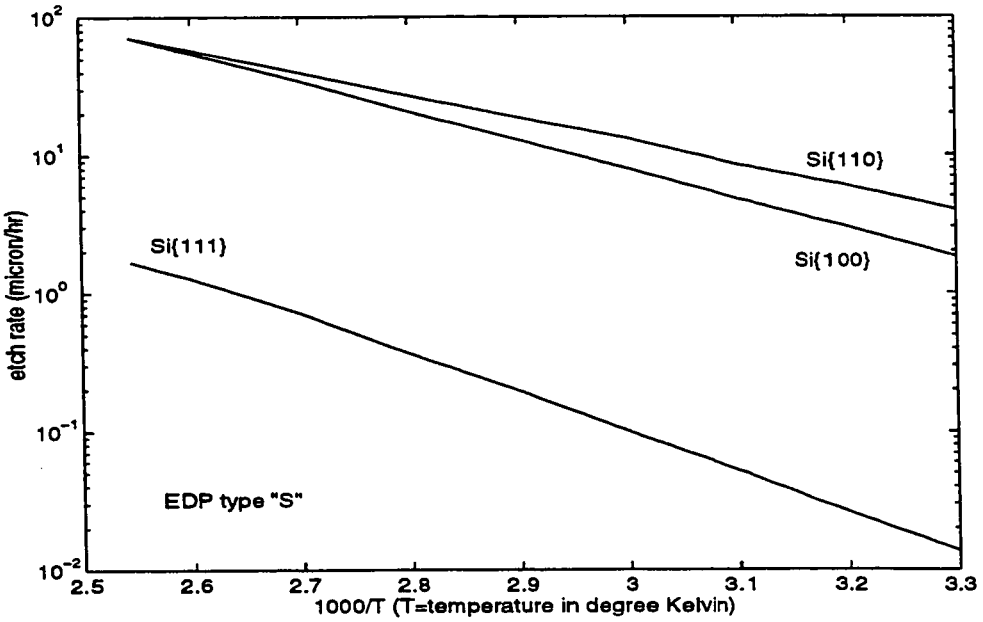

Fig. 2.16: Etch rate of silicon in EDP "type S" vs. temperature (from ref. [45]).

is shown. The surfaces of {111} plane are very clean and good quality [45]. The quality of {100} surfaces are also good but in the etched {110} surfaces some roughness can be seen even with naked eye. The etching of the convex corners generates the planes which are the fastest etching planes and they have been reported as {212}[48] and {331}[28].

Highly boron-doped etch stop effect- As in other etchants this effect is observed in EDP also [37,51]. In Fig.2.17 [37] this effect is shown. According to researchers [37] for boron concentration above10^{19} cm^{-3} etch rate of silicon, both {100} and {110} groups of planes show same behavior and their etch rate start dropping.

Passivation layer as etching mask- Silicon nitride and silicon oxide are both used as good mask for etching. Silicon nitride has an etch rate of very low value which is considered to be almost zero [45]. Silicon oxide has a nonzero etch rate but still it is very low, for example at 110^{0} C, thermal oxide etch rate in EDP type "S" is less than 100 Å/hr [45].The

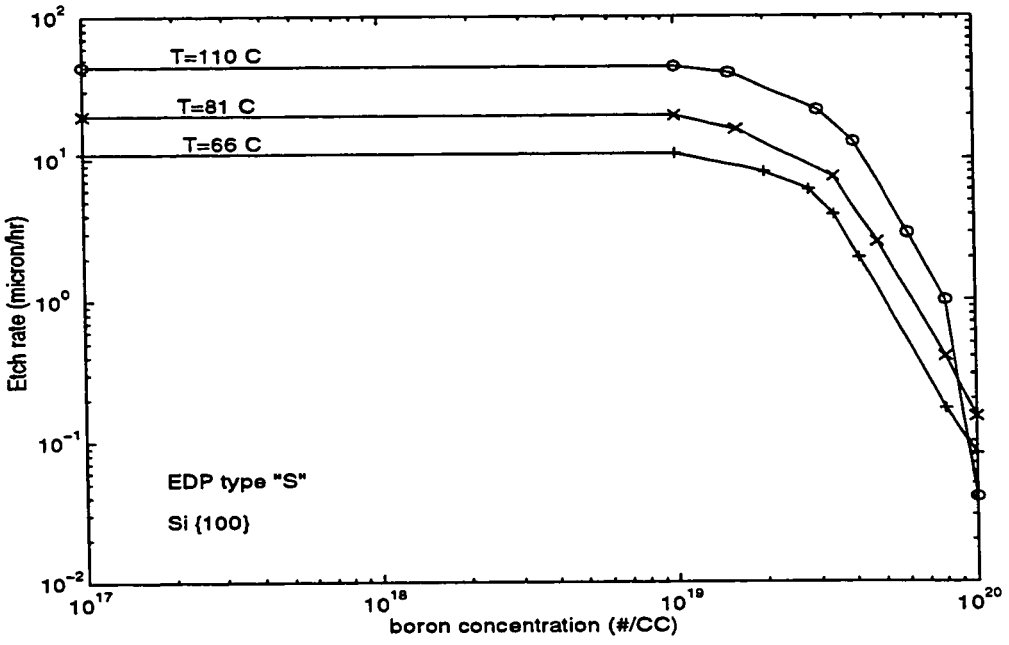

Fig. 2.17: Si {100} etch rate in EDP type "S" vs. boron concentration for some different temperatures (from ref. [37]).

main advantage of system EDP etch is that there are no alkaline metallic ions in it so it is a CMOS compatible etchant. Disadvantages of this system is that it is highly poisonous and because of this extreme care should be taken in handling EDP [13].

2.2.4 System CsOH-Water

Among the group I metals hydroxide, CsOH has the lowest etch rate of silicon dioxide [52,53]. The results of a study of etch rate and selectivity of this etch between silicon and passivation layers SiO_2 and Si_3N_4 are shown in the Table.2.1 [53]. By looking at the table it can be seen that for example, solution of 60 wt.% CsOH at 50^o C has an etch rate ratio of 200 between Si {110} and Si {111}, and a selectivity of 5500 between etching of Si {110} and etching of SiO_2. Also, it can be seen in the table that Si_3N_4 is a good mask for this etch system, like other etch systems.

Disadvantages of this system is the relatively high price of cesium hydroxide in contrast with KOH[4].

2.2.5 System NH_4OH-Water

The solution of ammonium hydroxide and water has been studied as an anisotropic etchant of silicon [15]. In that report the concentrations between 1 wt.% and 18.1 wt.% have been studied. A maximum etch rate of 30 μm/hr in {100} surface for the concentration of 9 wt.% has been observed. Even for concentration of 1 wt.% etch rate of 17 μm/hr has been measured. The solution of ammonium hydroxide water has a tendency to decompose at higher temperature and normal pressure. This problem is more serious for solutions with higher concentration. Therefore this should be considered in working with this etch system. Another problem with this system is roughness of the etched surface. For all concentrations studied, {100} surface was covered with pyramidal hillocks. Stirring

TABLE 2.1: CsOH-water characteristics as an anisotropic etchant (from ref. [53]).

CsOH wt.%	Temp. °C	Si {110}, μm/hr	Si {111}, μm/hr	SiO_2, Å/hr	Si_3N_4, Å/hr	etch rate of Si{110}/ etch rate of Si{111}	selectivity between Si{110} and SiO_2
10	50	0.89	0.56	5.7		1.6	1600
10	60	0.62	0.61	19		1	3300
10	70	1.2	1.2	43		1	280
30	50	0.68	0.59	7		1.2	970
30	60	1.3	0.77	24		1.7	540
30	70	5.4	1.1	70		4.9	770
45	50	10	0.22	11		45	9100
45	60	22	0.4	32		55	6900
45	70	52	0.88	110		59	4700
60	25	1.3	0.94	0.94		190	14000
60	50	8.3	15	15		200	5500
60	60	15	34	34		170	4400
60	70	27	85	85		180	3200
60	90	92	970	970	15	160	950

enhances the roughness of the surface but does not have a general influence on the hillocks formation. Addition of small concentration of H_2O_2 enhances the characteristics of {100} surface etching [16]. In 2.65 molar solution of NH_3 at 80° C the H_2O_2 concentrations between 0.65×10^{-2} mole/liter and 1.84×10^{-2} mole/liter in the solution increase the etch rate of (100) silicon to 75 μm/hr which is 2.5 times the solution without H_2O_2. In this range of concentration no pyramidal hillocks form. For concentrations below the above mentioned value pyramidal hillocks appear, and for the concentrations higher than that, no etching is done.

Highly boron-doped etch stop effect- The etch rate of highly boron doped (1.3×10^{20} mc^{-3}) silicon is almost 8000 times smaller than lightly doped silicon. This selectivity is much better than selectivity in KOH, EDP and hydrazine [15].

Passivation layers as etching mask- Different types of oxide and nitride can be used as good masks for etching in this system. In a 1.05 molar solution of AHW at T=80° C the

etch rate of thermal oxide and annealed LTO is about 35 Å/hr, etch rate of LPCVD Si_3N_4 about 16 Å/hr, etch rate of PECVD silicon nitride about 40 Å/hr and etch rate of non-annealed LTO is about 140 Å/hr.

The main advantages of this system are that it is a CMOS compatible etchant and also for silicon doping of more than 0.1 gr/liter in the pure AHW, aluminium will not be attacked. For solutions containing 2.65 mole NH_3 and 1.47×10^{-2}mole of H_2O_2, aluminium passivates above dissolved silicon concentration of 0.13 gr/liter [16]. Disadvantages of the system are that its concentration is not stable during etch time and also, the surface is covered with hillocks in the case of pure AHW [15].

2.3 Systems of Quaternary Ammonium Hydroxide-Water (QAHW)

Tetra-methyl ammonium hydroxide (TMAH) is the main topic that will be investigated in this thesis. It is relatively new and has not been fully characterized by other researchers.The existing research is summarized in some detail here.

TMAH, with molecular formula $(CH_3)_4NOH$ is one compound in a group of the materials called quaternary ammonium hydroxide (QAH). As another example of this group, tetra-ethyl ammonium hydroxide (TEAH) with molecular formula $(C_2H_5)_4NOH$ can be mentioned, which shows similar chemical and physical properties as TMAH [54]. Here the results of the previous researches about the properties of the TMAH (and some about TEAH) will be reviewed

As was mentioned in Chapter 1, TMAH has been used in the industry of semiconductor as a positive photoresist remover. For the first time in 1976 it was suggested as an anisotropic silicon etchant [6]. In that abstract it was reported that QAHW solutions etch silicon anisotropically and also etches thermal oxide and CVD oxide with a rate much lower than that of silicon, and etches native oxide very fast. In another paper about TMAH

the etch rate of solutions with different concentrations from 1 wt.% to 25 wt.% at temperature 80° C were reported [55]. According to this paper the pH value of the solution is the most significant factor affecting the etching characteristics of the solution. At higher pH values the etch rate will be lower but the quality of the {100} surface will be better. The surface of {100} planes will be covered by pyramidal shape hillocks, which their size become smaller by increasing pH value and finally they disappear completely at enough high values of pH. By increasing the silicon doping of the solution the pH value decreases and also it is possible to protect aluminium from etching.

Another report about TMAH gives the minimum value of 22 wt.% concentration for the solution to get a surface free of hillocks [56]. At lower concentrations the etch rate is higher but the surface is rougher. By increasing the concentration the etch rate decreases but the surface becomes smoother. Etch rates of {100} and {110} silicon for concentration from 5 wt.% to 40 wt.% for some different temperatures have been given in Fig.2.18 [56].

Also effect of high boron concentration of silicon has been studied by some other researchers[57] which the result is shown in the Fig.2.19. The same as other anisotropic etchant, thermally grown SiO_2 and Si_3N_4 has been found to be very good etching masks in this system [56].

There is also a report about the characteristics of mixture of TMAH-IPA (isopropyl alcohol)-Water [58]. The motivation for investigation of this system was to reduce the undercutting in the TMAH-Water system. The undercutting, which is defined as the ratio of the etched length of a <110> aligned silicon bar to the etched depth of {100} surface, can be important in the etching of the convex corners and shaping the structures on the silicon. This parameter in the TMAH and water solution is about 5-7, which is much higher than that of KOH-Water solution (about 2.7), but by adding alcohol to the solution it is improved by a factor of 2. In this system the concentration of TMAH is the main factor

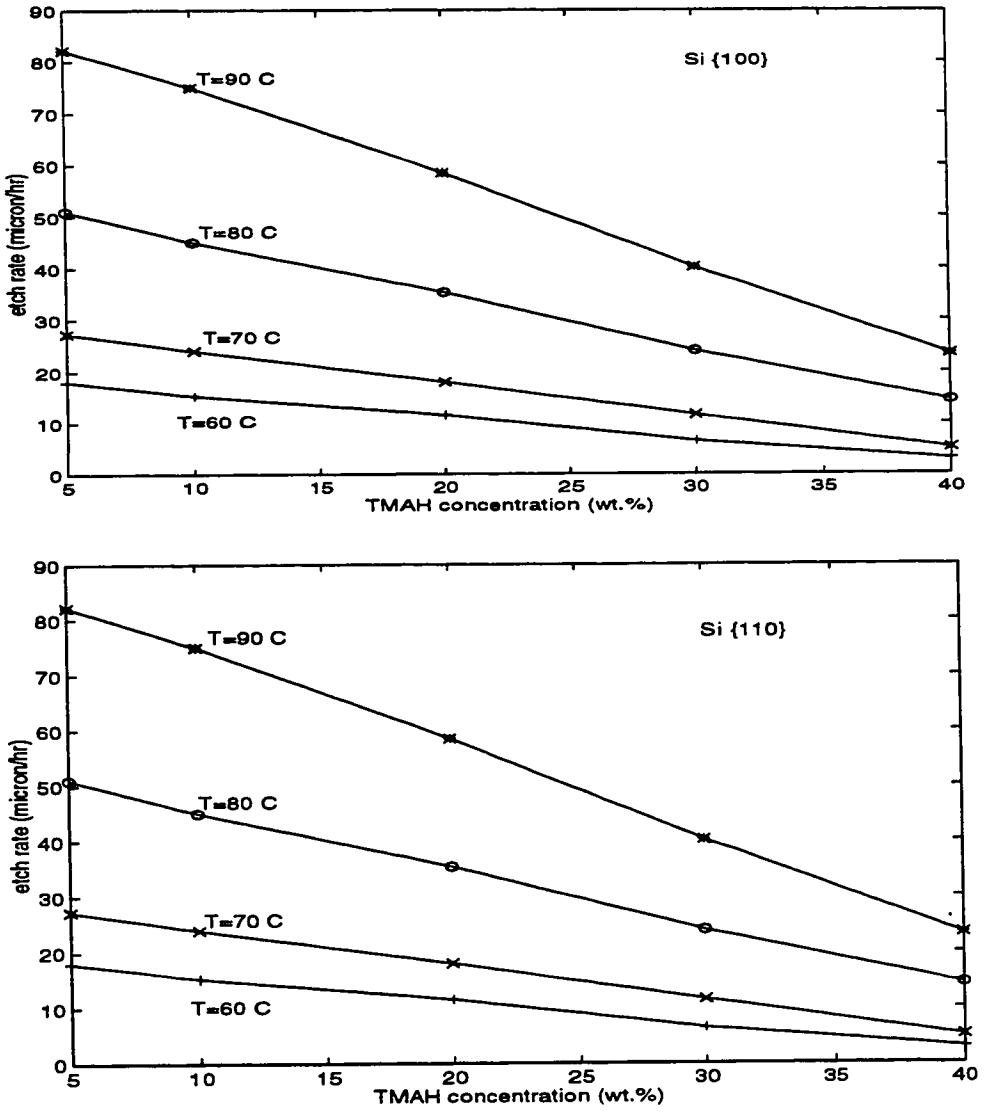

Fig. 2.18: Etch rate of {100} and {110} in TMAH for some different temperatures vs. TMAH concentration (from ref. [56]).

affecting the quality of surface [58].

In a report about TEAH [54] some data about the etch rate of silicon in TEAHW was submitted which is shown in Fig.2.20 [54]. The quality of the etched {100}surfaces is a function of the concentration of TEAH in the solution, for concentrations above 30 wt.% a very smooth surface is obtained and for lower concentrations the surface is covered by pyramidally or conically shaped hillocks. Thermally grown oxide and Si_3N_4 can be used

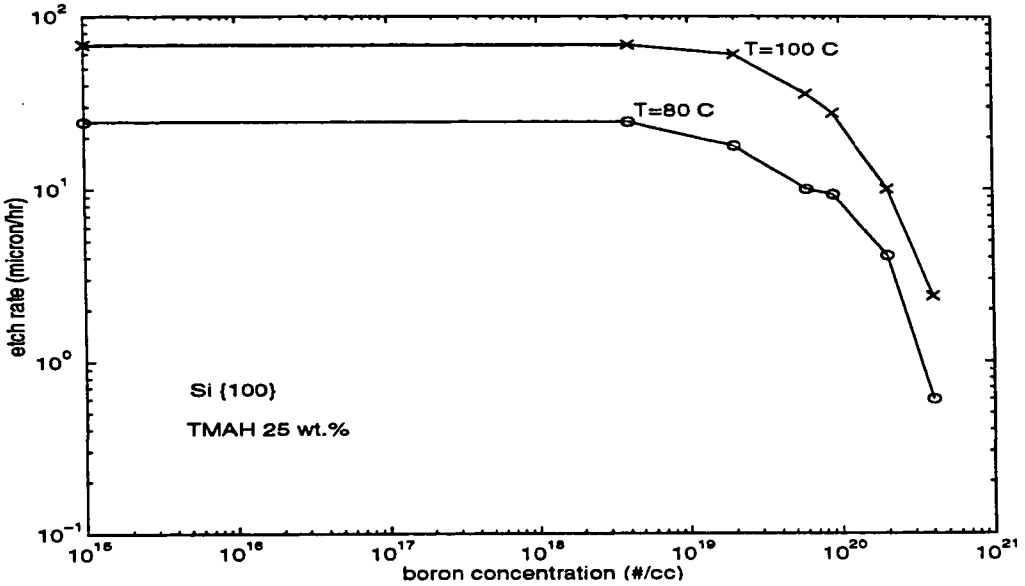

Fig. 2.19: Si {100} etch rate in TMAH 25 wt.% vs. boron concentration (from ref. [57]).

as excellent masks for etching. The etch rates of Si_3N_4 and SiO_2 have been measured to be zero and 4 Å/min. respectively, at solution temperature of 90^0 C and concentration of 40 wt.% TEAH. Since there is no alkaline metal ion in this solution it can be used in CMOS fabrication process.

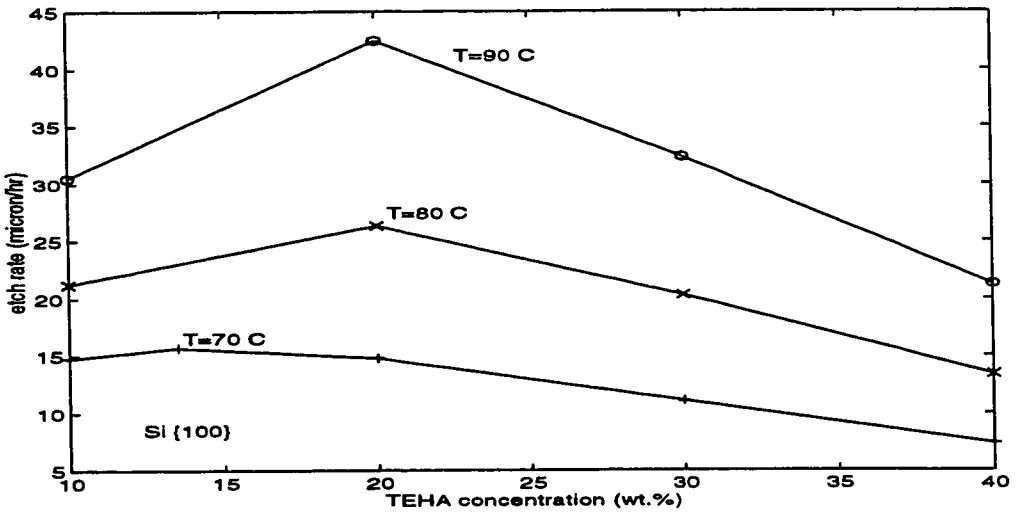

Fig. 2.20: Si {100} etch rate in TEAH solution vs. concentration for some different temperatures (from ref. [54]).

2.4 $HF:HNO_3$-Based Isotropic Etchants

These etchants have been being used for a long time. In 1959 a comprehensive study of $HF:HNO_3:H_2O$ and of $HF:HNO_3:CH_3COOH$ was reported [59,60]. The general mechanism of both of them are very similar, where hydrofluoric acid and nitric acid are the critical reactants of these two etchants which the water and acetic acid are used for the purpose of dilution [60]. The mechanism is simply as follows: the nitric acid oxidizes the silicon surface to a thin layer of oxide and this oxide is stripped off by the hydrofluoric acid. It should be noted that the etch rate of silicon in this system in contrast with anisotropic systems is much greater (about one order of magnitude). The different types of mask which are used for this system are thick thermal oxide [1,21], photoresist [21] and chrome-gold [1,20]. This etching system can be used for thinning of a silicon wafer. By bubbling gases like CO_2, CO and NO for agitation, a very uniform and blemish-free surface will be obtained [61].

CHAPTER 3

Measurement of Silicon Etch Rate in TMAH

This Chapter begins by explaining in detail the TMAH etching apparatus used in this research. Then the procedure for doing etch experiments in TMAH solution, and the mask used for basic etch rate determination are described. Then, the basic etch rate results are presented for etching of Si {100} and Si {110} in TMAH of different concentrations and temperatures, and compared with results from other researchers. Finally, the etch rate of various common passivation layers (and also of less common films) are studied.

3.1 TMAH Etching Station

The etching experiments explained in this thesis all have been done in the etching apparatus schematically shown in Fig.3.1:

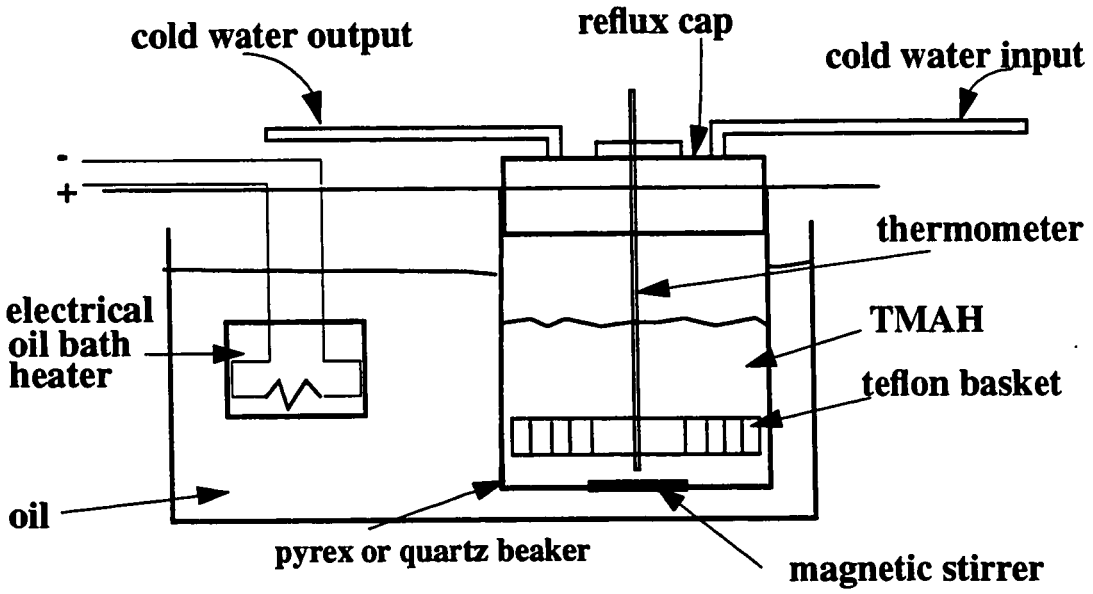

Fig. 3.1: TMAH etching apparatus.

The containers used for etching were quartz or pyrex. A reflux cap was used to condense the vapor of the etch solution in order to keep the concentration constant. The reflux cap is connected to running water with two hoses and cold running water is passing through it during all the etching time. The vapor of TMAH after contacting the cap is liquidized and drips back to the etchant solution in the beaker. The entire etching apparatus is kept in a fumehood to vent the vapors of the oil and TMAH. It has been observed that this reflux cap works well for the purpose of isolating the etch solution from air, because the TMAH which was kept in the beaker for 3 weeks had the same silicon etch rate as fresh TMAH (if TMAH is in contact with oxygen its characteristics change, as will be explained later). Usually the TMAH could be used for many numbers of experiments unless it got contaminated, or the silicon doping of the solution had become too high.

The TMAH used in all the experiments was bought from the same source [17]. The initial concentration of the TMAH is 25 wt.% in water, lower concentrations were obtained when necessary by diluting with the appropriate amounts of deionized water. No other additives were used in the experiments. A teflon basket was used to hold the silicon samples for etching in the etch solution. For handling the samples either steel or teflon tweezers were used. In some experiments in which stirring of the solution was required a teflon-covered magnetic stirrer was used. Speed of rotation was 120-240 rpm.

The temperature of the solution was measured using a mercury thermometer with an accuracy of $\pm$ 0.5^{o} C. The whole beaker was heated by oil bath, instead of hot plate, to have a better temperature uniformity of the etchant. The temperature of the etch solution is not controlled directly. The temperature of the oil used in the oil bath can be set to a desired level and it was observed that the temperature of the solution is always a few degrees lower than that of the oil. The higher the temperature of the oil, the bigger the difference between the temperature of the oil and etch solution. Therefore this point should

be always considered. For example, whenever a temperature of 80° C for the etch is desired the temperature of the oil should be set at about 87° C, and when the temperature of the etch is desired to be at 50° C the oil temperature should be set at about 52° C. The relation between oil and TMAH temperature, which has been measured during the experiments, is shown in Fig.3.2.

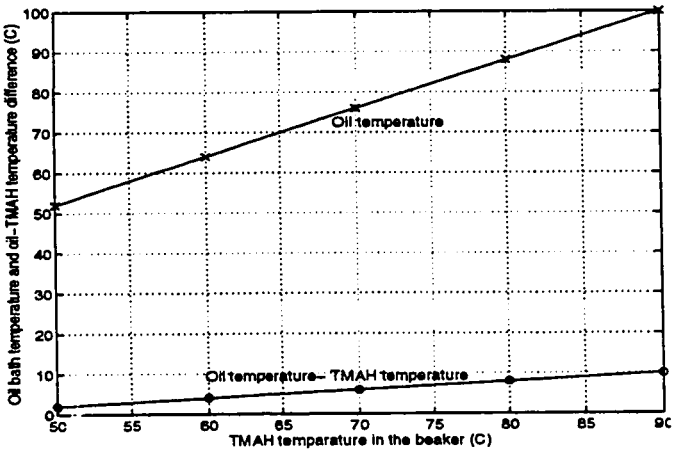

Fig. 3.2: Relation between oil bath temperature and TMAH solution temperature

3.2 Experiments for Etch Rate Determination

The samples were cut from wafers with low doping concentration with a resistivity in the range of 2-70 Ωcm n-type, single sided polished. All samples were cleaned using the RCA cleaning procedure [Appendix A] before any etch process.

As was mentioned in chapter 2, thermal oxide and silicon nitride are excellent masks for TMAH. In most of the experiments carried out thermal oxide was used as mask. The oxide was grown using wet oxidation at 1100° C for a sufficient length of time to grow thick enough to be used as a mask. The oxidation time was usually 2 hours. Common lithography procedures were used for generating the desired patterns on the polished side of the samples. The samples used in the experiments were single sided polished. In all

cases the oxide on the back of the sample was left to protect the back side of the samples from etching. All of the masks used in the lithography were made in the microelectronics lab using in-house facilities. Mask design was done in the Concordia Faculty of Engineering and Computer Science VLSI Lab using CADENCE or VALID software packages.

3.2.1 Etch Rate Measurements

The mask used for the measurement of the etch rate does not need to have a specific form. The only condition is that the open area of silicon exposed to TMAH should be large enough so that etch-stop planes are not reached too early. Here the mask used is an array of squares with different sizes where all of the squares are aligned together. This mask is shown in the Fig.3.3. Size of the edges of the biggest squares is 2 mm and that of the smallest is 50 μm.

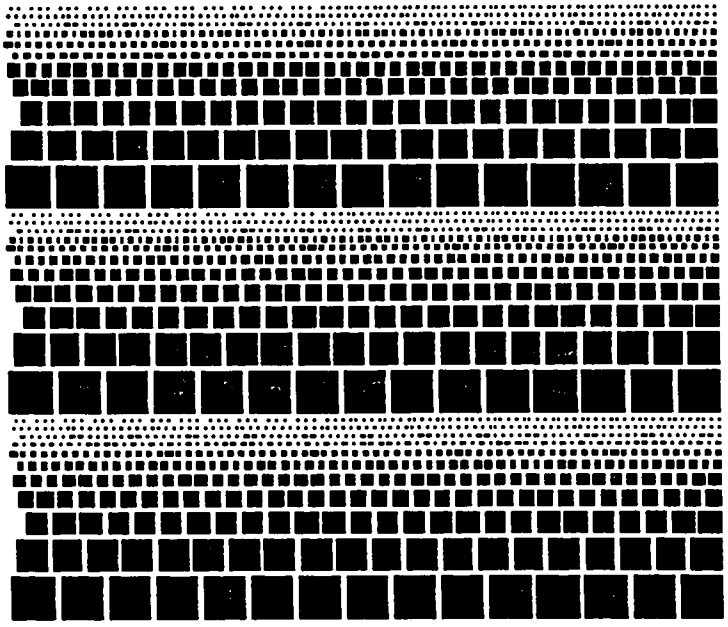

Fig. 3.3: Square array used as mask for etch rate measurement. The pattern is called squares.

Before etching, the samples were immersed in diluted HF(1:10) for 10 -30 seconds to

remove native oxide, but it seems that this step is not very critical. In both cases of samples with and without immersing in the diluted HF it was observed that the gas evolution from surface of the samples, which is an indication of the etching reaction, starts at the same time (approximately 30 to 90 seconds after immersing the samples in the etch solution). Also in the results of the measurement of both cases no difference was observed in the etch rate. The samples used in the experiments were {100} and {110}. The specific concentrations of TMAH used were 25, 15 and 5 wt.%. In each experiment 2 samples of each orientation were used and each experiment was repeated twice. The temperatures under test for most of the experiments were 50, 60, 70, 80 or 90 ^{o}C. Etching was done for different lengths of time. For higher temperatures, etching was done for shorter lengths of time. After etching, all of the samples were rinsed with DI water for 10 to 20 seconds, dried with blow of nitrogen and examined through an optical microscope. Measurement of depth was also done by optical microscope, with an accuracy of ± 1 μm. The surfaces of etched area of {100} samples were usually very clean and smooth and etch depth was very uniform. In this respect, TMAH acts like KOH and EDP [45]. The surface of the oxide area was also very smooth. When the surface of the larger squares are looked with the naked eye they have a mirror like appearance, same as an un-etched, polished surface. However, when they are checked through the microscope the surface shows a very slight waviness, which in some papers it has been described as an "orange peel" surface [55].

In the case of etching {110} surface, same as observed in other etchants [45], the etched surface is quite rough and its roughness can be even seen with the naked eye. The depth of etch is also nonuniform. This non-uniformity sometimes reaches 12 μm for an etch depth of 100 μm for all temperatures of etching (The discrepancy in the result of this work and the results obtained by Tabata *et al.* [56] in the case of Si {110} etched in TMAH 15 wt.% (Fig.3.7) is probably due to this reason.)

TABLE 3.1: Etch rate of silicon in different concentrations of TMAH

Concentration of TMAH (wt.%)	surface orientation	Temperature	Etch rate (μm/hr), unstirred	Etch rate (μm/hr), stirred
25	(100)	50° C	4.45	4.16
25	(100)	60° C	7.9	8.17
25	(100)	70° C	14.8	14.56
25	(100)	80° C	23.2	24.63
25	(100)	89.2° C	41.85	43.2
25	(110)	50° C	9.35	10.94
25	(110)	60° C	18.3	20.07
25	(110)	70° C	30.45	32.7
25	(110)	80° C	56.56	55.35
25	(110)	89.2° C	83.5	83.8
15	(100)	50° C	6.6	6.6
15	(100)	80° C	35	35
15	(110)	50° C	4.7	4.7
15	(110)	80° C	57	57
5	(100)	80° C	39 (large squares), 13 (small squares)	47 (large squares) 35 (small squares)
5	(110)	80° C	48 (large squares), 21 (small square)	62 (large squares), 41 (small squares)

Table.3.1 shows the measurements results.

For the case of Si {111}, the etched area has a staircase appearance. The reason could be due to the deviation of {111} wafers from real <111> direction by about 3° which usually happens during manufacturing of these wafers [62]. Therefore to measure {111} etch rate, underetch rate of {111} walls were measured instead.The surfaces of the {111} walls which emerge in both {100} samples and {110} samples are all very smooth and have a

TABLE 3.2: Surface condition as a function of experimental conditions

TMAH Concentration (wt.%)	Si Surface Orientation	T (^{o}C)	State of Agitation	Surface Quality
25	{100}	50-90	stirred & unstirred	smooth, uniform etch depth
25	{110}	50-90	stirred & unstirred	very rough, textured appearance
15	{100}	50, 80	stirred & unstirred	uniform etch depth, many hillocks
15	{110}	50, 80	stirred & unstirred	very rough, textured appearance
5	{100}	80	stirred & unstirred	very rough, nonuniform etch depth
5	{110}	80	stirred & unstirred	very rough, textured appearance

mirror-like quality. Table.3.2 shows the quality of etched surfaces for different conditions of etching. It was observed that stirring of the solution at all temperatures does not have any effect on the etch rate of the TMAH **at 15 and 25 wt.% concentration.** However, for the case of TMAH 5 wt.% stirring and also size of the etch window, as shown in Table.3.1, have effect on the etch rate. The Arrhenius curves for {110} and {100} direction for 15 wt.% and 25 wt.% concentration of TMAH are shown in Fig.3.4 to Fig.3.7. In these figures the results of some other researchers are included for comparison. Arrhenius' formula:

$$R = R_0 e^{\frac{-E_a}{kT}} \qquad (3.1)$$

where R is the reaction rate, R_0 is called frequency factor [63], E_a is activation energy (eV), k=8.62 $\times$ 10^{-5} (eV) is Boltzman constant and T is temperature in Kelvin, describes the relation between reaction rate and temperature. The units of the R and R_0 can be chosen as μm/hr. By using the curves the values of the parameters R_0 and E_a are calculated for {100} and {110} surfaces which are shown in the Table.3.3 and Table.3.4. The etch rates

for squares of different sizes are all same. By considering the facts that state of stirring of the solution and the size of the open area does not have any effect on the etch rate it is known that the process of etching silicon in TMAH 15 wt.% and 25 wt.% is a reaction limited, and not a diffusion limited process.

Bare wafers have also been etched in TMAH 25 wt.%. For this experiment first the samples were thermally oxidized and the oxide from polished side was removed and then the sample were etched in TMAH. The etched surface, except a small number of scars on it, looks like the surface before etching, shiny and mirror-like. The etch rate is also same as the etch rate of the open windows in the oxide mask.

TABLE 3.3: Activation energy for the etching of silicon in TMAH.

Si Surface Orientation	TMAH Concentration, (wt.%)	E_a (eV) (This work)	E_a (eV) (Tabata *et al.*)[56]	E_a (eV) (Merlos *et al.*) [58]
{100}	25	0.5717	0.5613	0.6285
{110}	25	0.5637	0.4238	-
{100}	15	0.5466	0.5598	0.419

TABLE 3.4: Frequency factor for the etching of silicon in TMAH.

Si Surface Orientation	TMAH Concentration, (wt.%)	Frequency factor (μm/hr) (This work)	Frequency factor (μm/hr) (Tabata *et al.*) [56]	Frequency factor (μm/hr) (Merlos *et al.*) [58]
{100}	25	3.6054×10^9	3.0112×10^9	2.0461×10^{10}
{110}	25	5.9437×10^9	5.8568×10^7	-
{100}	15	2.2119×10^9	3.7884×10^9	2.1364×10^8
{110}	15	2.6578×10^{13}	6.1141×10^7	-

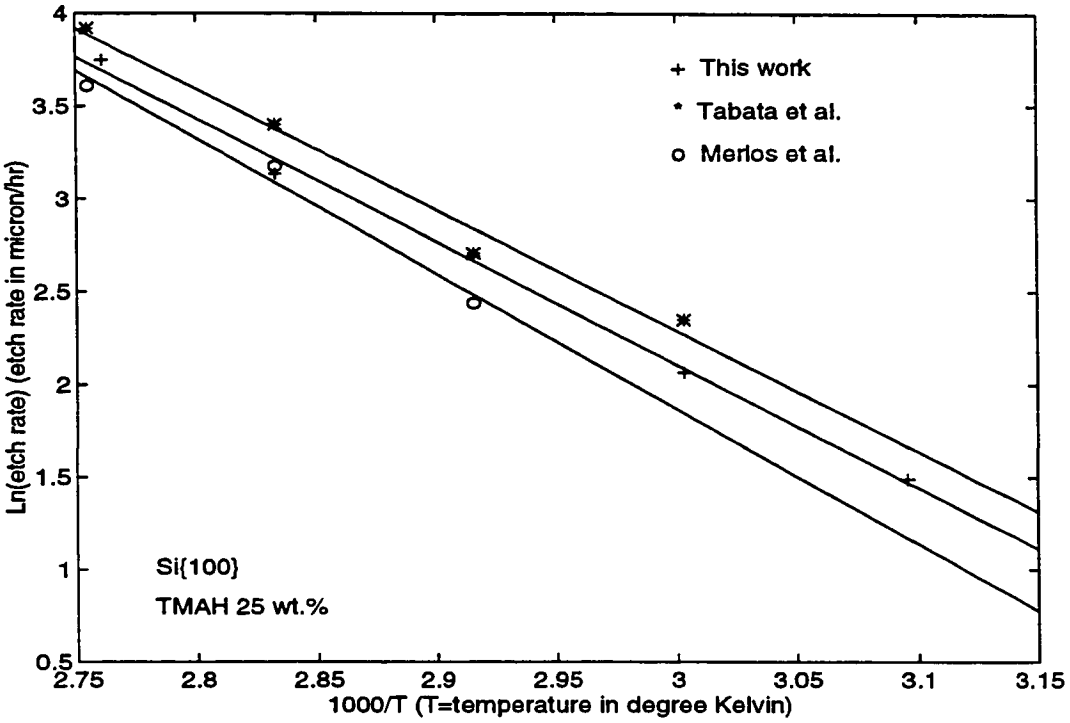

Fig. 3.4: Arrhenius curve for TMAH 25 wt.%, {100} surface.

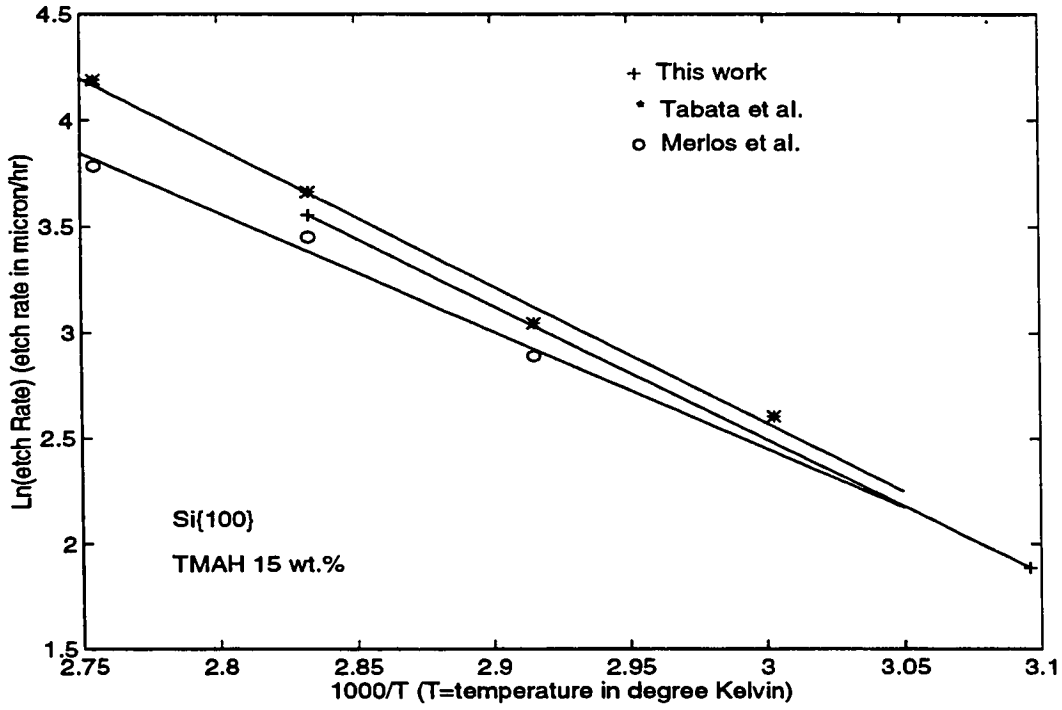

Fig. 3.5: Arrhenius curve for TMAH 15 wt.%, {100} surface.

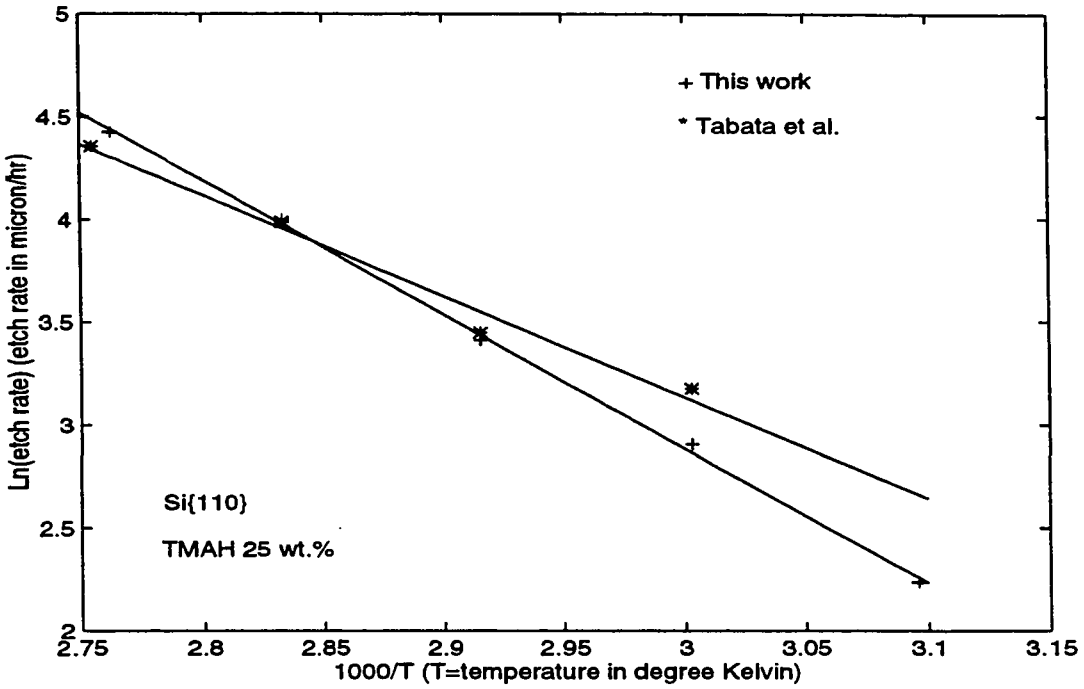

Fig. 3.6: Arrhenius curve for TMAH 25 wt.%, {110} surface.

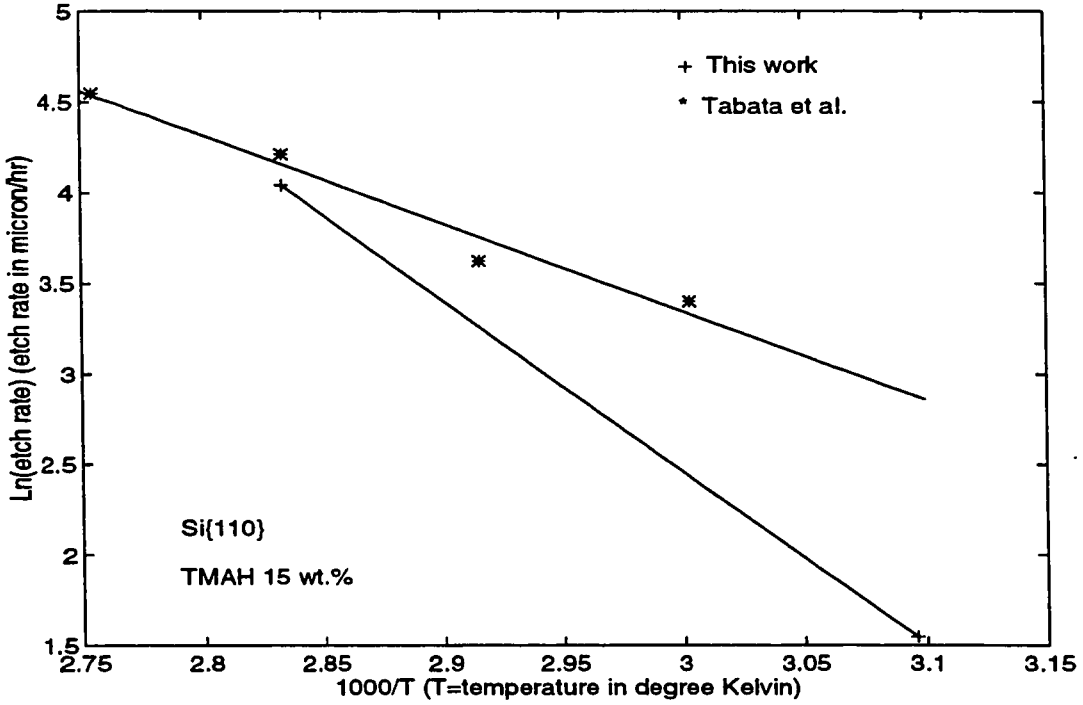

Fig. 3.7: Arrhenius curve for TMAH 15 wt.%, {110} surface.

3.3 Etch Rate of Various Films and Passivation Layers in TMAH.

As it was explained in chapter 2 among common passivation layers used for different etchants, silicon oxide and silicon nitride are very good passivation layers used in micro-machining. This section will present experimental results to supplement those available in the literature.

3.3.1 Experiments and Results

The results of measurements are shown in the Table.3.5. The thicknesses were measured by ellipsometer (where applicable), the etch rates were found to be approximately constant through the etch, and the average etch rates are presented in Table.3.5.

Silicon nitride-For measurement of etch rate of Si_3N_4 in TMAH, some samples which were cut from a wafers covered with silicon nitride were used[1]. Two types of nitride, LPCVD and PECVD were examined. The TMAH used was 25 wt.% and etch temperature was 80° C. Samples were etched for long time, about 15 hours (the etching time should be such a long time because silicon nitride etch rate is very low and in order to be able to measure its etch rate long time of etching is required.). The thickness of the nitride layer was measured before and after etching using an ellipsometer, and by measuring the etch time its etch rate was measured.

Thermally grown silicon dioxide-For measurement of the thermal oxide etch rate in TMAH, some silicon samples were RCA cleaned and thermally oxidized in wet oxygen at 1100° C for 65 minutes. A grid mask as shown in Fig.3.8 was used to confine the measured surface to a small area to avoid the non-uniformity of the oxide thickness usually happens on a large sample oxidized in wet oxidation.

1. The wafer used in this experiment were received from Mitel.

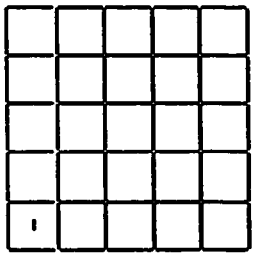

Fig. 3.8: Mask used for oxide and SOG etch rate measurement

The grid mask is consisting of squares with edges equal to 5 mm. This pattern on the surface of samples creates some opening on the oxide which exposes bare silicon to TMAH. After etching in TMAH, on the place of these openings, long cavities will be created. In this way the area confined to each small square will be recognized before and after etching and thickness of oxide in each square will have a much more uniform thickness, therefore the results of measurement will be much more reliable.

Spin-on glass- One of the materials which can be used in micromachining as a mask is spin on glass, (SOG). The motivation for using SOG as mask was to protect thin layer of deposited aluminium on the silicon surface. In our investigation the SOG was bought from Alliedsignal corporation [64]. The deposition of SOG was done as it is recommended in instruction sheet received from producer. The procedure is as following:

1) Droplets of SOG were applied on the sample surface when the sample was rotating with 3000 rpm. The spinning of the sample continued for 30 seconds.

2) After spinning the sample was soft-baked, in the dry air flow at 150^{o} C for 1 minute.

3) Then the sample was hard-baked for 1 hour at 420^{o} C within a nitrogen ambient.

According to the producer data sheet, following these steps gives a thickness of about 700 Å of SOG. In the course of experiments it was realized that only one layer of SOG is not enough to protect the silicon surface for long time of etching. Therefore SOG deposi-

tion was done 4 times, one on top of the previous one on the same sample. For deposition of SOG, Minisart filter was used to reduce the number of floating particle in the SOG. Same as in the case of thermally grown oxide, a grid like pattern was created on the SOG covered samples because the thickness of SOG on the surface of the samples is not uniform. For creating the pattern on SOG covered samples common lithography method and buffered HF (HF:NH_4F-1:4) were used which etches SOG the same way as it etches thermal oxide. As was done with thermal oxide, the thickness of SOG layer was measured before and after TMAH etch using ellipsometer and its etch rate was measured by knowing the etch time. It was observed that SOG can be used as good etching mask in TMAH for masking bare silicon surface from etchant. The etch rate of SOG is comparable with LTO etch rate. The results of different measurements are shown in Table.3.5.

TABLE 3.5: Etch rate of different types of masking films

Passivation Layer	TMAH Concentration (wt.%)	T (^oC)	Etch Rate (Å/hr) (This work)	Etch Rate (Å/hr) (Tabata *et al.*)[56]	Etch Rate (Å/hr) (Merlos *et al.*)[58]
Thermal SiO_2	25	80	57	56	25
LPCVD Si_3N_4	25	80	7	very low~0	7
PECVD Si_3N_4	25	80	15	-	-
SOG	25	80	440	-	-

Although SOG deposited on top of the bare polished silicon wafers shows good behavior as a mask for TMAH etching, in using SOG as a protector for metal pattern on silicon wafer some problems were observed. During the attempt of spin SOG on the surface of a sample of silicon covered by a thin film of aluminum, many cracks appear on the SOG film during the soft-bake step. The reason is most probably due to the large differ-

ence in the thermal expansion coefficients of SOG film and aluminum film on the wafer. An attempt was made for solving this problem, by spinning a second layer of SOG on top of the first layer (with many cracks on it) with the idea that new layer of SOG might cover the first layer and fill the cracks and gaps in it. However, this also did not work and in fact showed a worsening effect in the number and the size of cracks after soft-baking of the second SOG layer. In another attempt, the sample was simply immersed in the SOG solution, removed and dried. As a result, a thicker layer of SOG on the top of the aluminum film was deposited. The result of etching on this sample was also failed and cracks were observed.

Although efforts to protect patterns of metal with narrow features (as opposed to wide film of metal on the whole surface of the sample) was not fully satisfactory, it showed a relative success. A pattern (consist of narrow features) of aluminum was generated on the surface of an oxidized sample. The aluminum pattern was repeated for both positive and negative masks. In the case of use of negative mask, the remover was phosphoric acid. Then SOG was deposited on the pattern. In order to protect the metal during long time TMAH etching (e.g. 4 hours), the SOG layer should be thick enough to stand the etching. Thus, SOG deposition was repeated for several layers. During the SOG deposition it was observed that in the area which the SOG layer is directly on the top of the thermal oxide the layer was intact and did not have any crack or defect. But in the areas which the aluminum features were sandwiched between thermal oxide and SOG, some cracks developed on the SOG after the hard-bake step. More cracks appeared after depositing a new layer on the top of the old one. Fig.3.9 shows an optical micrograph of aluminum film covered with three layers of SOG. The dark spots are the defects on the metal film and the very vague traces seen in the picture are the cracks appeared on the SOG films after annealing at 420^{o} C for 1 hour.

Another defect observed on SOG layer, was presence of pinholes on the surface of the layer after the etching process. When SOG layer deposited on a metal pattern was checked under the microscope, in the areas which pinholes exist, TMAH penetrates through the hole and attacks the metal film. Fig.3.10 shows the aluminum pattern (white areas) covered by three layers of SOG and baked at 420° C. The presence of irregular spots on the metal film shows the penetration of the TMAH through SOG layers during etching and damaging the metal.

It was found that the variation of hard-baking temperature (in the range of 370-420° C) has no or little effect on the quality of the SOG layers.

Fig. 3.9: Optical micrograph of aluminum covered with 3 layers of SOG after annealing at 420° C for 1 hour. The cracks emanates from the central defect (magnification = x 500).

Titanium nitride- This layer which is a conductor, is used in the fabrication of semiconductor devices and increases the adhesion of metal layers to the underneath surface. In the course of some experiments with silicon samples covered with a thin film of titanium nitride with chemical formula TiN, it was observed that it can be used as a good mask in

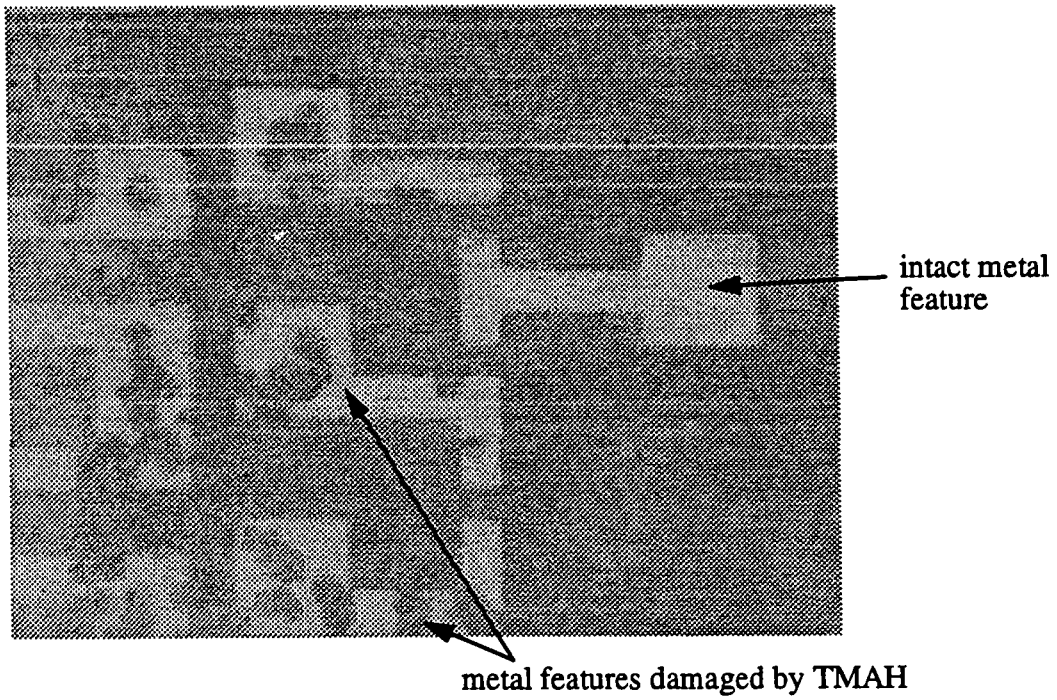

Fig. 3.10: Optical micrograph of aluminium covered by 3 layers of SOG (annealed for 1 hour at 420° C after deposition of each layer) and etched in TMAH 25 wt.% at 80° C for 1 hour. The circular region of Al are due to TMAH penetrating the SOG.

TMAH etching. Since this layer is not transparent its thickness cannot be measured with ellipsometer. So its etch rate could not be measured. An experiment was carried out on the samples covered with a thin layer of titanium nitride with thickness of 950 Å (determined by supplier, Mitel) to see how this layer resists in TMAH etching. Different steps of the experiment are as follows:

1) Some of the samples were immersed in diluted HF for 1-2 minutes. Other samples were not treated with HF.

2) All of the samples were immersed in TMAH 15 wt.% at temperature 80 ° C for 2 hours. And again all of them were immersed in TMAH 25 wt.% at 80° C for another 2 hours. The surfaces of all of the samples were checked through the optical microscope. They appear to be unchanged and they are as solid as they were before etching in TMAH.

Result of this experiment shows that titanium nitride stands in TMAH very well.

3.4 Effect of Oxygenation of TMAH

At the beginning of this Chapter it was mentioned that TMAH should be isolated from air. To investigate the effect of air exposure on TMAH, an experiment was carried out in which TMAH solution with 25 wt.% concentration was bubbled by a flow of oxygen for 3 hours at room temperature. The flow rate was 2 liter per minute and the TMAH was stirred during bubbling. This TMAH was used for an etch experiment at 80^{o} C using the "square" mask pattern and the etch rate was measured. It was observed that the etch rate had increased from about 24 μm/hr to 28 μm/hr.

3.5 Conclusion

The basic etch rate of Si {100} and Si{110} at temperatures 50^{o} and 80^{o} C and concentration of 25 wt.% and 15 wt.% TMAH were measured. Activation energies for these conditions of etching were calculated and were found to be in good agreement with other researchers results. Also, it was found that stirring of etchant during etching for TMAH concentration of 15 wt.% and 25 wt.% has no effect on etching of silicon for temperatures of 50-90^{o} C but at 5 wt.% at 80^{o} C of stirring of the etchant was observed to have a considerable effect.

Etch rate of thermally grown SiO_2, LPCVD and PECVD Si_3N_4 in TMAH 25 wt.% at 80^{o} C was measured. It was found that titanium nitride (TiN) in the form of a thin film is very resistant in TMAH. SOG was also tested as a masking film and its etch rate was measured or a particular condition of etching. More experiments are required to determine the suitable conditions of applying SOG as mask for thin metal film protection.

CHAPTER 4

Underetch Measurement in Si {100} and {110}

4.1 Introduction

In the fabrication of various structures on the surface of silicon using bulk micromachining, sometimes it is necessary to know the etch rate of undercut of mask edges having different angles of deviation from intersection of (001)-(100) on a {100} wafer. Also, in studying the fundamental mechanisms of anisotropic etching of crystalline silicon, by knowing the behavior of different orientations of silicon crystal in the anisotropic etchant, useful information can be extracted. In this chapter the experiments carried out for measurement of underetch rate of Si {100} at some different temperatures and concentrations of TMAH, are explained and some important observations are highlighted. Also, in one particular case of etchant composition and temperature, a simple model is offered to explain the different planes which emerge as a function of different angles of deviation.

4.2 Mask Design and Justification

For clarifying the geometry of underetch experiments, the following example can be helpful. If a square-shaped window is patterned on a {100} wafer such that the edges of the square are aligned with the <110> wafer flat, "deviation angle" of the edges of this square is considered to be 45^{o}. At this deviation = 45^{o}, the underetched surfaces which emerge after etching are {111} surfaces, which have the lowest etch rate and underetch rate. If this square window is rotated around its center by an angle of θ, (remaining in the plane of the {100} wafer surface), the planes which emerge underneath the edges of the square during an etch will not be {111} planes, but some other planes. In these cases the

deviation angle, called δ from now on, is defined as $\delta=45^{o}-\theta$.

For the purpose of studying the different emerging planes at different deviation angles, δ, a special mask was designed. During this work, in the experiments carried out for obtaining underetch rates, a group of right-angled triangles are used as windows for etching. In each triangle, the length of one of the edges of the right angle is kept at constant value of 850 μm and the angle opposite this edge varies from 45^{o} to 5^{o}, in steps of 1^{o}. In fact, this angle corresponds to θ mentioned above. All of these triangles are arranged beside each other in a way that the edges with the constant value of 850 μm are aligned together, and also aligned to the intersection of {111} planes with the surface of the wafer (the <110> wafer flat). By considering the symmetry of the crystallographic planes on a {100} wafer it can be seen that only a range of δ between 0^{o} and 45^{o} is enough for obtaining all information about underetch rate. However, by rotation of the group of the triangles to 90^{o}, 180^{o} and 270^{o}, useful redundancy is provided to enhance the reliability of the experiments. The mask designed in this way is shown in the Fig.4.1.

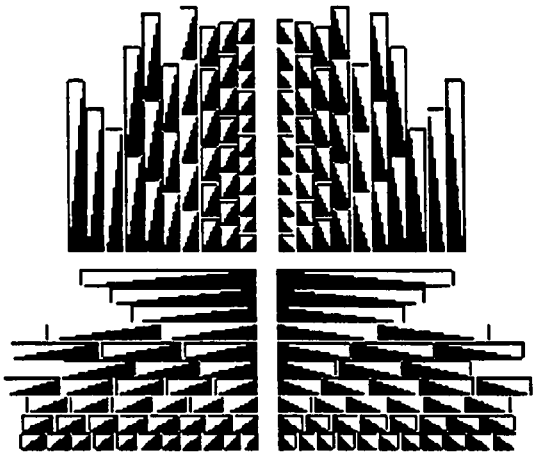

Fig. 4.1: Mask with triangle pattern used for underetch rate measurements. (In reality hypotenuse of the triangles are straight lines. The roughness in the edges is an artifact of the plotting program.)

Dark region in Fig.4.1 represents etched regin. Also, one point which should be remarked is that, as it can be verified easily, the range of deviation angle δ is from 0^o to 40^o, and not to 45^o. The reason is that for the values of δ very close to 45^o, the dimensions of the triangles would be too large. Because of this reason the deviation angles 41^o to 44^o were omitted. For measurements of the underetch at $\delta=45^o$, the underetch of the one of the other two edges of any of the triangles can be measured instead.

4.3 Experimental Procedure

Samples of Si {100} and Si {110} were oxidized using wet thermal oxidation at 1100^o C for 2 hours. Then, by using the mask shown in Fig.4.1, the samples were patterned such that one of the edges of the right angles was aligned with (a) the flat side of the wafers (on {100} wafers) and (b) with the intersection of a {111} plane and the wafer surface (on {110} wafers). Then the samples were etched in fresh TMAH solution (without silicon dissolved in it) unless otherwise indicated, at different concentrations and temperatures. After etching, the samples were rinsed with DI water and carefully dried by blowing nitrogen very gently, so as to keep the overhanging oxide intact and unbroken.

Measurement of underetch rate was done by measuring the width of this overhanging oxide using an optical microscope as is schematically illustrated in Fig.4.2. Also, for investigating the orientation and quality of emerging planes underneath the deviated edge of the triangles, on some samples the oxide was stripped off using HF solution, and SEM pictures were taken. Some of the photographs are shown in the next sections.

In Fig.4.2 the schematic of a typical triangle with underetching is shown. For measuring the angles of the slope of the emerging planes the following method was used. First, the scaning electronic microscope was focused on the emerging plane by looking at the surface of the sample from a right angle from top. Then the microscope chuck on

which the sample was placed was tilted gradually so that the sloped planes appear like a line. At this position, the angle by which the chuck is tilted is equal to the angle which the emerging plane makes with the vertical direction. In this way, by some calculation and by knowing the angle of the edge of the triangle, it is possible to find the Miller indices of the emerging plane (see Chapter 5). In the following sections, 4.3.1-4.3.5, several different cases of etching are discussed.

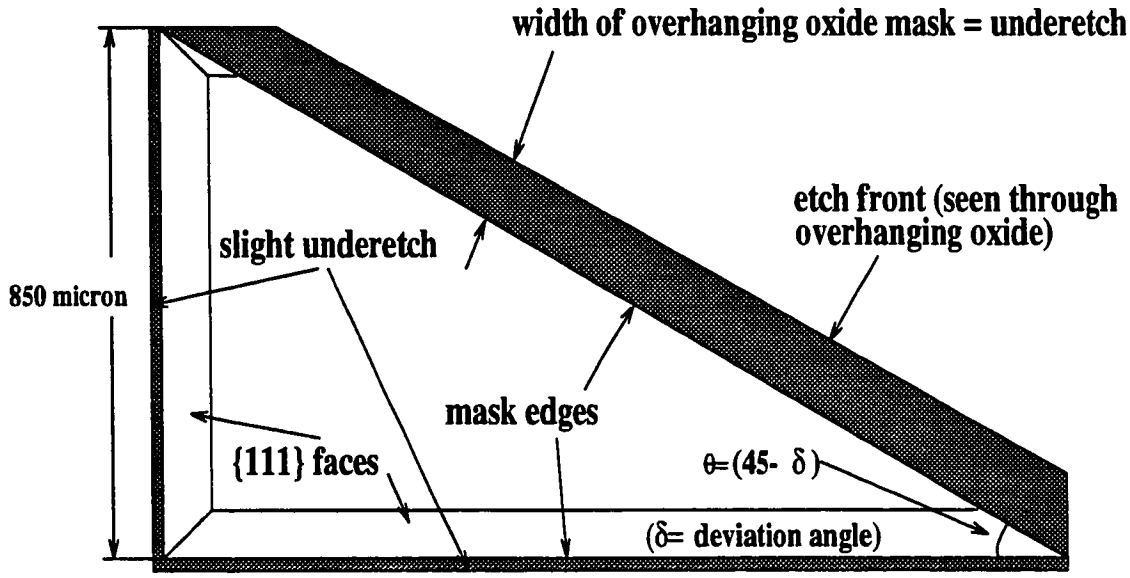

Fig. 4.2: Demonstration of measurement of the underetch rate in a sample triangle.

4.3.1 Emerging Planes in Si {100} Etched in TMAH 25 wt.% at 80° C and 50° C.

Since the type and the quality of emerging planes in these two cases (50° C and 80° C) were very similar, they are discussed in one section. Considering "first" triangle in Fig.4.1 (for example see the center bottom of Fig.4.1) the hypotenuse of this triangle has a 0° deviation, that is ($\delta=0^{o}$). Moving from triangle to triangle in the pattern, δ increases and finally reaches 40°. The emerging inclined surface in the first triangle, is shown in Fig.4.3.

It consists of two different planes, one a vertical {100} plane with a very smooth surface, and the other, a sloped plane with a rough surface (appearing at the intersection with the bottom of the etched pit).

As δ increases from 0^o to higher values, the top part of the emerged surfaces becomes rougher, which might be compared to a staircase shape. This staircase shape surface consists of {100} sections plus some rougher sections which connect each of the {100} sections together. This is shown in Fig.4.4. At the same time the bottom sloped part of the emerged plane, becomes smaller. This trend continues until the staircase part becomes the dominant part of the emerged surface and simultaneously this staircase-like surface becomes a sloped and rather smooth surface, as shown in Fig.4.6. At deviation angles δ very close to 45^o, this sloped smooth surface, changes to another staircase shape as is shown in Fig.4.7. At $\delta=45^o$, the emerged surfaces are {111} surfaces. In all experiments done in this work for all conditions of temperature and concentration of TMAH, {111} planes have been very smooth and had a mirror-like quality.

The etch rate, underetch rate and slope of the emerging planes vs. deviation angle, for these two cases are shown in Fig.4.8 and Fig.4.9. The shape of the underetch curve in the case of 50^o C is same as that of 80^o C the overall magnitudes of the underetch rates are about 5 times lower. The variation of the slope of the emerged planes with δ looks similar in both cases.

In the top curve of Fig.4.8 the emerging planes at $\delta=0^o$, 22^o and 45^o have also been specified. As is shown, the fastest underetching plane, which is at $\delta=22^o$, has Miller indices between {253} and {252} families. The method used for determining the Miller indices will be explained in the next chapter.

An important result which can be extracted from the underetch curve shown in Fig.4.8 and Fig.4.10 is that {100} surfaces have a relative minimum underetch rate, when

etching in TMAH 25 wt.%. The effect of this strong local minimum in the underetch rate curve can be seen in the emerging planes of triangles with underetch rate higher than the underetch rate at $\delta=0^{o}$. This occurs at $\delta=1$ to 35^{o}, according to Fig.4.8. Fig.4.4 shows an example of an underetched surface at $\delta = 11^{o}$. The masking oxide has been removed for this micrograph. The opening in the mask was clearly triangular both before and after the TMAH etch. The underetched surface at the side of the etched pit corresponding to the original hypotenuse is now made of several facets. In particular at the more acute-angled end of the triangle, a {100} vertical wall emerges. Fig.4.5 diagrams the evolution of the etched surfaces in TMAH 25 wt.% at 80^{o} C in triangles having $\delta=1$-35^{o}.

Similar to Fig.4.8, in Fig.4.9 it can be seen that there is a local minimum in the underetch rate at $\delta=0^{o}$ corresponding to Si {100} plane and an absolute minimum at $\delta=45^{o}$ corresponding to the Si {111} plane. While fewer inclination angle measurements were taken, the slopes appear to be very similar to those in Fig.4.8. The fastest etching plane appears at almost the same angle of deviation $\delta=22^{o}$.

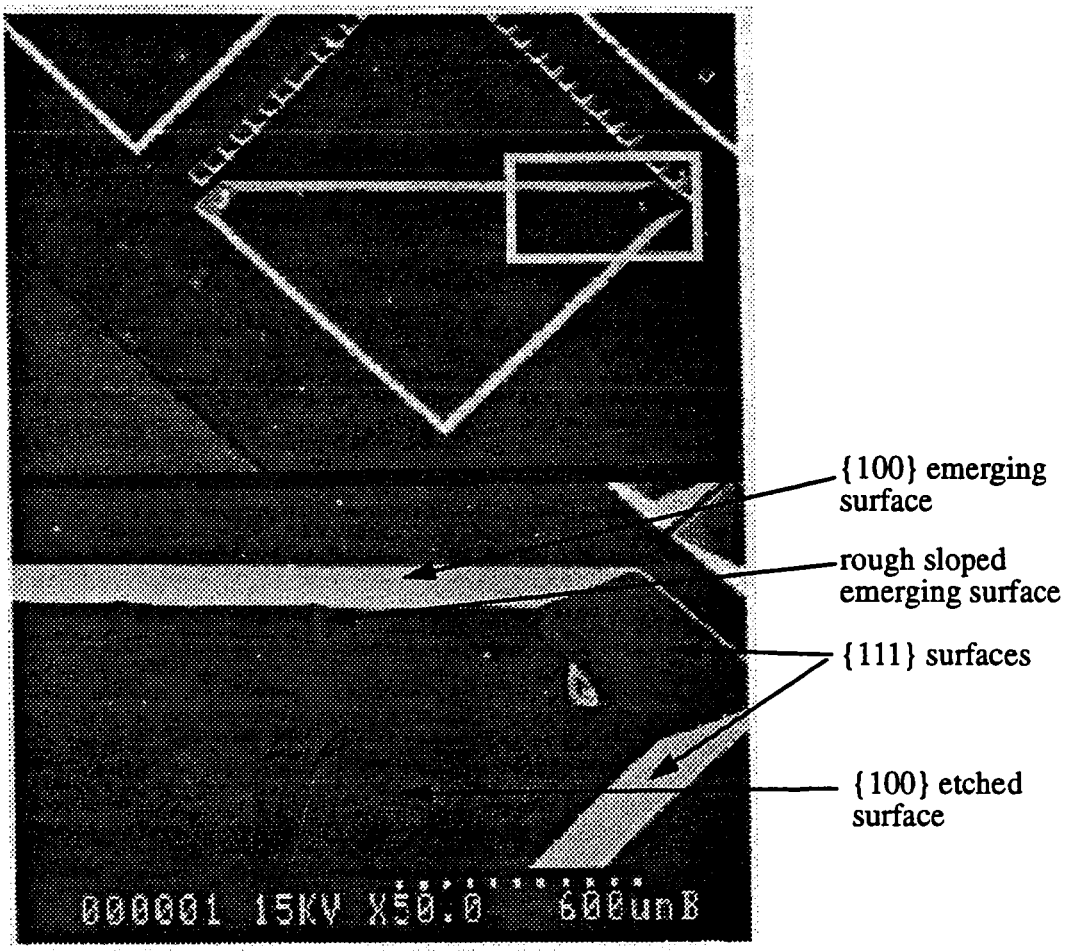

Fig. 4.3: SEM micrograph (viewed from a tilt of ~15-25^0 from vertical) of underetched surface at 0^0 deviation from the intersection of (100)-(001) in Si {100} sample, etched in TMAH 25 wt.% at 50^0 C for 14:15 hours. Note that the underetch surface is composed of a vertical {100} plane and a rougher plane adjacent to the base {100} etched plane.

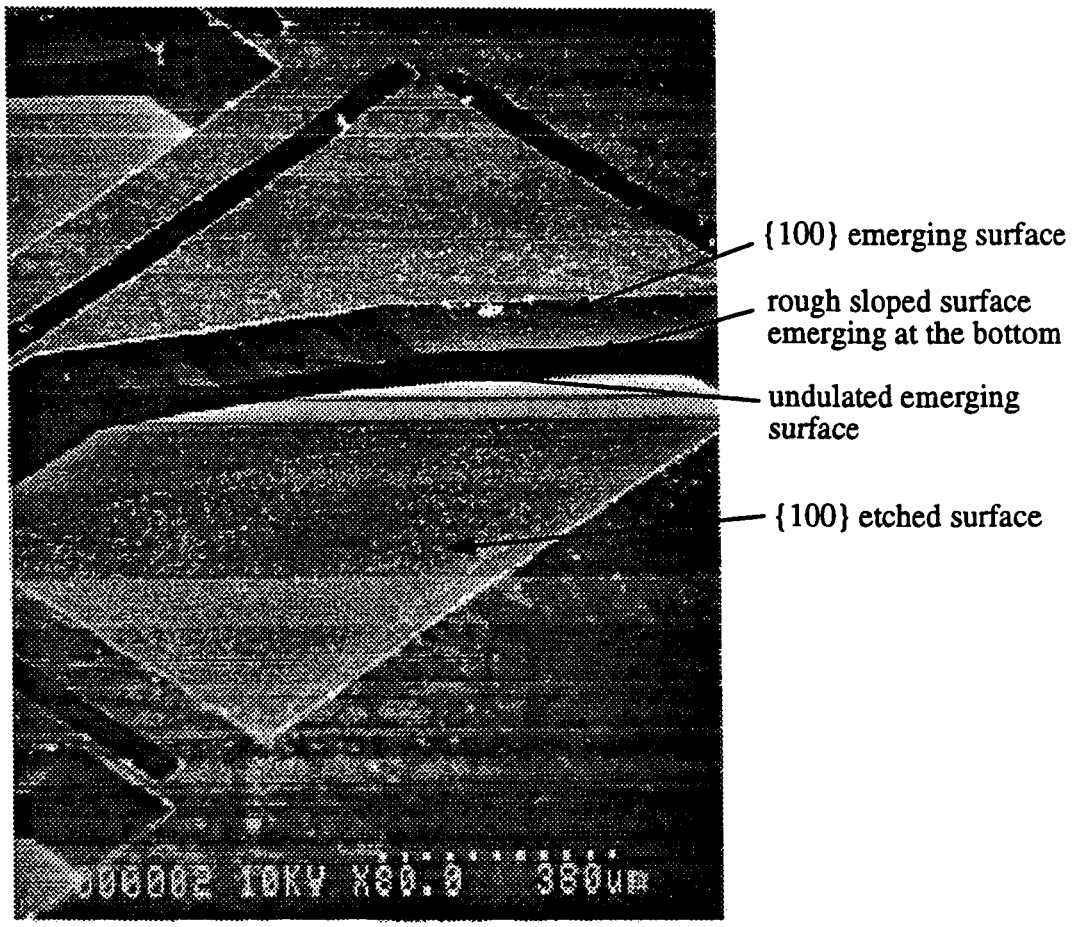

Fig. 4.4: SEM micrograph (viewed from a tilt of ~45-55° from vertical) of underetched surface at 11° deviation from the intersection of (100)-(001) in Si {100} sample, etched in TMAH 25 wt.% at 80° C for 5:15 hours. Note that the underetch surface is composed of a vertical {100} plane with some undulation at left and a rougher plane adjacent to the base {100} etched plane.

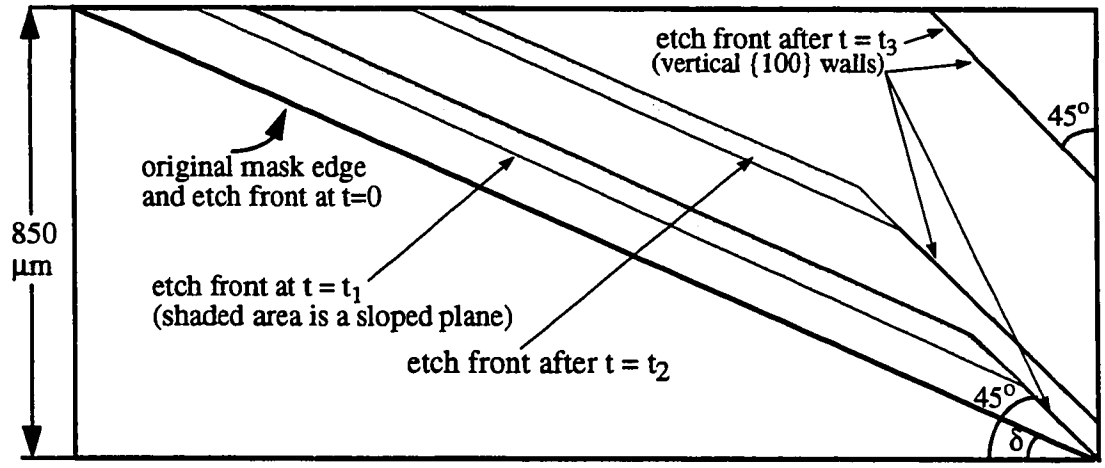

Fig. 4.5: Evolution of etch front (viewed from top) during etching in TMAH 25 wt.% at 80° C at four different times after the start of the etch ($t_1 < t_2 < t_3$). In this case $1^\circ \leq \delta \leq 35^\circ$.

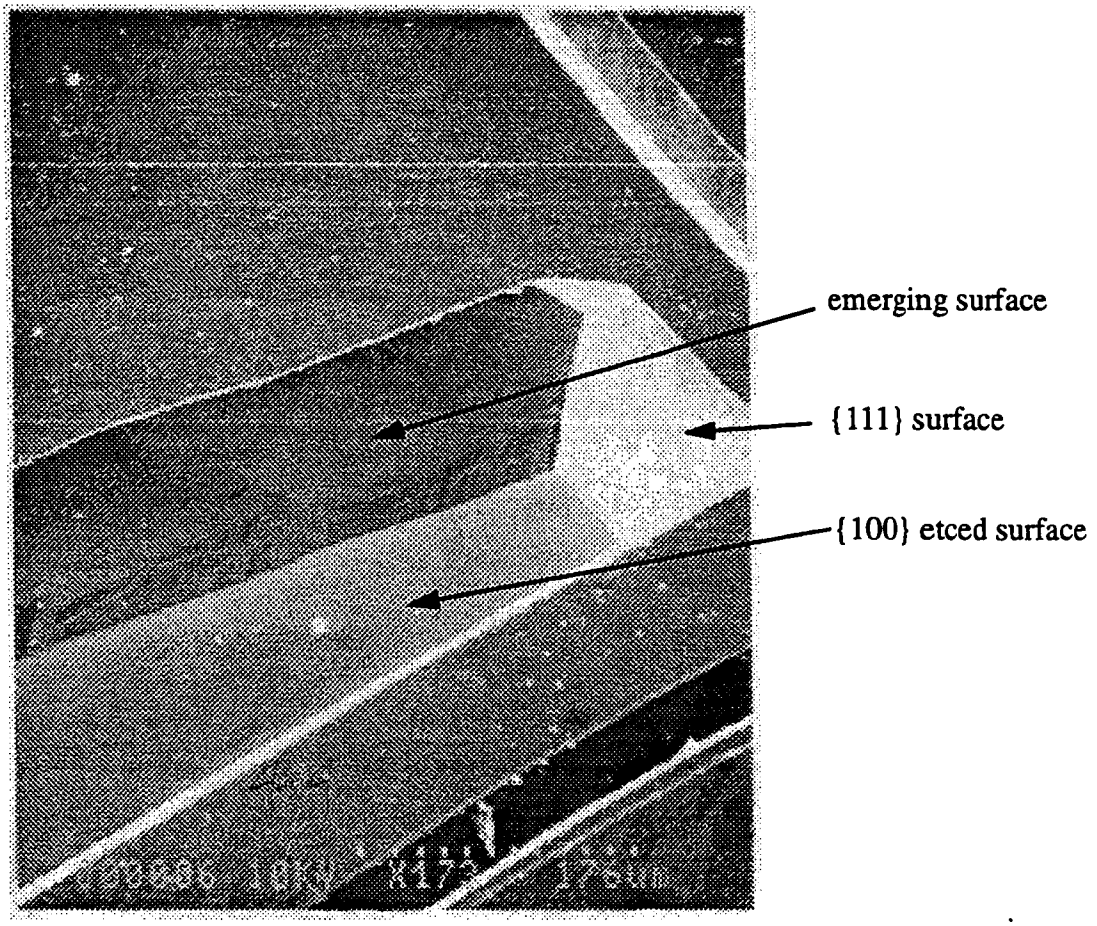

Fig. 4.6: SEM micrograph (viewed from a tilt of ~45-55° from vertical) of underetched surface at 33° deviation from the intersection of (100)-(001) in Si {100} sample, etched in TMAH 25 wt.% at 80° C for 5:15 hours. Note that the underetch surface is composed of a larger smoother plane and a rougher plane adjacent to the base {100} etched plane.

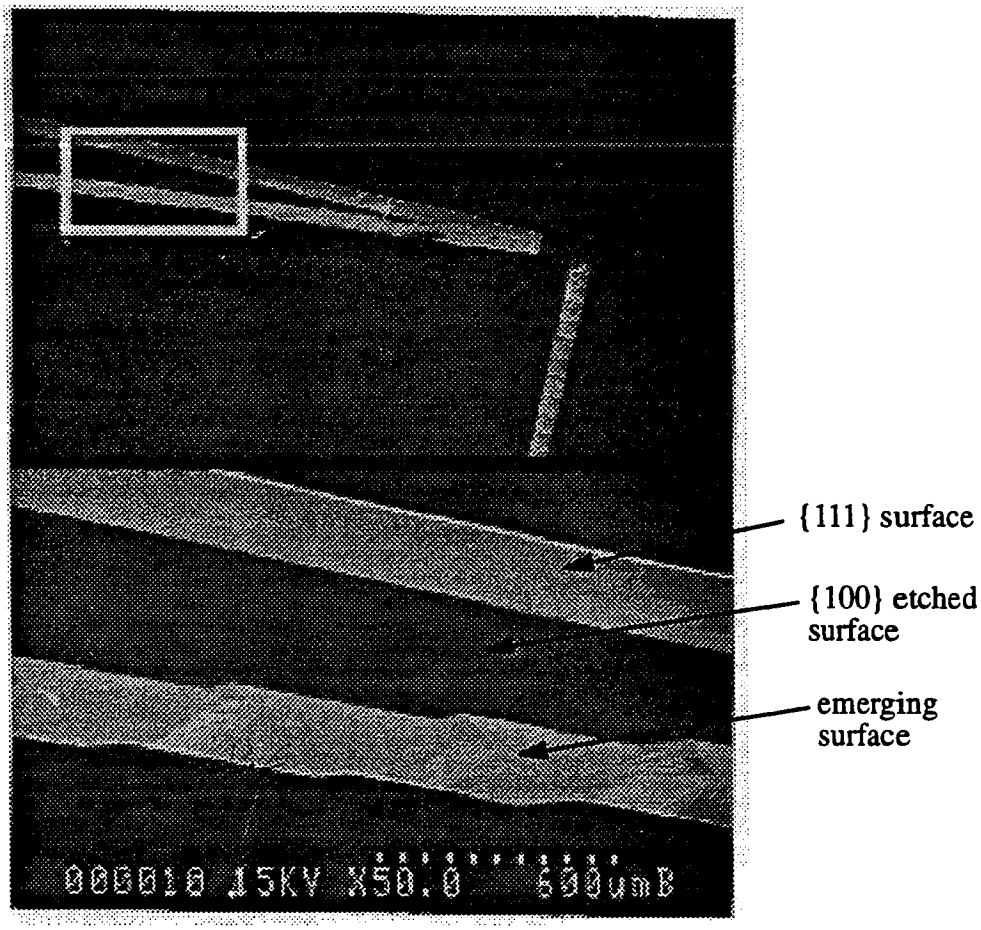

Fig. 4.7: SEM micrograph (viewed from top) of underetched surface at 40° deviation from the intersection of (100)-(001) in Si {100} sample, etched in TMAH 25 wt.% at 50° C for 14:15 hours. Note that the underetch surface is composed of a smooth plane and a rougher plane connecting each of the two adjacent smooth plane.

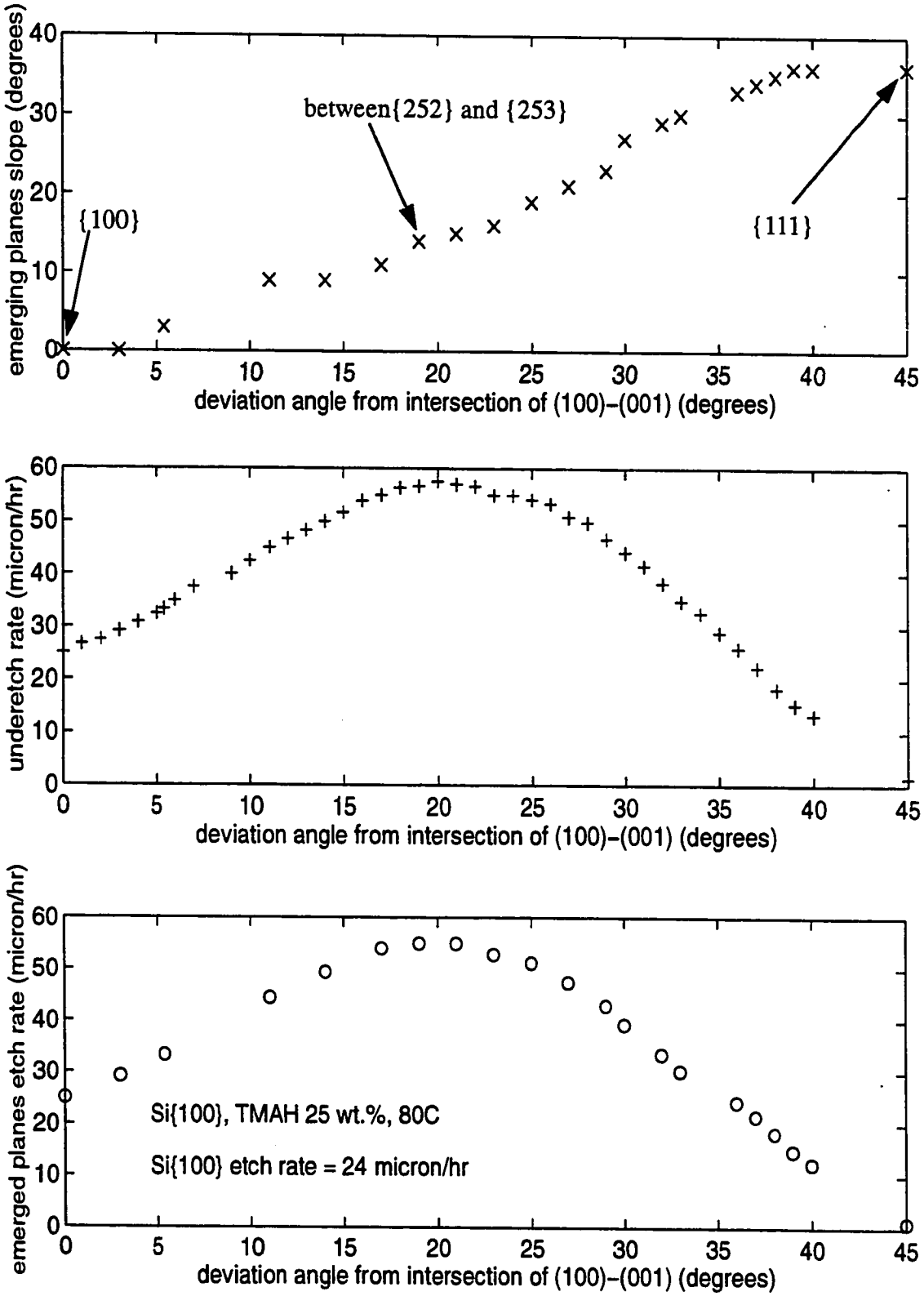

Fig. 4.8: Slope, underetch rate and etch rate of emerged planes in Si {100} etched in TMAH 25 wt.% at 80° C.

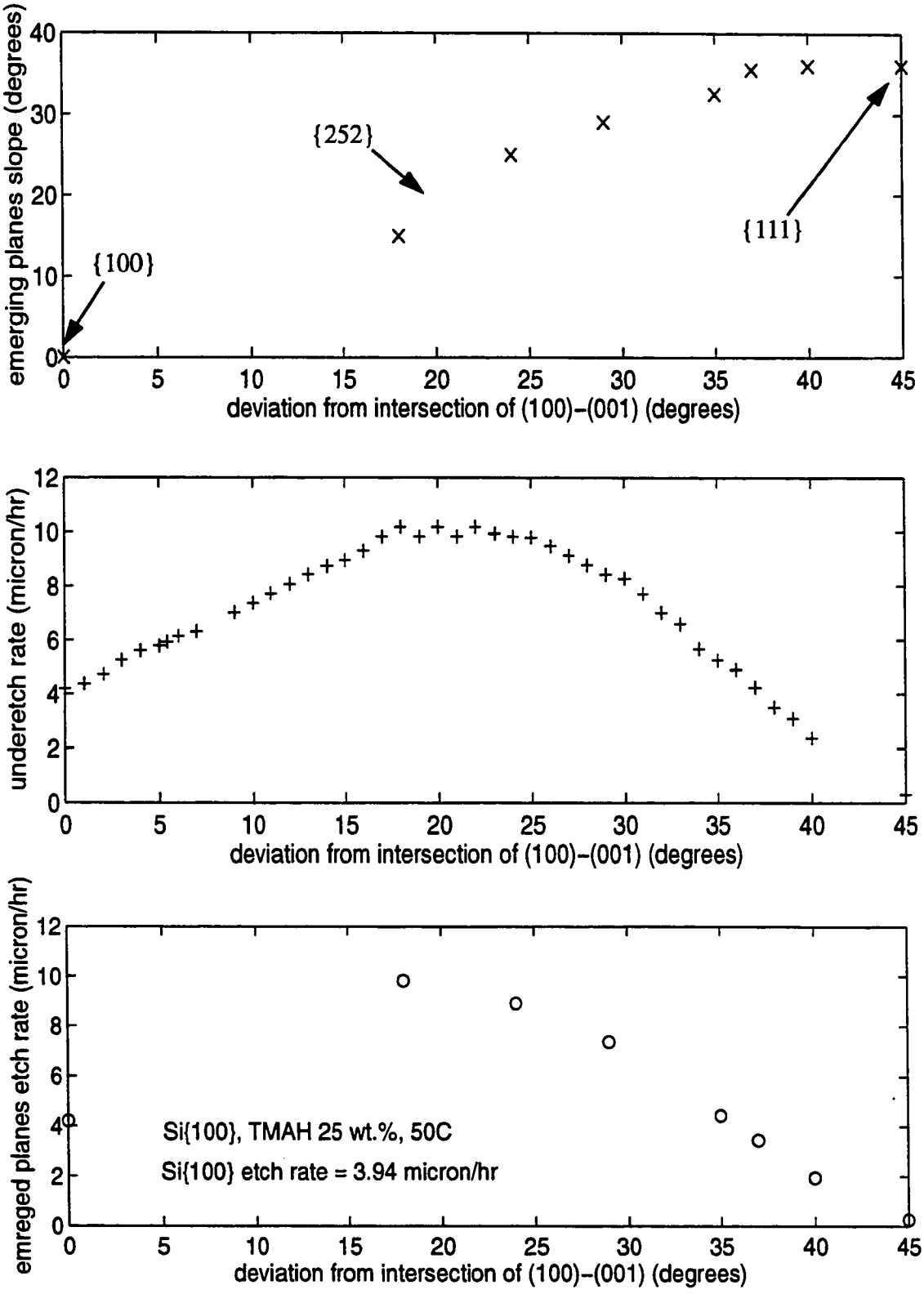

Fig. 4.9: Underetch rate and slope of emerged planes in Si {100} etched in fresh TMAH 25 wt.% at 50° C.

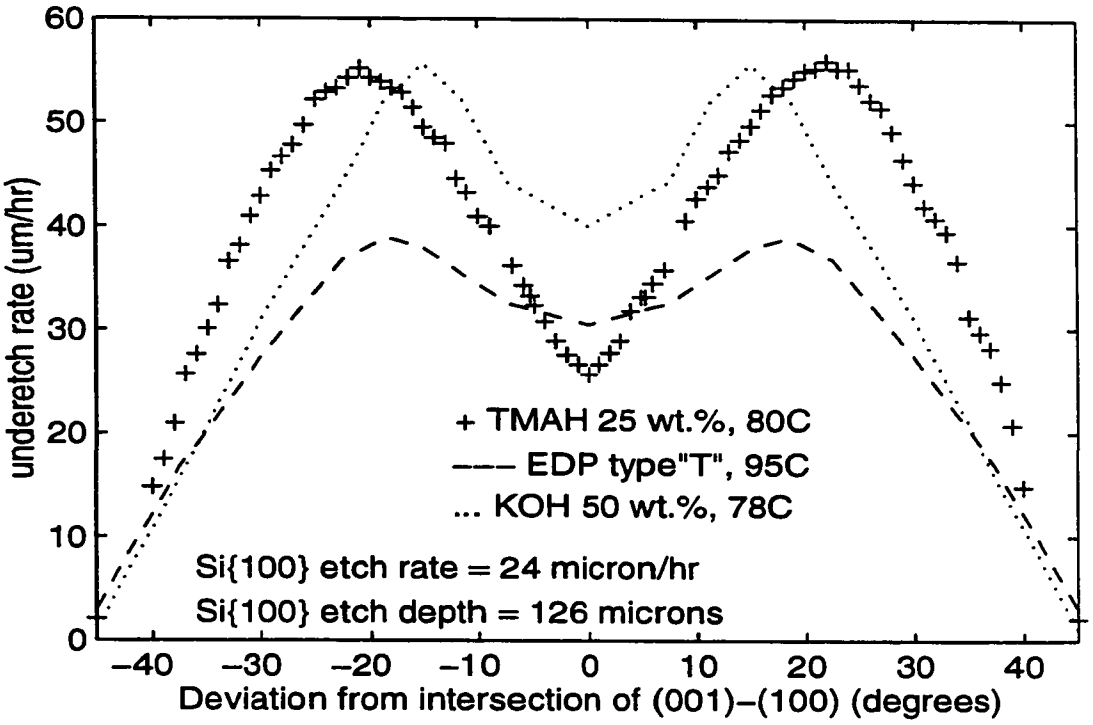

Fig. 4.10: Underetch rate of Si {100} in TMAH 25 wt.% at 80° C. Underetch rate in KOH and EDP type "T" are also shown for comparison.

In Fig.4.10 the underetch rate of Si {100} in TMAH 25 wt.% at 80° C is shown, in comparison with KOH and EDP type "T" underetch data from other researchers [45]. This graph is basically same as the curve shown in Fig.4.8 but with a range of variation of δ from -45° to 45°. These three curves are qualitatively similar. However, quantitatively there are some differences, notably in the values of the maximum underetch rate and location at which they occur. Also, it can be seen that all of the etchants shown in Fig.4.10 have a local minimum at the δ=0°. As mentioned before, the emerging plane at δ=0° in TMAH in this curve is a Si {100} plane. The emerging plane at δ=0° in KOH is also a Si {100} plane, but in EDP the emerging plane is a Si {110} plane [45]. The location of the maxima in the three curves differe by a few degrees. In KOH and EDP the maxima are at lower deviation angles. A quantitative difference which can be extracted from this figure

is the ratio of the highest underetch rate to its value at $\delta=0^{o}$. These are approximately 2.2, 1.33 and 1.25 for these particular conditions of TMAH, KOH and EDP, respectively.

4.3.2 Emerging Planes in Si {100} Etched in TMAH 15 wt.% at 80° C.

Samples were covered with thermal oxide and patterned with the triangles mask and etched in fresh TMAH 15 wt.% at 80° C for 2 hours. In this case, the emerging plane in the first triangle ($\delta=0^{o}$) is a rather rough surface but on average it is a {110} surface. In particular the intersection of this plane with the base {100} etched plane is sharp. At deviation angles very close to $\delta=45^{o}$ deviation, the emerging surfaces are staircase-shaped, very similar to cases found in TMAH 25 wt.%. In general, emerging surfaces are rougher than those found in TMAH 25 wt.%. One examples of emerging planes are shown in Fig.4.11.

The etch rate, underetch rate and angle of inclination of emerging surfaces are graphed vs. deviation angle (δ) for TMAH 15 wt.% at 80° C, in Fig.4.12. Comparing Fig.4.8 with Fig.4.12, it can be seen that the slopes of the emerging planes (shown in the top curves in both figures) are totally different from those found in TMAH 25 wt.%. Only at $\delta=45^{o}$ the emerging planes are the same. In Fig.4.8 the angles which the emerging planes make with vertical are between 0° and 35.3° but Fig.4.12 the angles are between 45° and 35.3°. The underetch rate curves show a maximum at the same angle of deviation ($\delta\sim22^{o}$) but the fastest underetch plane in TMAH 15 wt.% was identified as being between {525} and {524}, as opposed to {252} in the case of TMAH 25 wt.%. The local minimum in Fig.4.12, occuring at $\delta=0^{o}$, is not as strong as the one in Fig.4.8. The ratio of highest underetch rate to its value at $\delta=0^{o}$ is about 1.4 in the case of TMAH 15 wt.% at 80° C.

4.3.3 Emerging Planes in Si {100} Etched in TMAH 15 wt.% at 50° C.

Using the same method as in previous cases, a {100} sample patterned with triangles was etched in TMAH 15 wt.% at 50.3° C for 14 hours. The appearance of the emerged surfaces in this case are to some extent similar to the case discussed in 4.3.2 but since the surfaces were very rough and sometimes nonuniform, no accurate measurement could be done on them. In Fig.4.13 the underetch rate vs. deviation angle for this case is shown. There is some scattering in the underetch data points, because of some damage to the over-hanging oxide but in general the shape of the curve looks similar to the case of etching in TMAH 15 wt.% at 80° C shown in Fig.4.12. The overall etch rates are lower than in Fig.4.12 by a factor of about 6. It can be seen that the fastest underetching planes in this case appear at the same angle of deviation ($\delta \sim 22^{\circ}$) as in the previous cases.

In the curves shown in Fig.4.15, the results of etch rate, underetch rate and slope of the emerging planes measured for TMAH 15 wt.% at 50° C are shown, but in this case the TMAH was silicon doped to a level of approximately 0.6 gr/liter. By comparing Fig.4.13 and Fig.4.15 it can be seen that silicon doping of TMAH has a considerable effect on the underetch rate at $\delta=0^{\circ}$ (in Fig.4.15 underetch rate at $\delta=0^{\circ}$ has decreased to about 0.6 times of its value in Fig.4.13) but not much effect on the etch rate of the base Si {100} surface (6.3 μm/hr vs. 6.5 μm/hr). The shape of the underetch rate curve in this case is relatively flat for deviation angles of $\delta=0-22^{\circ}$. The emerging plane at $\delta=0^{\circ}$ (Fig.4.14) was identified as a {110} plane and at $\delta=22^{\circ}$ the emerging plane was in {525} family of planes.

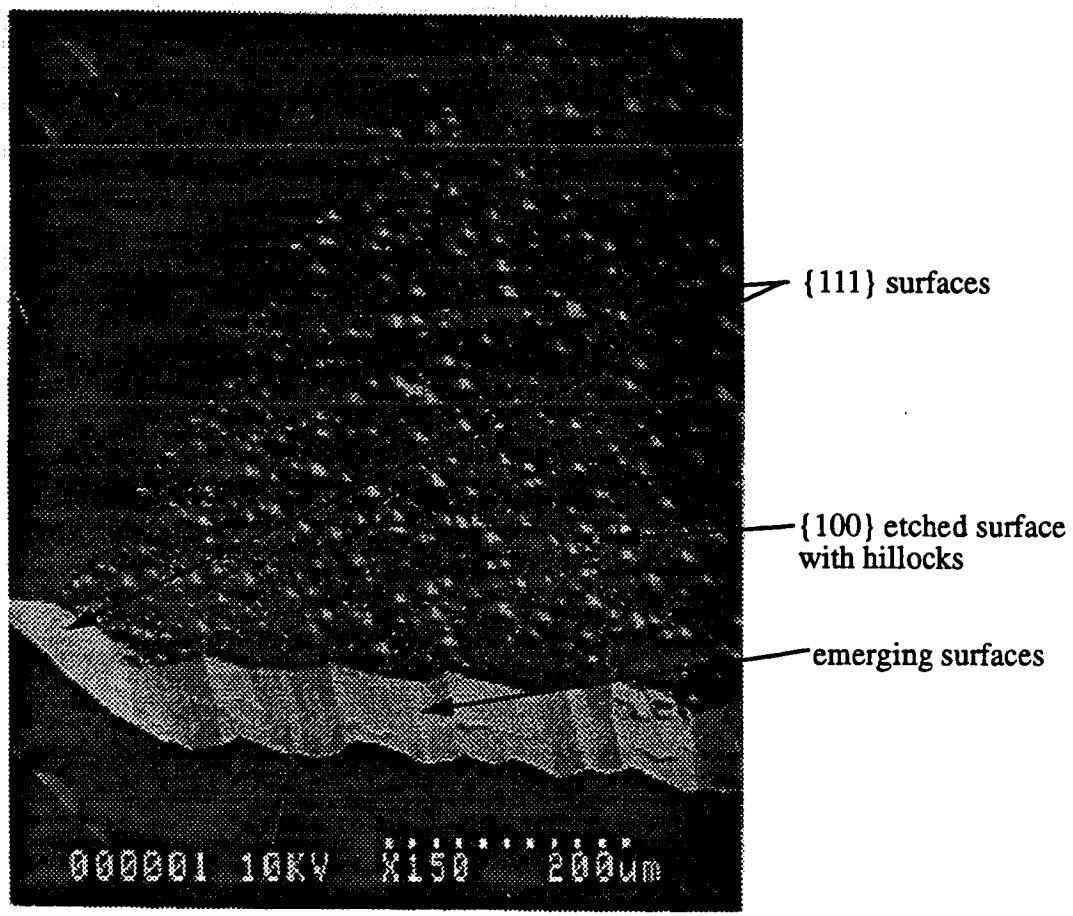

Fig. 4.11: SEM micrograph (viewed from an angle of ~10-20° from vertical) of underetched surface at 10° deviation from the intersection of (100)-(001) Si {100} sample, etched in TMAH 15 wt.% at 80° C for 2 hours. The bottom of the etched region is covered with hillocks. The masking oxide has been removed.

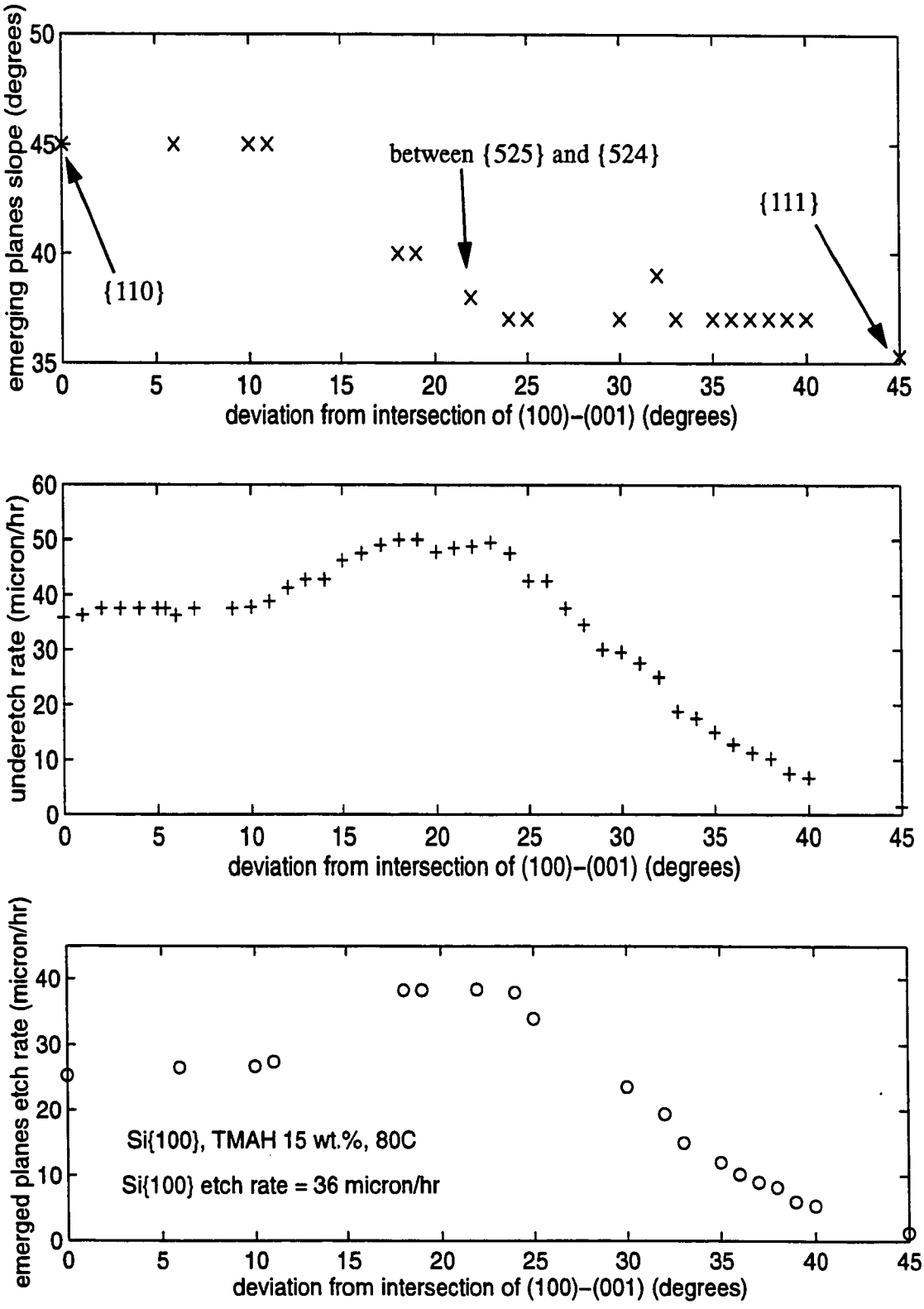

Fig. 4.12: Underetch rate and slope of emerged planes in Si {100} etched in fresh TMAH 15 wt.% at 80° C.

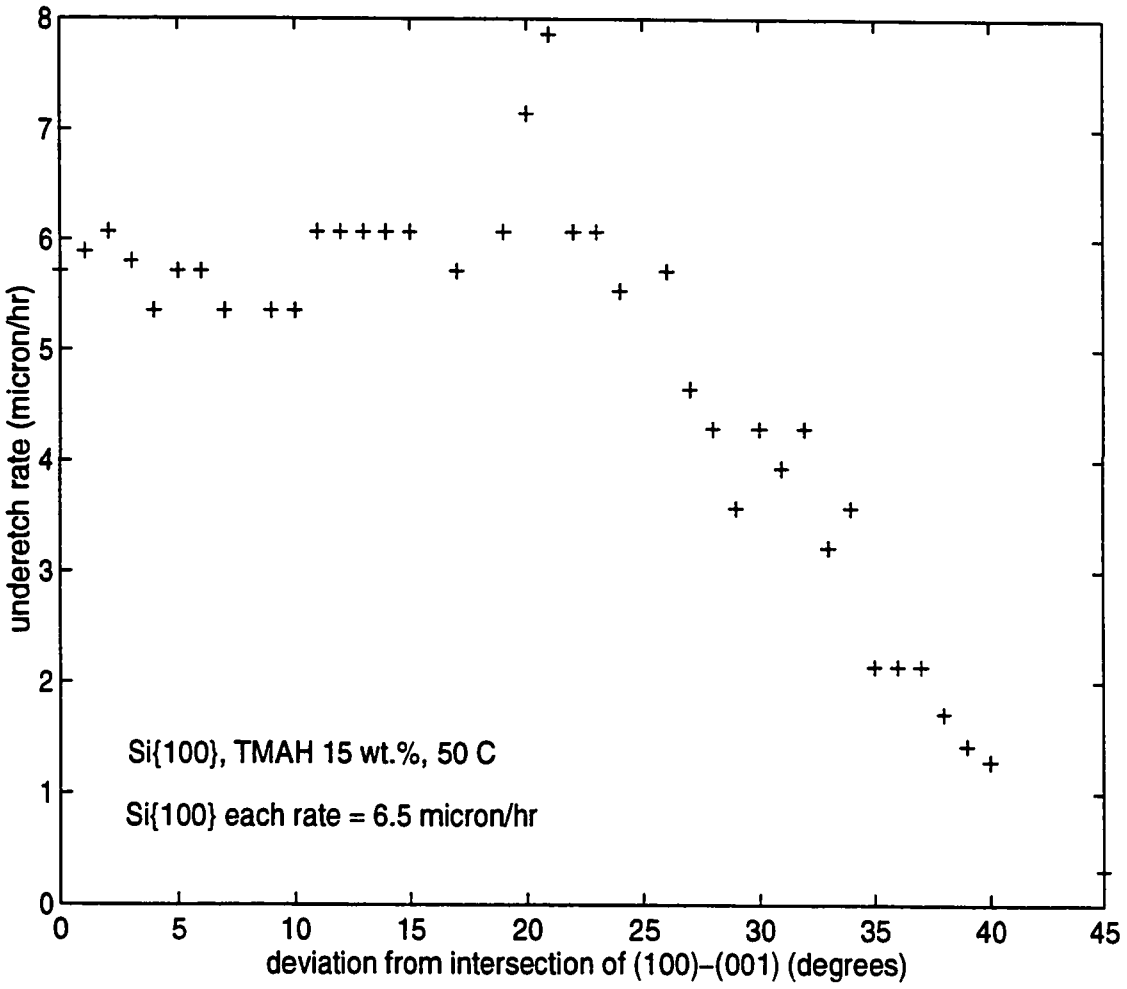

Fig. 4.13: Underetch rate in Si {100} etched in fresh TMAH 15 wt.% at 50°.

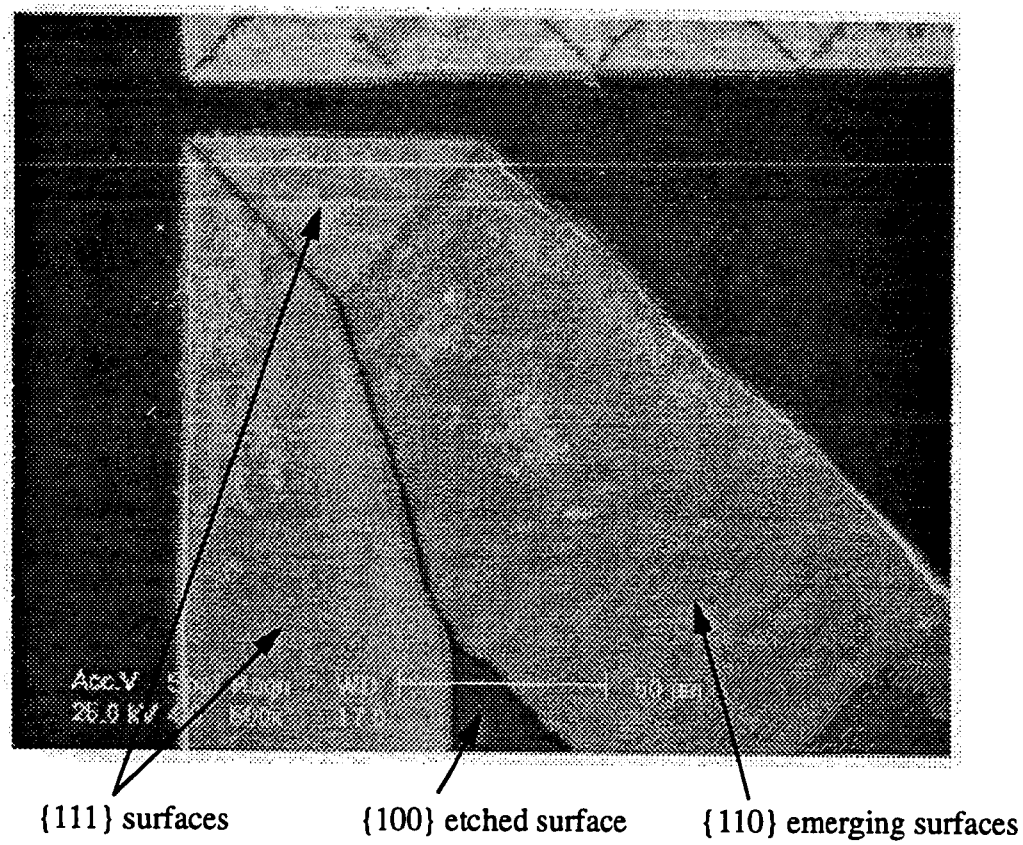

Fig. 4.14: SEM micrograph (viewed from top) of underetched surface at 0° deviation from the intersection of (100)-(001) Si {100} sample, etched in TMAH 15 wt.% at 50° C for14 hours. The masking oxide has been removed.

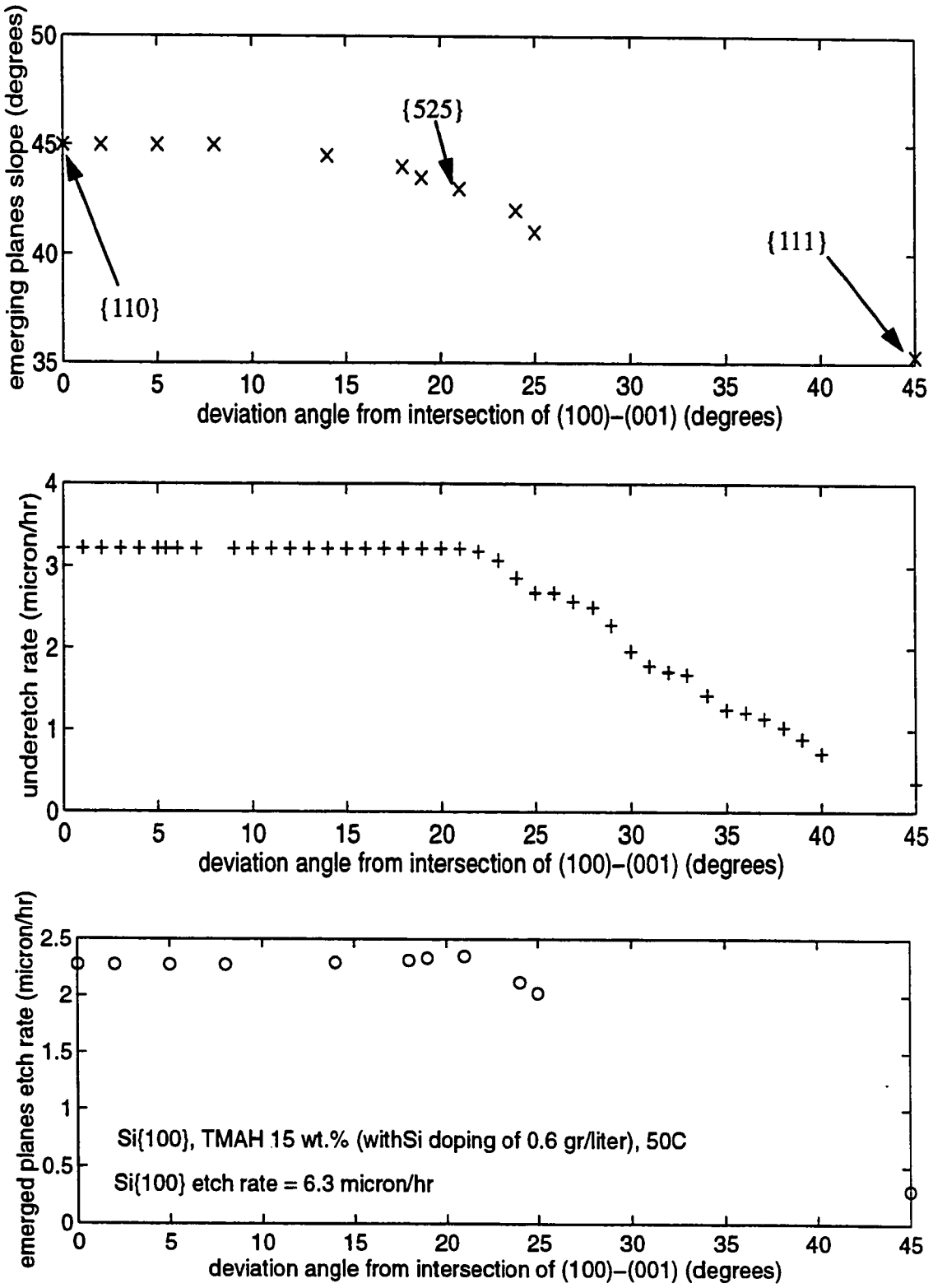

Fig. 4.15: Underetch rate and slope of emerged planes in Si {100} etched in rather highly silicon doped TMAH (0.6 gr/liter) 15 wt.% at 50° C

4.3.4 A simple Model for Explaining the Angle of Inclination of Sloped Surfaces.

A geometrical model is suggested here which can be useful for some of the cases of etching silicon in TMAH. The model gives the angle of the slope of the emerged planes vs. deviation of the edge of the triangle, δ, used so far.

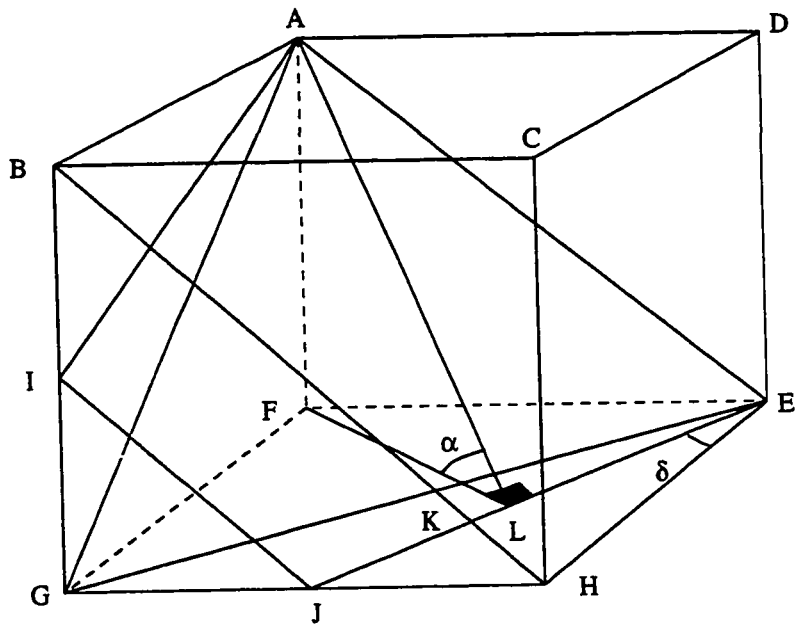

Fig. 4.16: Demonstration of rotation of a {110} plane around a line in that {110} plane and perpendicular to the intersection of {110}-{100}, AE in this figure.

To explain this model, first the cube cell ABCDEFGH shown in Fig.4.16 is considered with length of all of the edges equal to 1. If plane ABHE is rotated around the line AE, the intersection of the new plane AIJE and plane EFGH, that is EJ, makes the angle $\angle HEJ$ which is called δ. In fact this angle corresponds to δ defined in section 4.2.

The angle which plane AIJE makes with plane EFGH is shown in Fig.4.16 as $\angle ALF$. By looking at the Fig.4.16 following relations can be written:

$$FL = \sin\angle FEL = \sin(90^o - \delta) \tag{4.1}$$

$$\tan(\angle ALF) = \frac{1}{FL} \tag{4.2}$$

Therefore the angle $\angle ALF$ which is called α can be written in terms of δ as follows:

$$\alpha = \angle ALF = \text{atan}\left(\frac{1}{\sin(90^o - \delta)}\right) \tag{4.3}$$

The cube shown in Fig.4.16 can be compared to a silicon crystal unit cell. All of the faces of the cube correspond to {100} planes, plane ABHE corresponds to {110} planes and plane AGE corresponds to a {111} plane. According to this model by variation of δ from 0^o to 45^o the {110} plane transforms to {111} plane. It should be noted that Figs.4.8, 4.9, 4.13, 4.13 report the underetched plane with respect to the vertical while this model derives a with respect to the horizontal.Therefore $(90^o-\alpha)$ will be compared to the experimental data.

If the value of $(90^o-\alpha)$ is drawn in terms of δ using the Eq.(4.3), and compared to

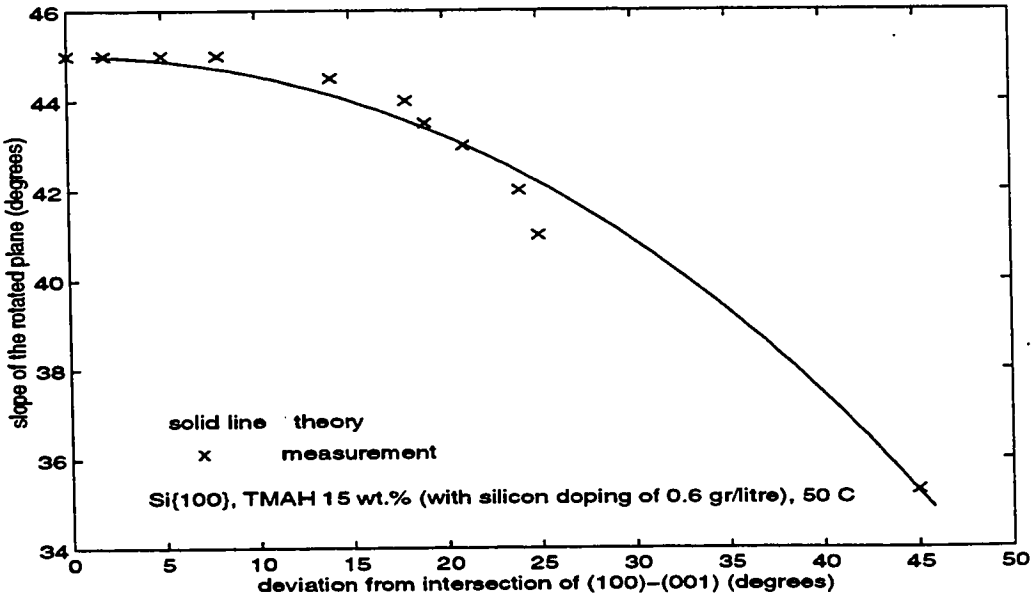

Fig. 4.17: Comparison of theory and measurement.

measured data points provided by SEM, a very close agreement between these two is observed. This comparison is shown in Fig.4.17. In this figure the crosses are the values of measurements done on the sample which was etched in TMAH 15 wt.% with rather high doping of silicon (0.6 gr/liter) shown in Fig.4.15.

The plane which corresponds to $\delta=0^o$ gives $\alpha=45^o$, which corresponds to a {110} plane and $\delta=45^o$ gives $\alpha=54.7^o$, which corresponds to a {111} plane.

4.3.5 Underetch Rate of Si {110} in TMAH 25 wt.% at 80° C.

The results of measurement for this condition are shown in Fig.4.18. In this case the deviation angle is the deviation from the intersection of {110}-{111} which in the Fig.4.18 has a variation from 0^o to180^o. 0^o deviation in this case is aligned with the intersection of the wafer surface with those {111} planes which make an angle of 35.3^o to the horizontal. The other two minima in the curve, which occur at deviation angles of 54.26^o and 125.3^o are also {111} planes, but these are vertical. (For alignment of the mask, the natural cleavage lines of the {110} wafers were used in this work). The emerging planes at the local minima at $\delta=0^o$ in the curve were observed to have a 45^o slope. the etch rate of this plane (as opposed to underetch rate) can be obtained by calculation $25\ \mu m = \sin(45^o) \times 35.4\ \mu m$. This is same as the etch rate of {100} planes in Fig.4.8.

In Fig.4.18, the underetch rate of KOH and EDP type "T" are also shown for comparison. As can be seen, there are qualitative similarities between KOH curve and TMAH curve but the location of maxima on the curves are a few degrees off from each other. The emerging plane at local minimum in the case of KOH is also a {100} [45]. In the curve of EDP underetch rate, three local minima can be seen. Their emerging planes have been identified as {110} planes [45]. Also, the curve related to EDP has a local maximum at about $\delta=45^o$ which cannot be seen in the KOH and TMAH curves.

Same as the case of Si {100}, the ratio of maximum underetch rate to the local minimum at $\delta=0^{o}$ in each curve can be obtained from Fig.4.18. In this case this ratio for TMAH 25 wt.% is 1.6 and for KOH this ratio is about 1.07. For EDP, more than one value is obtained because there are more than one maximum and minimum. The ratio most relevant to the others is 1.3.

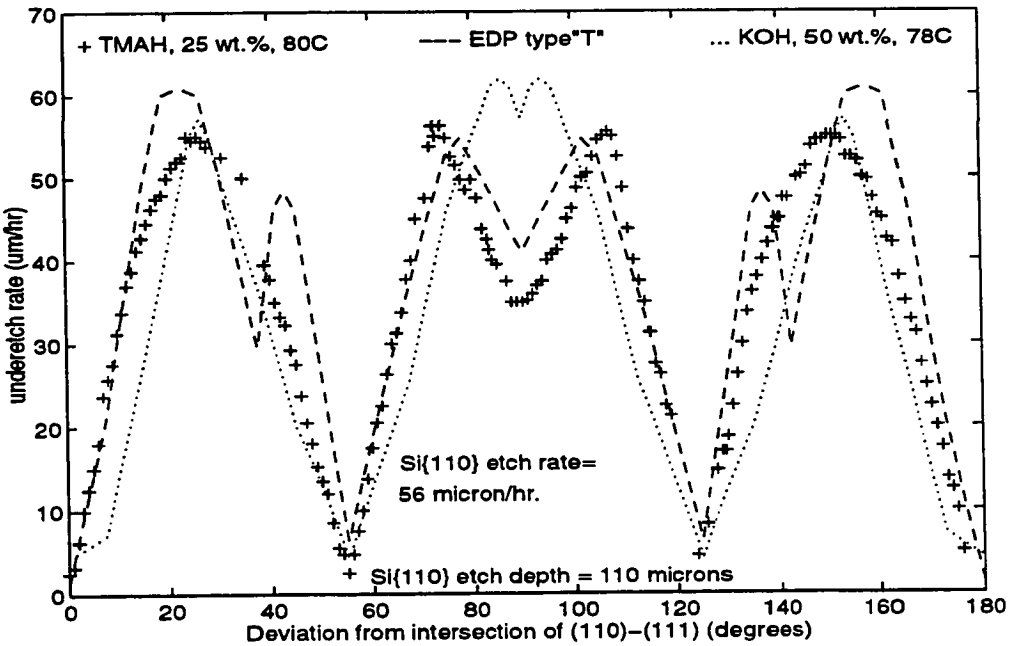

Fig. 4.18: Underetch rate of Si {110} in TMAH 25 wt.% at 80° C. Underetch rate in KOH and EDP type "T" are also shown for comparison.

4.4 Summary

In a series of experiments carried out with different concentrations of TMAH at two different temperatures, it was found that Si etch anisotropy is a strong function of composition of the etchant. Also, different planes emerging during etching for different mask edge deviation is also a strong function of etchant concentrations. It was found that the content of silicon in etchant can also have considerable effect on the underetch curve.

All of these observations suggest that by continuing similar experiments at other tem-

peratures, concentrations, and silicon content, useful information can be extracted for the modelling of the atomic mechanism of Si anisotropic etching.

CHAPTER 5

Investigation of Hillocks Formation During Anisotropic Etching in TMAH

5.1 Introduction

Pyramidal hillocks are the most important defect type observed during anisotropic etching of Si. Pyramidal-shaped hillocks are protrusions appearing on {100} etched surface after anisotropic etching. The study of hillocks is important because in some applications, the quality of the {100} etched surface can be critical. For example in creating the V-shape and U-shape grooves on the silicon wafers for holding the fiber optic waveguides it is necessary to have a very smooth surface otherwise the fiber will be damaged. Also, studying the mechanism of hillocks formation may be helpful in the study of the basic physical mechanism of the anisotropic etching of silicon.

In this chapter the experiments and the observations done regarding the hillocks are described.

5.2 Previous Studies

The mechanism responsible for the formation of hillocks is at present not well understood. It should be noted that hillocks have been found not to be related to mask defects [46], lithography problems [46] or surface conditions [46] such as small patches of SiO_2 left on the surface. They are not correlated with any specific wafer supplier either [46]. Hillocks are created or removed during the etching process [46].

In general, two mechanisms can be considered for the formation of hillocks. It can be either hinderance in the etching process, or it can be a growth process. Current under-

standing in the literature has proven neither of these to be right or wrong. In a report about hillock formation in KOH [46] the factors affecting its formation have been studied. According to this report there are four factors affecting the formation of hillocks in KOH:

1) State of agitation of etchant: by stirring the KOH solution the hillocks density is reduced by one order of magnitude.

2) KOH concentration: by increasing the concentration of KOH in the solution the density of hillocks decreases until it vanishes completely. For example at temperature of 60^{o} C a concentration above 30 wt.% does not allow any hillocks to appear.

3) Temperature: at higher temperature the density of hillocks is higher.

4) Effect of surfactants: addition of some kind of surfactants can reduce the roughness of surface. The surfactant used for KOH is FC129 [1]which is added to the solution to reduce the surface tension of etchant. The amount of additive is about 0.01 wt.%.

Also, it has been shown that hillocks formed in etching Si {100} in KOH which are not perfect pyramids. Instead, each of the 4 main faces is made of 2 sub-faces, which are planes having Miller indices {567} [46].

In another investigation by Bhatnegar *et al.* [47] which is mostly about the formation of hillocks on {100} surface etched in EDP, the presence of defects in the crystalline structure of bulk silicon, and incomplete dissolution of hydrated silica (a product of etching reaction) have been considered as main causes of appearance of hillocks. It is found [47] that thermal annealing and residual stress affect the appearance of hillocks because these two affect the structural defects in the bulk of the silicon. In this report they have supposed that the walls of the pyramids are {111} planes. Also they reported that they have not been able to find any hillocks in the state of either formation or annihilation. Some other observations about pyramidal hillocks which hold for all kinds of etchants are as follows [12,

1. A fluorocarbon compound made by the 3M company.

46, 47, 55, 56]:

a) by changing the composition of the etchant in an appropriate way it is possible to prevent the creation of hillocks.

b) The location of pyramids can be affected by the thermal and stress history of the silicon substrate.

c) The pyramids may appear and disappear on the etch plane as the etching proceeds.

d) The density distribution of pyramid sizes is in a way that bigger size hillocks have a lower density and smaller pyramids have higher density.

e) The walls of the pyramids meet each other at a bevelled planes, not at sharp edges.

f) Pyramids may overlap on each other, some times in a way that their base look to be bowed somewhat.

In a recent paper [65], by some pictures taken from same hillocks during different times of etching, destruction of a hillocks has been shown clearly.

5.3 Experiments and Observations

5.3.1 Determination of the Orientation of Hillock Surfaces

When a single hillock is observed through an optical microscope it looks very similar to a tetrahedron with a square-shaped base and four similar triangular facets, and all hillocks on a surface are aligned with each other. In actuality the shape of the hillocks is more complicated than this. Investigation of hillocks using a higher magnification optical microscope or scanning electron microscopy (SEM) shows that the base of the hillocks has an octagonal shape [46]. The view of an etched surface (in TMAH 15 wt.%) with hillocks and the view of one single hillock on this surface are shown in Fig.5.1 and Fig.5.2. For determining these surfaces the same method as the one used by Tan *et al.* [65] was

used here. But first some points about calculation of the Miller indices are explained.

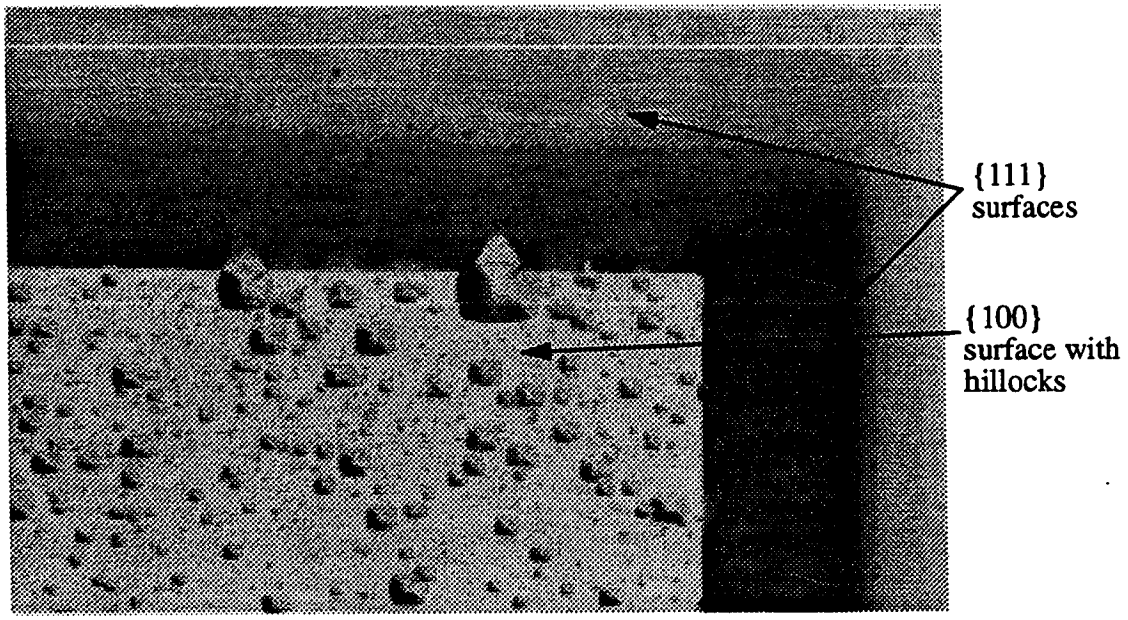

Fig. 5.1: Optical micrograph of the surface of a Si {100} sample etched in TMAH 15 wt.% 80° C for 2 hours, covered with hillocks.

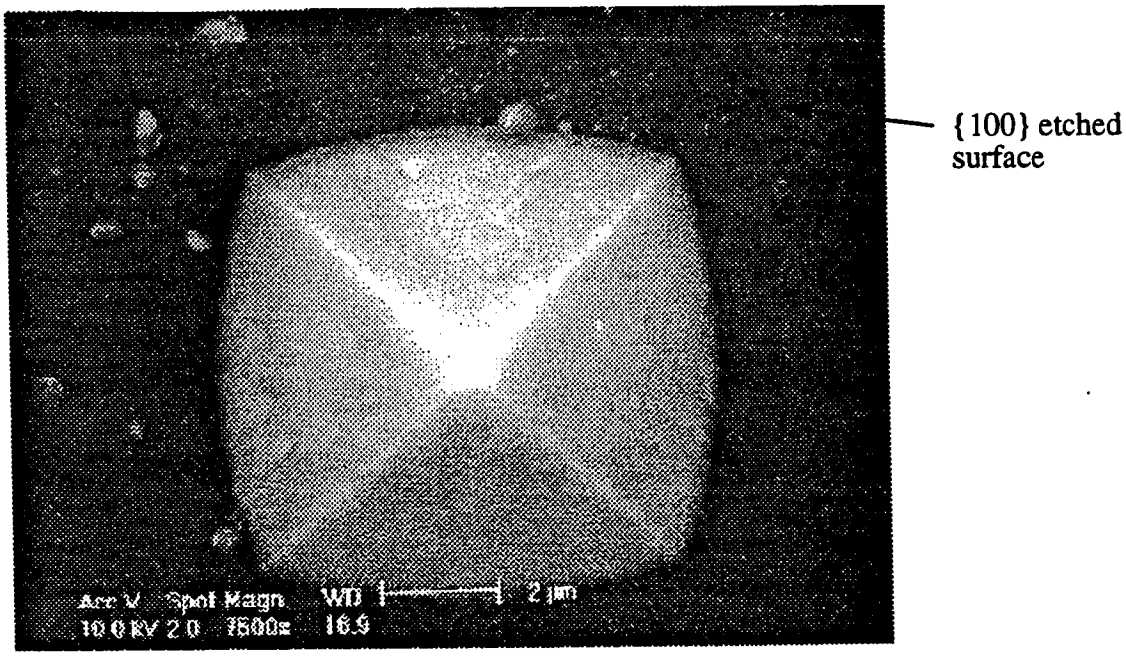

Fig. 5.2: SEM micrograph of a top view of a hillock etched in TMAH 15 wt.% at 80° C (α=0).

By having angles by which a plane intersects coordinates axis, it is possible to calculate the Miller indices of that plane. This is shown in Fig.5.3. In this figure planes XY, XZ and YZ are parallel to {100} planes in a silicon crystal.

If angles $\angle OMN$ and $\angle PQO$ are available, following calculations provide the Miller indices:

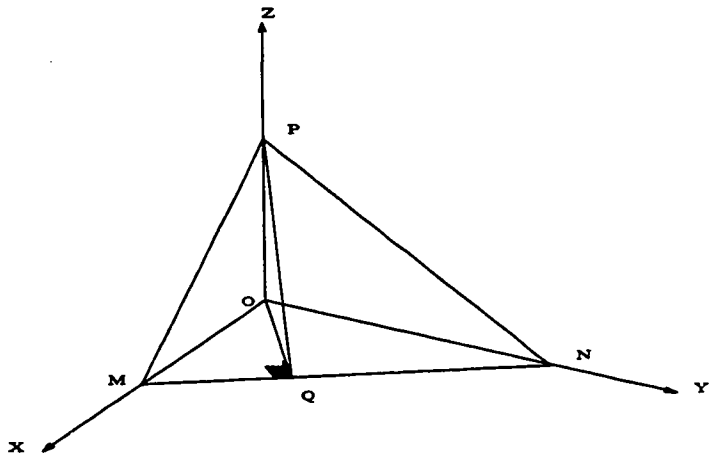

Fig. 5.3: Geometry used to calculate Miller indices.

$$ON = OM \cdot \tan\angle OMN \tag{5.1}$$

$$OQ = OM \cdot \sin\angle OMN \tag{5.2}$$

$$OP = OQ \cdot \tan\angle PQO \tag{5.3}$$

Therefore values of ON and OP are obtained in terms of the length of OM. For the plane MNP the Miller indices are $(\frac{1}{OM}\ \frac{1}{ON}\ \frac{1}{OP})$, which by using Eq.(5.1), Eq.(5.2) and Eq.(5.3) all of them are stated in terms of one variable OM. By choosing the value of OM in an appropriate way the three Miller indices are expressed as close as possible to integer numbers.

This method is used for calculation of Miller indices of hillocks walls as follows. By

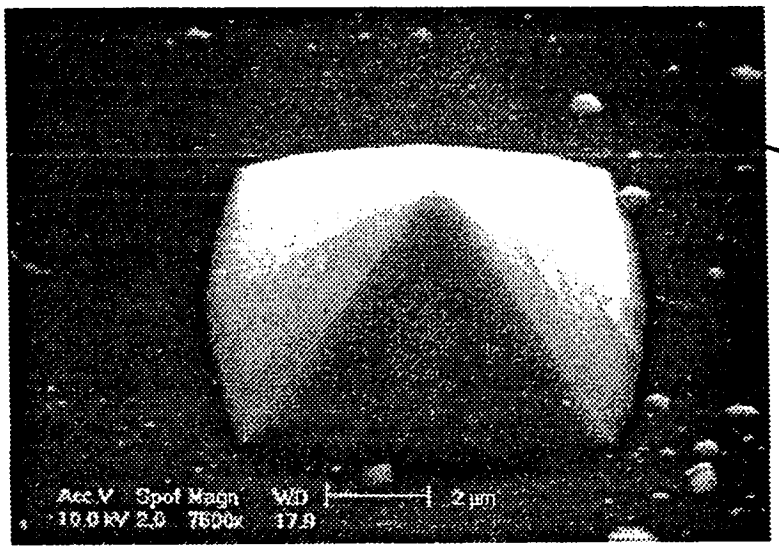

Fig. 5.4: SEM micrograph of the same single hillock as shown in Fig.5.2, tilted by α=33°.

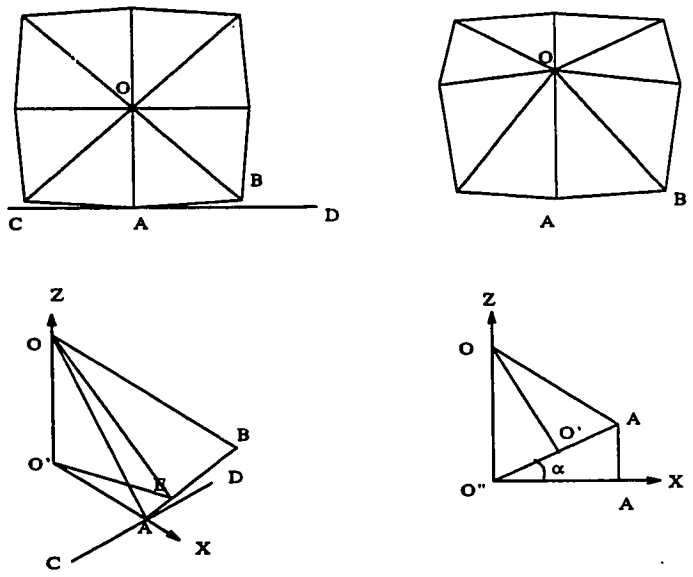

Fig. 5.5: Outline of top view and tilted view of a hillock (Analysis method from Tan *et al.* [65]).

looking at the top view of a hillock shown in Fig.5.2 and measuring the angles which is made of the line of intersection of hillock walls and wafer surface, and the line of intersection of {111} walls and bottom surface, two of the Miller indices can be calculated. This is demonstrated in Fig.5.3. For determining the third Miller index of these walls, the sample

is tilted by an arbitrary angle of α, here α was chosen to be 33°. This situation is depicted in Fig.5.5. The top left feature in Fig.5.5 shows the outlines of the hillock viewed from top. By drawing outlines on a copy of Fig.5.2 the angle $\angle BAD$ and length of $O'A$ are measured. By drawing similar kinds of outlines on the magnified copy of the SEM picture of the tilted sample shown in Fig.5.4 and measuring the length of lines $O''A'$ and using relations shown below, the inclination angle of the hillock walls can be obtained:

$$\tan\angle OEO' = \frac{OO'}{EO'} = \frac{OO'}{AO'}\frac{AO'}{EO'} = \frac{\tan(\angle OAO')}{\cos(\angle AO'E)} \tag{5.4}$$

The denominator of the most right term can be evaluated by direct measurement of the angle $\angle DAB$ which is congruent to $\angle AO'B$. For determining the numerator by looking at the bottom left part of Fig.5.5 it can be seen that

$$\frac{\cos(\angle OAO')}{\cos(\angle OAO'-\alpha)} = \frac{O'A}{O''A'}. \tag{5.5}$$

In the Eq.(5.5) all parameters can be obtained by measurement from Fig.5.2 and Fig.5.4 and the only unknown is $\angle OAO'$ which by substituting values in Eq.(5.4) and Eq.(5.5) the value of $\angle OEO'$ can be calculated.

The values of parameters measured here was: α=33°, $\angle AO'E$ = 11.5°, $O'A$ = 34 mm, $O''A'$ = 50 mm which give the Miller indices of {3 1.986 3.04}.

In another measurement where the tilt angle was α=20° and $O''A'$ = 44 mm the Miller indices of the planes were calculated to be {3 1.986 3.4}, near to {332}, for example {578} or {6 9 10}.

5.3.2 Tracking a Single Hillock

In the experiments carried out regarding hillocks explained in this section, it has been

tried to investigate the formation of hillocks in TMAH. In all experiments the sample was Si {100} and the concentration of TMAH was 15 wt.% unless specified. After cutting and cleaning the samples, they were oxidized at a temperature 1100° C using wet oxygen for different oxidation time to produce thicknesses between 0.6 to 1 μm. The square array mask shown in Fig.3.3 was used for opening windows on the samples.

In the first series of experiments carried out it was tried to track the evolution of one hillock and check if its formation is the result of a growth process or the result of hindrance in the process of etching. For this purpose two samples were etched in a solution of 15 wt.% TMAH (which certainly produces hillocks on the etched {100} surface) for 2 hours at temperature of 80° C. After this one of the samples was checked through the microscope and a few hillocks were identified for later observations. Selection of these hillocks was based on their size so that the biggest hillocks found were chosen. The reason is that since the microscope magnification is limited, the bigger the hillocks the easier it is to observe them. The etch depth of the {100} surface and the height of selected hillocks was measured. The height of hillocks were measured by alternately focusing at the apex and the bottom of etched surface. Then samples were etched in the TMAH solution with the same concentration of 15 wt.% for 6 minutes and after this the samples were taken out of etchant, rinsed with DI water and checked through the optical microscope. It was expected to see the hillocks with similar pyramidal structure with either higher height or lower height. But instead it was observed that the shapes of hillocks have changed to an octagonal shape and also some distortion had appeared on the apex of the hillocks. These changes of shape are shown in figures Fig.5.6 and Fig.5.7. The same sample was etched for two more steps of 6 minutes each and checked through the microscope. The same process of destruction as in Fig.5.6 was observed to be continuing as is shown in Fig.5.8 and Fig.5.9 (The etch rate of Si {100} in the re-etch conditions was 0.4 μm/min.).

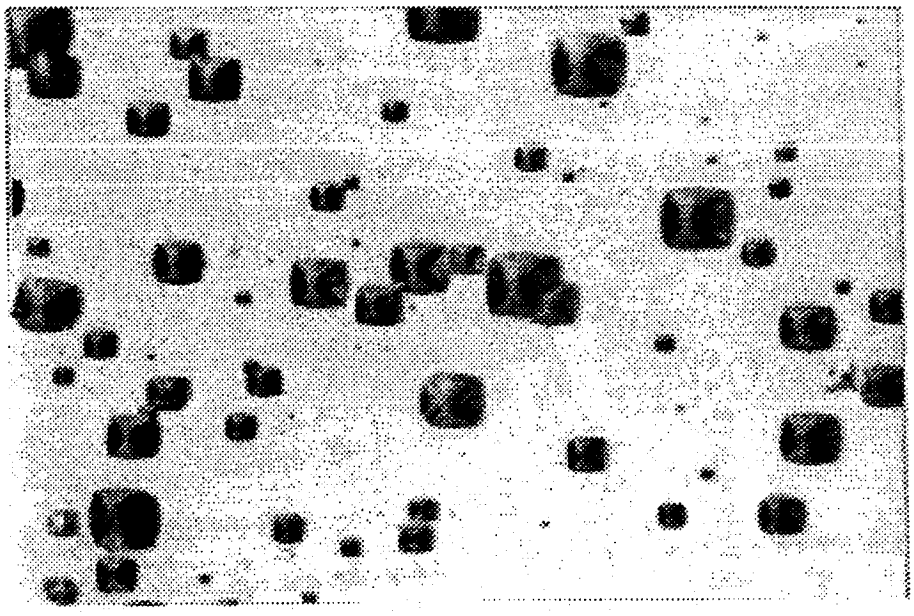

Fig. 5.6: Optical micrograph of Si {100} surface etched for the first time in TMAH 15 wt.% at 80° C for 2 hours continuously (magnification = x 500). Hillocks are predominantly pyramidal with maximum size about 18 μm.

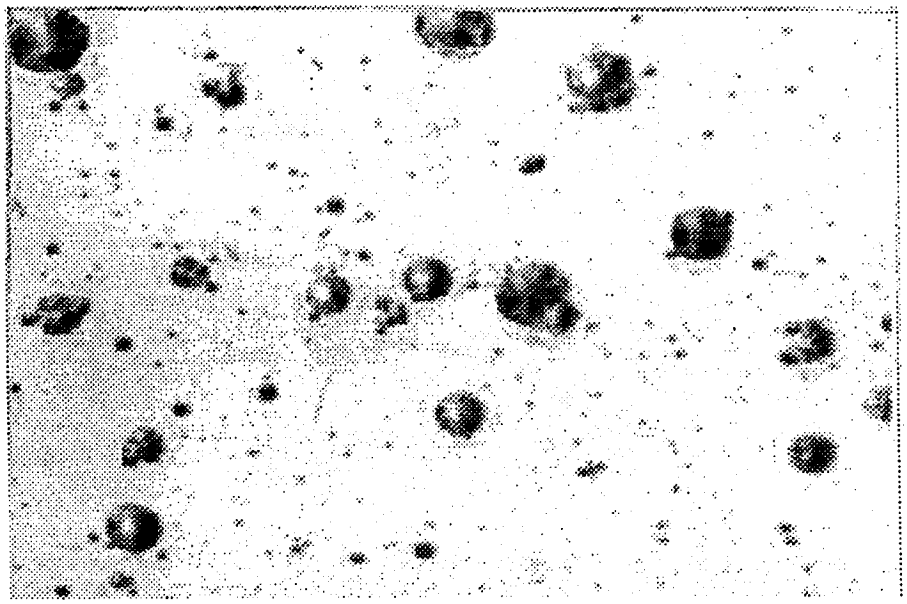

Fig. 5.7: The same sample as in Fig.5.6 after re-etching for 6 minutes in the same etchant bath. (magnification = x 500). The hillocks have changed size and shape.

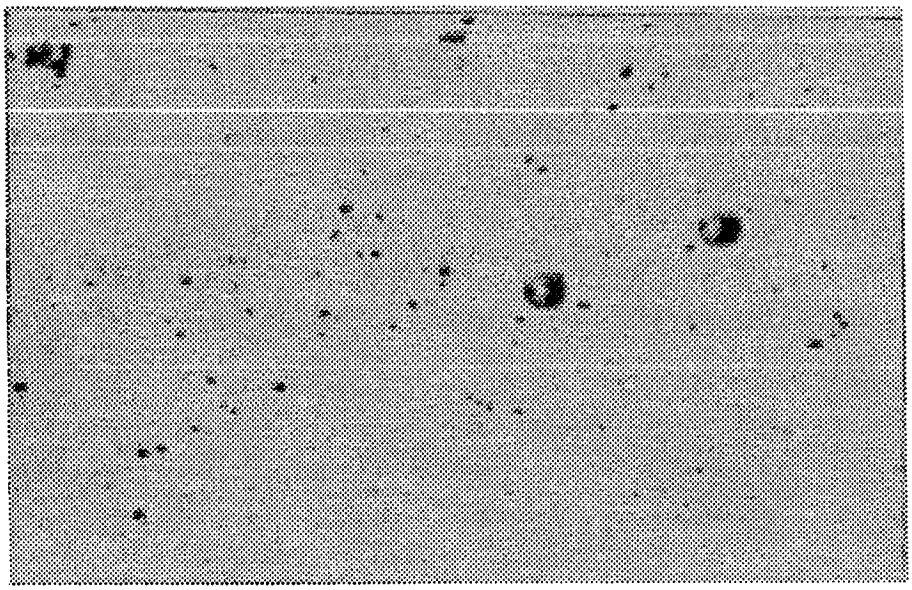

Fig. 5.8: The same sample in the two previous figures after a second 6 minute re-etch step in the same etchant bath (magnification = x 500). Most of the hillocks have been severely diminished.

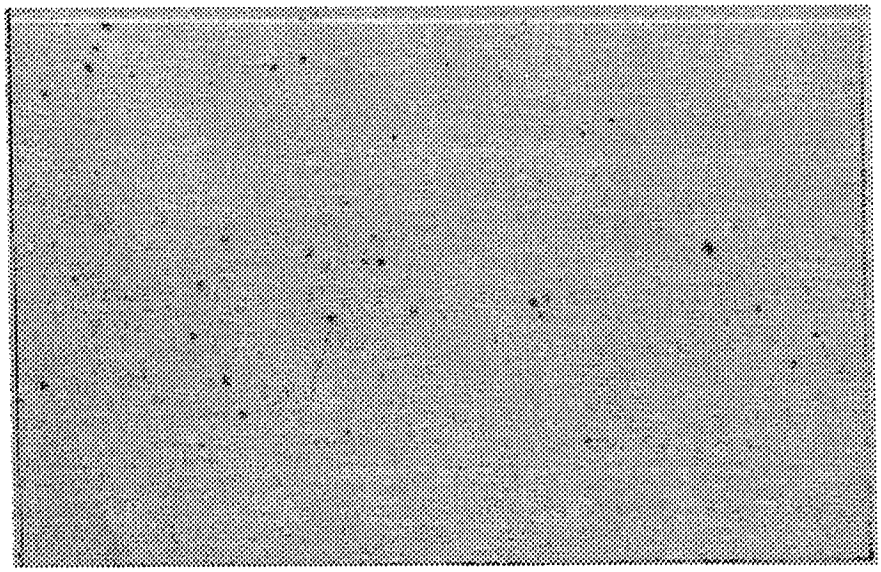

Fig. 5.9: The same sample after a third re-etch step for 6 minutes in the same etching bath. (magnification = x 500). Most of the hillocks have disappeared.

This experiment was repeated several times and same phenomenon (change of shape of hillocks base from an octagonal very close to square-shape, to a regular octagonal shape) was observed each time.

Also, in another experiment it was observed that the shape of hillocks appearing on the samples etched continuously in TMAH 15 wt.% at 80^{o} C for lengths of etch time of 2 hours, 5 hours and 7 hours are the same and similar to what is shown in Fig.5.1. Considering this observation and the result explained before this, shows that the act of interrupting the etching of samples (which consists of taking the sample out of TMAH, rinsing it with DI water and drying it by blow of nitrogen) disturbs the normal life cycle of a hillock so that after re-etching a sample having normal-shaped hillocks (Fig.5.1) their shape changes quickly and the hillock disappears. For this reason it was not possible to track the normal life cycle of hillocks as this would require in situ observation.

Along the same idea, a new experiment was devised to study the dissolution of hillocks during re-etching. For this purpose, 10 samples of Si {100} after growing thermal oxide and patterning them with squares array, were etched in TMAH 15 wt.% at 80^{o} C for 2 hours. As it was expected hillocks appeared on all of the samples. Then all of the samples were put in the same TMAH at the same conditions and every 3 minutes one sample was taken out of the etch solution and rinsed with DI water and dried using blow of nitrogen. The aerial density of hillocks on the samples were measured and drawn. For counting the number of the hillocks, first squares whose sizes were in a range that fitted in the photograph frame were chosen and their picture were taken. The number of hillocks was counted either on the picture itself or on the magnified copy of the pictures. Of course, the hillocks whose size was too small to be seen were not counted. The minimum size of hillocks counted was about 1 μm. Also, a SEM photograph of a dissolving hillock is shown in Fig.5.10. As can be seen in the figure the hillock starts dissolving from its apex. In

Fig.5.11 the density of hillocks vs. their sizes are shown after different times of re-etching. Also, by checking the sample through the SEM it can be seen that the shapes of hillocks are affected by the length of re-etching process. All of the hillocks on the sample re-etched for 3 minutes, as observed through the optical microscope, were octagonal. On the next sample re-etched for 6 minutes, hillocks with edge size below 2 μm had a normal pyramidal shape of hillocks and above this size they had regular octagonal shape. For

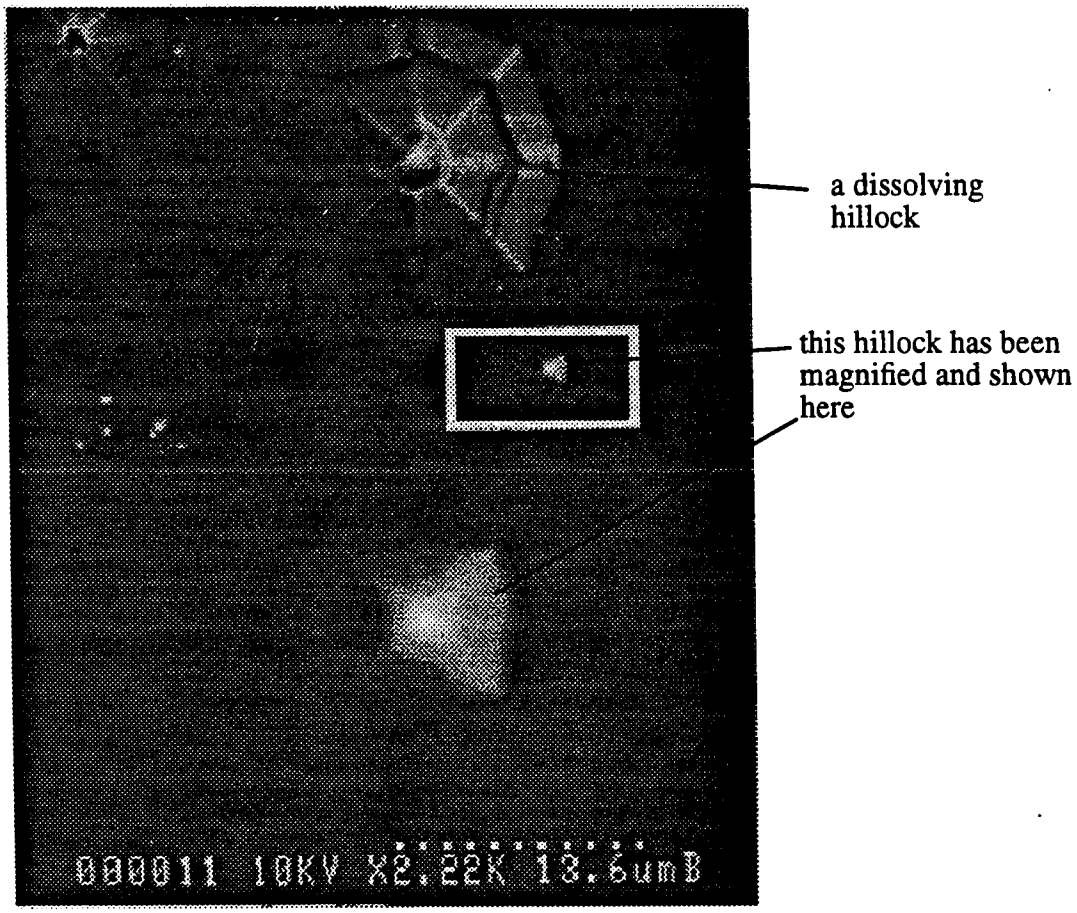

Fig. 5.10: SEM micrograph of Si {100} surface after 2 hours of initial etch and 6 minutes re-etch at 80° C. Top center: a large hillock (~15μm side) in a stage of dissolution. Magnified inset: a small pyramidal hillock. Inset is magnified x 5.

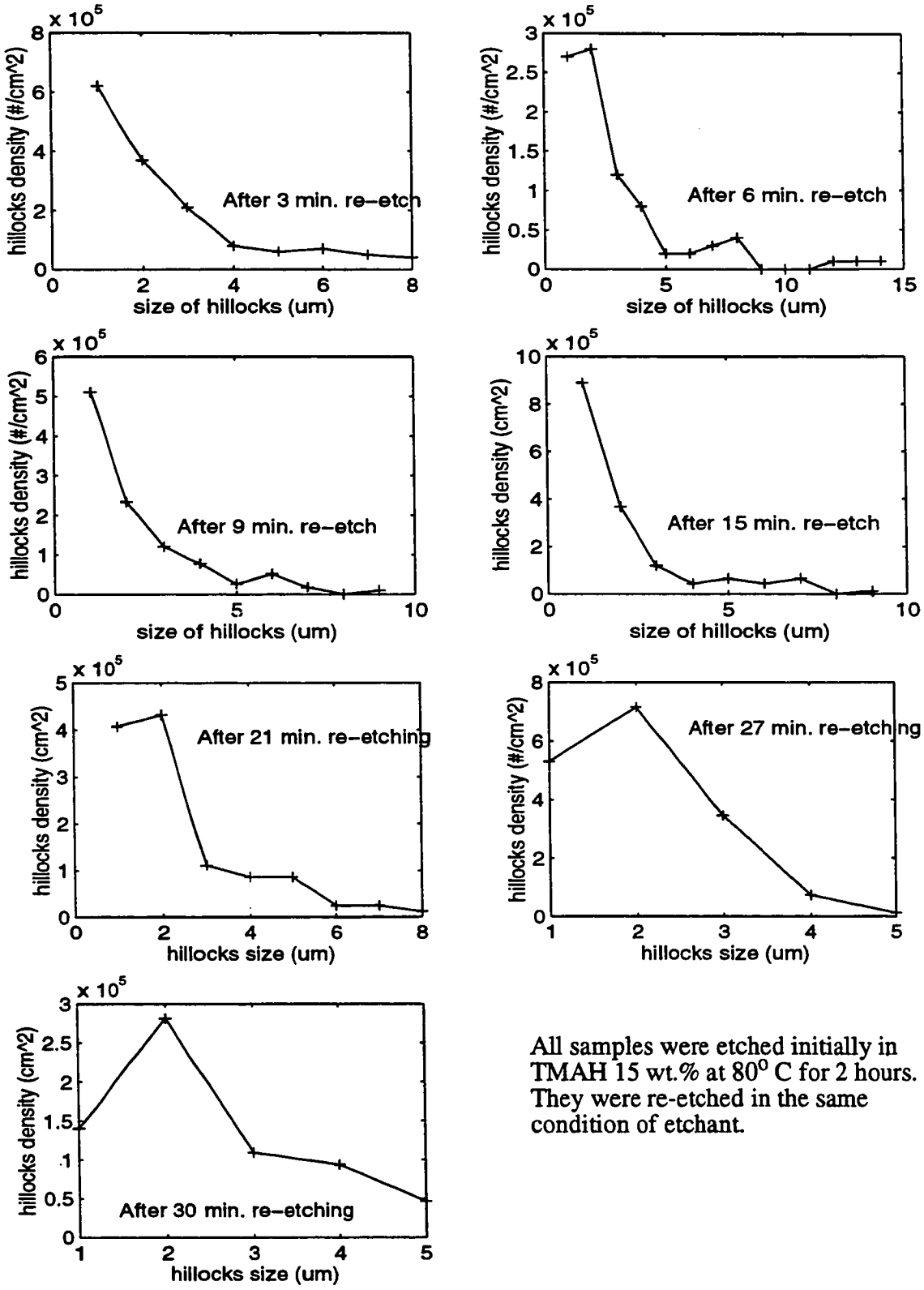

All samples were etched initially in TMAH 15 wt.% at 80° C for 2 hours. They were re-etched in the same condition of etchant.

Fig. 5.11: Density of hillocks vs. size in samples re-etched for different times.

sample re-etched for 9 minutes this limit size of edges was 6 μm and for sample re-etched 27 minutes the limit size is 8 μm. After 30 minutes re-etch all of the hillocks had the normal shape of a hillock. In Fig.5.10 two hillocks with different sizes are shown on the sample re-etched for 6 minutes. The hillock with bigger size has a regular octagonal shape and is dissolving from apex, and a smaller hillock which has the normal shape of a hillock.

When the etched and re-etched samples mentioned above are put in the TMAH solution again for long time of etching, 2 hours for instance, again some hillocks appear on the surface of the sample but the aerial distribution and size of new hillocks is different from the case which a sample is etched for the first time. In the re-etched sample, at the area of the etched surface on the {100} surface close to the edge of the {111} walls there is almost a zero density of hillocks and at the center of the area there is a rather uniform distribution of hillocks with smaller size. And in small squares the hillocks density reaches zero over the whole surface of the square. The range of the sizes of hillocks in re-etched samples is 1-4 μm.

In another experiment two samples of silicon were first etched in TMAH 25 wt.% for 2 hours at 78^{o} C. The surface of samples, as was expected, did not have any hillocks on them. Then the samples were re-etched in TMAH 15 wt.% for another 2 hours at 80^{o} C. The maximum size of the hillocks was about 0.5 μm, which was much smaller than in any other case observed in etching done simply with TMAH 15 wt.% at different temperatures. The density of hillocks also, in this case was much lower than that of the case of just TMAH 15 wt.% but because of small size of hillocks it was not possible to determine the density accurately.

5.3.3 Effect of Temperature of Etching on Hillocks Formation

It has been observed that after etching the samples in TMAH 15 wt.% at two temper-

atures of 50° C and 80° C the density and size of hillocks are different. Usually in samples etched at 80° C the density of hillocks is uniform on the etched surface and hillocks are separate from each other but on the samples etched at 50° C the density of hillocks is not uniform on the etched surface and hillocks overlap.

It should be mentioned that on the samples etched for the first time in different experiments at etch temperature of 80° C, in TMAH 15 wt.% and same length of etching, the maximum sizes of hillocks were variable. One possible reason for this observation can be the different temperatures and lengths of oxidation of samples (growing oxide as etch mask).

5.3.4 Effect of Stirring on Hillock Formation

In another experiment, a sample of Si {100} was patterned with triangles mask shown in Fig.4.1 and etched in TMAH 15 wt.% at T= 80° C for 2 hours with stirring. The TMAH used in this experiment had been used for only one etching experiment (and therefore was relatively fresh, having the dissolved Si content of less than 0.05 gr./liter). After etching, the sample was rinsed with DI water and dried with nitrogen (carefully so as not to break the overhanging oxide on the edge of triangles). Then the sample was checked through the microscope and it was observed that on the etched surface there was a high density of hillocks on all {100} surfaces except the area which is underneath the overhanging oxide. This is shown in figure Fig.5.12. As can be seen in this picture there is a distinctive border between the area covered with hillocks and hillock-free area, which had been underneath the overhanging oxide during etching. This observation strengthens the idea that hillock creation is a diffusion-limited process. (Diffusion limited processes are types of processes in which the rate of the process is determined more by the rate of transport of reactants, to the reaction interface than by the rate of the chemical reaction).

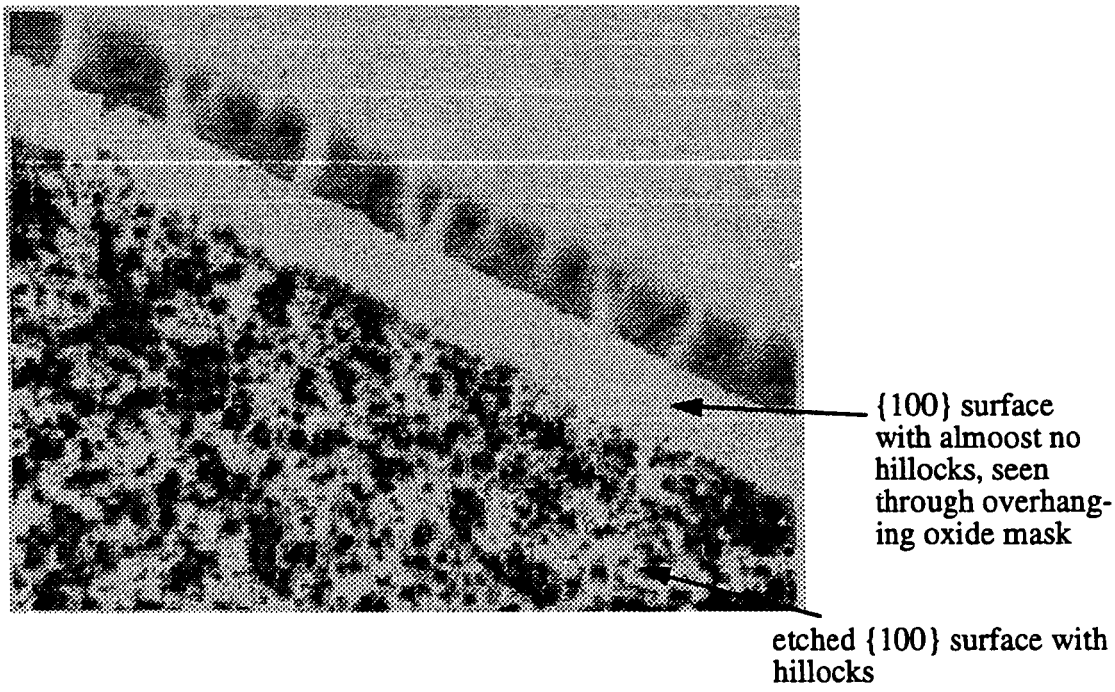

Fig. 5.12: Optical micrograph of an underetch sample etched in TMAH 15 wt.% at 80° C with stirring. The mask oxide overhangs the etched region up to the onset of many hillocks.

5.3.5 Possible Effect of Contamination on Hillocks Formation

In all research work reported about TMAH and in almost all experiments carried out with TMAH in this work it was observed that in TMAH solutions with concentrations more than 22 wt.% the surface of etched Si {100} is hillocks-free. But in one experiment done with TMAH 25 wt.% at T= 87° C for 2 hours in this work, an extraordinary density of hillocks was observed on the Si {100} etched surface. The reason is that most probably a small amount of oil has contaminated TMAH solution which has caused hillocks creation. For testing this assumption in another experiment a small amount of oil (a few droplets) from an oil bath was added intentionally to a fresh solution of TMAH 25 wt.% and Si {100} samples were etched at T=78° C for 2:30 hour, to see if hillocks appear or not. Although hillock density in this case was lower than in the case with accidental oil contamination as was seen on the etched surface, there was a nonzero density of hillocks

which was not observed in uncontaminated TMAH. In any case no hillocks are expected in the range of T=78° C to T=87° C for TMAH 25 wt.%. So, these observations are consistent with a hypothesis that the contamination contributes to causing the hillocks.

5.4 Conclusions

Some of the main points regarding the observations on hillocks are remarked here. The following are some factors which are likely to affect the density and size of hillocks, each of them to different extents:

a) Cleanliness of the sample before oxidation: It is possible that if the surfaces of the samples are not cleaned well before thermal oxidation, contaminants on the surface may diffuse into the bulk of the silicon and be a source of hillocks, or influence their formation.

b) Temperature and length of oxidation time: Since there is a possibility that hillocks are produced because of the presence of defects in the silicon crystal, and defects in the crystal are affected by high temperature steps, therefore hillocks can be affected by any high temperature step.

c) Temperature of etching: As was described in section 5.3.3 the samples etched at 80° C have hillocks with bigger sizes and different density from that of the samples etched at 50° C.

d) Length of the etching time. Apparently, after a certain time, further etching does not have much effect on the size and density of hillocks. It was observed that between the samples etched for 2 hours and the samples etched for 7 hours there is not much difference in the appearance of the etched surfaces. That is, the sizes and density of hillocks look the same for both groups of samples.

The mechanism responsible for creation of hillocks is more complicated than can

explained by the experiments carried out in this work and demands more experiments to be done. Considering the observations in this work, when doing any new experiments regarding hillocks it is recommended to use samples which are cut from the same wafer or batch of wafers, which have gone through the same cleaning process and the same high temperature steps, in order to avoid variations in the factors which have possible effects on the formation of hillocks.

CHAPTER 6

Effect of the State of Stress on Etching of Si {100} in TMAH

Different aspects of anisotropic etching have been the subjects of many investigations. One aspect which is still an unsolved question is the drastic decrease of etch rate of silicon when boron dopant concentration is very high. In Chapter 2, it was indicated that this property applies to almost all known Si anisotropic etchants. Also it was mentioned that for explaining this phenomena there are some theories submitted. One of them [34] states that at a high enough concentration of boron a state of stress reduces the etch rate of silicon. Although the result of one experiment done by a group of researchers [34] shows that there is no major effect caused by state of stress on the etch rate of silicon, in another report [66], it is said that a considerable change in etch rate has been observed due to state of bending stress in silicon.

Also, it is known that masking films such as SiO_2 and Si_3N_4 apply significant stress to the silicon substrate. This topic has been addressed for KOH etching of Si [66] and some significant effects were found.

This chapter presents some experiments carried out to determine how stressed Si (both due to thin film mismatch stress and due to bending stress) behaves during etching in TMAH.

6.1 Experimental Procedure

To study the effect of stress applied to silicon substrate due to thin film masks, samples covered with SiO_2 and Si_3N_4 were used. Silicon dioxide film were grown thermally using wet oxidation at 1100^0 C to thicknesses about 0.6 to 1 μm. Silicon dioxide always

applies tensile stress to the substrate and in this case it is in the range of 2-8 $\times 10^8$ Pascal [66]. On other samples, silicon nitride layers were deposited in states of both compressive and tensile stress of similar values as that of the oxide films. The patterns on the samples covered with nitride were donut-shaped openings, while on the samples covered with oxide, square-shaped opening were created. These samples were etched in TMAH 25 wt.% at 80^0 C for 2 to 4 hours and no difference was observed in the etch rate of the samples and quality of the etched surfaces.

The stress that the masking film applies to the Si is mostly concentrated at or near the film/Si interface. Therefore it is possible that during an etch to a depth of several tens of microns, this stress might not have enough of an effect to be visible.

Therefore, as a supplement to the above film-stress tests, another experiment was attempted, wherein the entire wafer was macroscopically bent. In this way the entire thickness of the wafer was subject to significant stress. In Fig.6.1 it is shown how bending stress was applied to a rectangular piece of silicon. Strips of {100} silicon with dimensions about 1.5 cm $\times$ 7cm were cut and patterned using a square array pattern (Fig.3.3) or triangles pattern (Fig.4.1). The bending of the sample was accomplished by squeezing the sample in the blades of the teflon basket used to hold the samples during etching. As is shown in the Fig.6.1, bending in the range of 1.2-1.3 mm has been obtained. By using the relation for mechanical stress in this case [67] the value of stress, τ, is calculated to be a function of distance x from center of bending. the relation is as follows:

$$\tau = \frac{12 \cdot E \cdot \Delta \cdot t \cdot (\frac{l}{2} - x)}{l^3} \qquad (6.1)$$

in which τ is stress, E is the Young's modulus of Si (1.9×10^7Newton/cm^2), Δ is the amount of bending, t is the thickness and l is the length of the silicon sample and x is the

distance from center of bending (the units of Δ, t, x and l all should be the same as each other). By substituting the values of parameters in Eq.(6.1) and Eq.(6.2), value of stress is obtained in terms of x (x is in cm):

$$\tau = 1.954 \times 10^9 \times (3.5 - x) \text{ Newton/m}^2\text{(Pascal)} \qquad (6.2)$$

Experiments were carried out at concentrations of 15 and 25 wt.% at 80° C. In some of the experiments three samples were used: (1) one with pattern at the side with compressive bending stress and (2) one at the side of the sample with tensile bending stress.

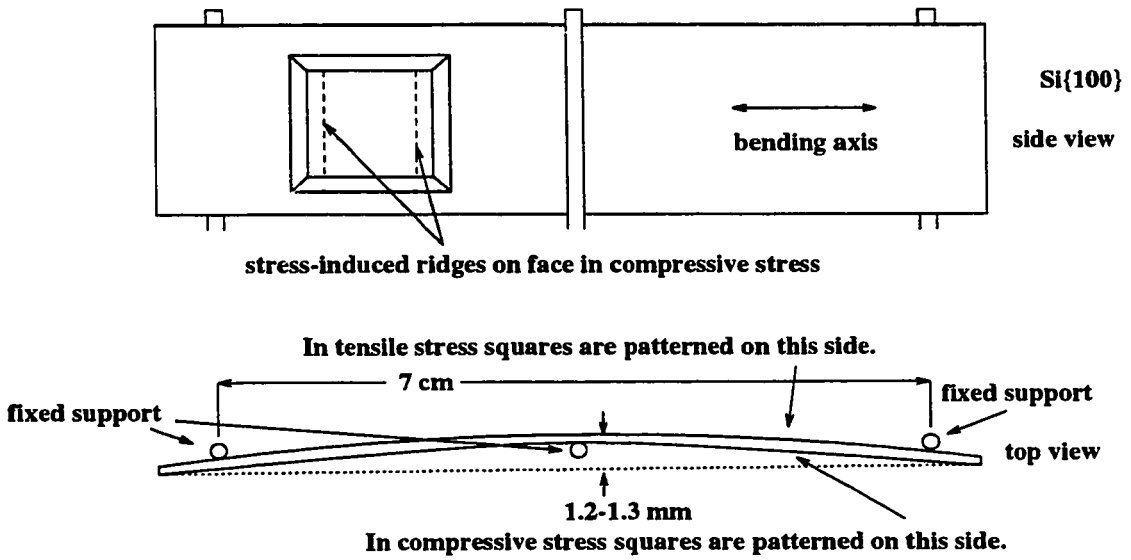

Fig. 6.1: Description of application of stress

The third sample, if used, was for the purpose of having a stress-free sample for comparison with the other two samples.

6.2 Etch Rate Result

For the experimental conditions described above, the etch rate of the base {100}

plane of stressed samples was found to be unchanged within the resolution of the optical microscope used. Also the quality of the surfaces of samples were observed not to change. The only effect observed, which was definitely due to the state of compressive stress was the appearing of ridges in the etched area wherever the edges are perpendicular to the axis of bending as shown in Fig.6.1. Examples of these ridges are shown in the photographs in Fig.6.2 and Fig.6.3. The ridges seem to be the result of intersection of slightly sloped surfaces with the base {100} surface, but attempts to find any etch depth difference in these two surface failed (difference<1 μm). It is observed that the width of ridges are maximum at the center of bending. As the distance of the square windows from the center of bending increases the width of ridges also decreases. This is shown in graphs drawn in Fig.6.4. At the two outer supports, the stress reduces to 0, and the ridges no longer appear. In these two graphs the width of ridges are shown as a function of distance from center and applied stress. Fig.6.5 shows a magnified version of the lower part of the Fig.6.1 to show the match between value of stress and the distance from center of bending in silicon sample.

6.3 Underetch Rate Under Conditions of Applied Stress

In the same way that it was explained in Chapter 4, a pattern of group of triangles were created on rectangular silicon samples. Two samples were etched in TMAH 25 wt.% at 80^0 C for 3 hours. One of the samples was in compressive stress and the other one in tensile stress. The amount of stress was very similar to what is shown in Fig.6.4.. The underetch rates of these two samples were measured with the result shown in Fig.6.6. There is no observable difference in between the underetch rate of the two cases of stress.

6.4 Conclusion

As indicated at the beginning of this chapter, the aim of these bending stress tests was

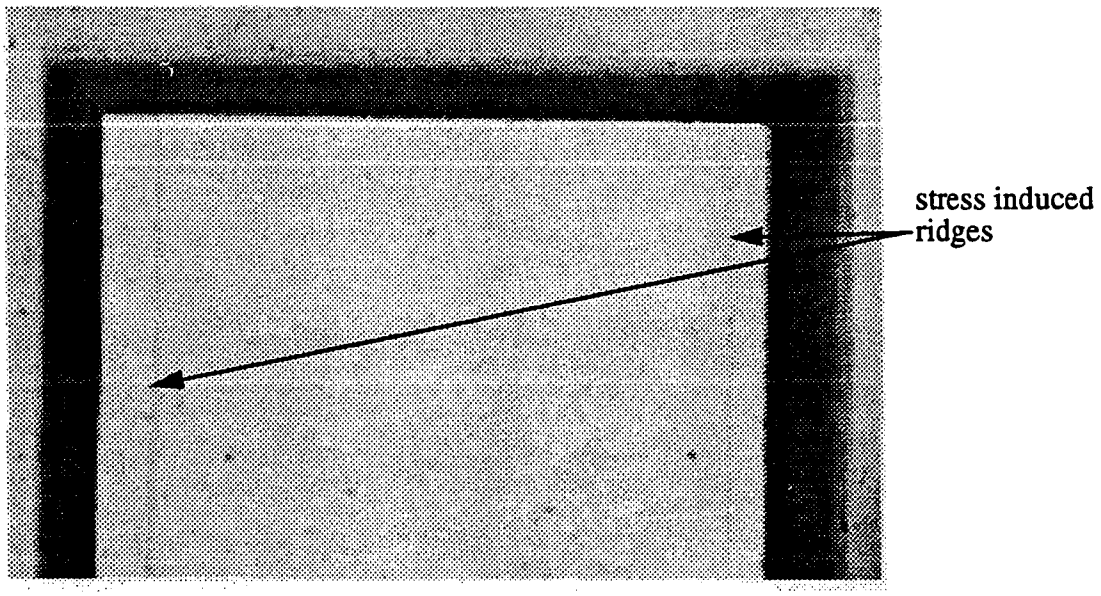

Fig. 6.2: Optical micrograph of the square opening in the oxide mask, after 2:30 hours etch in TMAH 25 wt.% at 80° C under compressive stress, showing stress induced ridges at left and right. (Magnification= x 500)

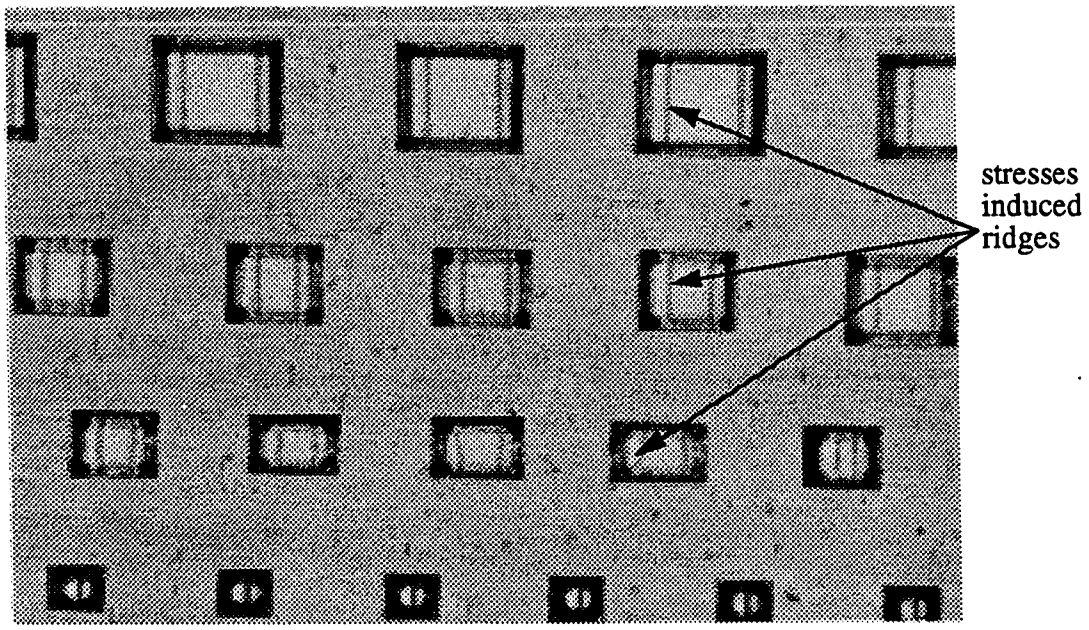

Fig. 6.3: Optical micrograph of array of squares demonstrating stressed induced ridges only at left and right of each square (magnification= x 50).

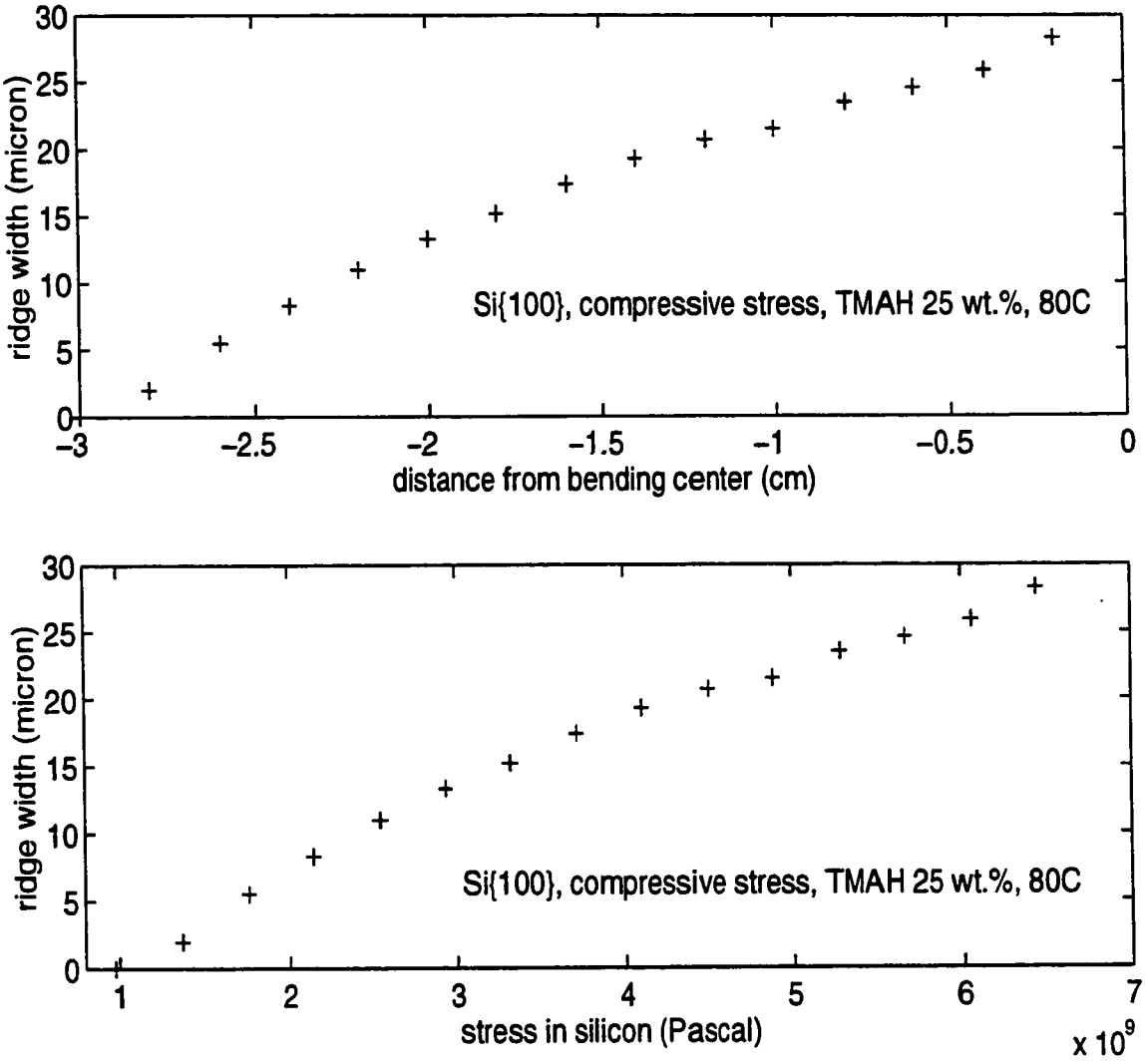

Fig. 6.4: Width of ridges vs. applied stress and distance from center of bending

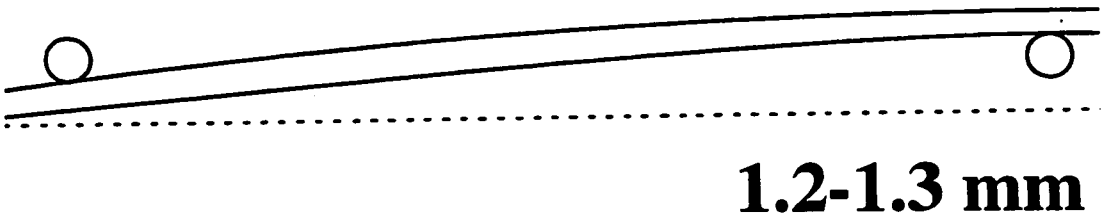

Fig. 6.5: Magnified copy of lower part of Fig.6.1 to show the relation between stress and bending of silicon

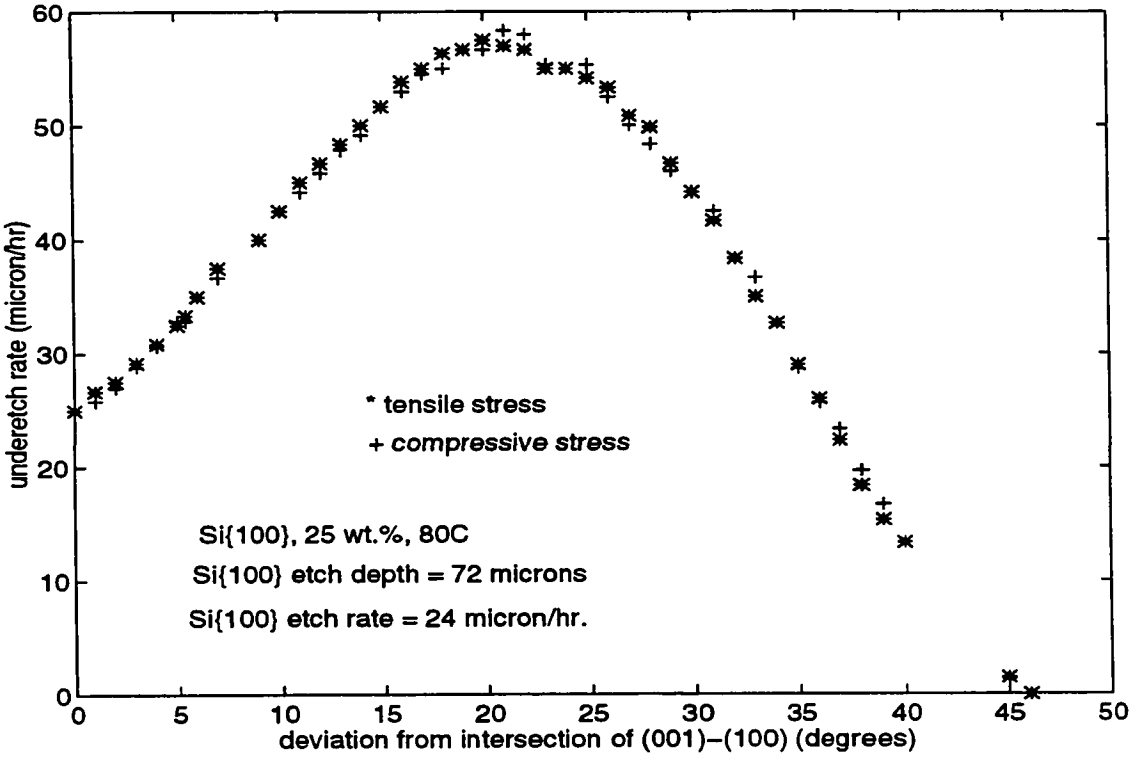

Fig. 6.6: Comparison of underetch rate of samples in tensile stress and compressive stress.

to investigate the possibility of the state of stress being involved in the etching mechanism. In summary, no stress-induced effect was observed for etching of Si {100} in TMAH 25 wt.% at 80° C, except for the presence of subtle ridges under compressive stress. Therefore, it can be deduced that the etching mechanism at 80° C in 25 wt.% is not determined by sensitive variations in bond energies but rather by more robust phenomena such as number of back-bonds, availability of kinks and steps on the surface of silicon, etc.

CHAPTER 7

Examples of the Use of TMAH in MEMS Device Fabrication

7.1 Introduction

As was mentioned in Chapter 1 the mature techniques and methods of planar microelectronics fabrication devices can be used in the fabrication of micro electromechanical systems and devices. Because of its distinctive properties, as explained in Chapter 3, TMAH is a very suitable etchant to be used for post-processing of devices and structures fabricated by standard CMOS processes. In this chapter two examples of application of TMAH etching in fabrication CMOS based microelectromechanical devices are explained.

By using the CMC-Mitel-1.5 μm process (Appendix B) typical oxide cantilevers as described in Fig.7.1can be made. Such a structure can be used as piezoresistive accelerometer. Such devices can be created readily by leaving some area of silicon around the oxide cantilever exposed so that it can be attacked by anisotropic Si etchant. As was mentioned in Chapter 3 silicon dioxide and nitride are not etched in TMAH appreciably.

However, the release of oxide cantilever structure can have problems due to the stress in the oxide layers, which can lead to device failure[1]. This chapter will demonstrate one possible strategy for alleviation of these problems by using release-control structures and careful consideration of etch anisotropy.

1. This was discovered and explained by researchers at the LISA lab at Ecole Polytechnic: Professor John Currie, Robert Antaki and Gord Harling.

7.2 Cantilever Structure and Release Problem.

Cantilevers, whether they are made of silicon or silicon oxide can have various applications in microsensor devices [20]. The cantilevers designed and implemented here are made of silicon dioxide. Fig.7.1 shows how a meandering resistance made of poly silicon is sandwiched between thermal oxide and all the other layers deposited on top of it. Before release the area around the cantilever is bare silicon. To expose the silicon to the anisotropic etch, different opening masks are defined on top of each other, all of them on top of the active area. The region defined by the active area is covered by a thin layer of gate oxide (thin, as opposed to field oxide which is much thicker). The opening masks mentioned above are: contact cut opening, via cut opening and passivation layer opening respectively. The contact cut allows contact between the metal 1 layer and the poly silicon layers or substrate. Thc via cut opening allows contact between the metal 2 and metal 1 layers; and the passivation opening creates an opening which exposes metal 2 layer to the air. By looking at the Fig.1.B (Appendix B) it is clear that by stacking all of these openings on top of active area, the silicon substrate will be exposed.

When such a structure is immersed in an anisotropic etchant, the open area will be attacked and gradually the silicon underneath the oxide cantilever will be etched in the way shown in Fig.7.2. In this design the edges of the cantilever are aligned with the intersection of a {111} plane and {100} plane. After the cantilever is fully released, its cross section is ideally expected to be as shown in Fig.7.1 b. By bending the cantilever with any external force applied to it the poly silicon resistor embedded in the cantilever will also be bent, and, because of piezoresistivity, the value of its resistance will change. This property

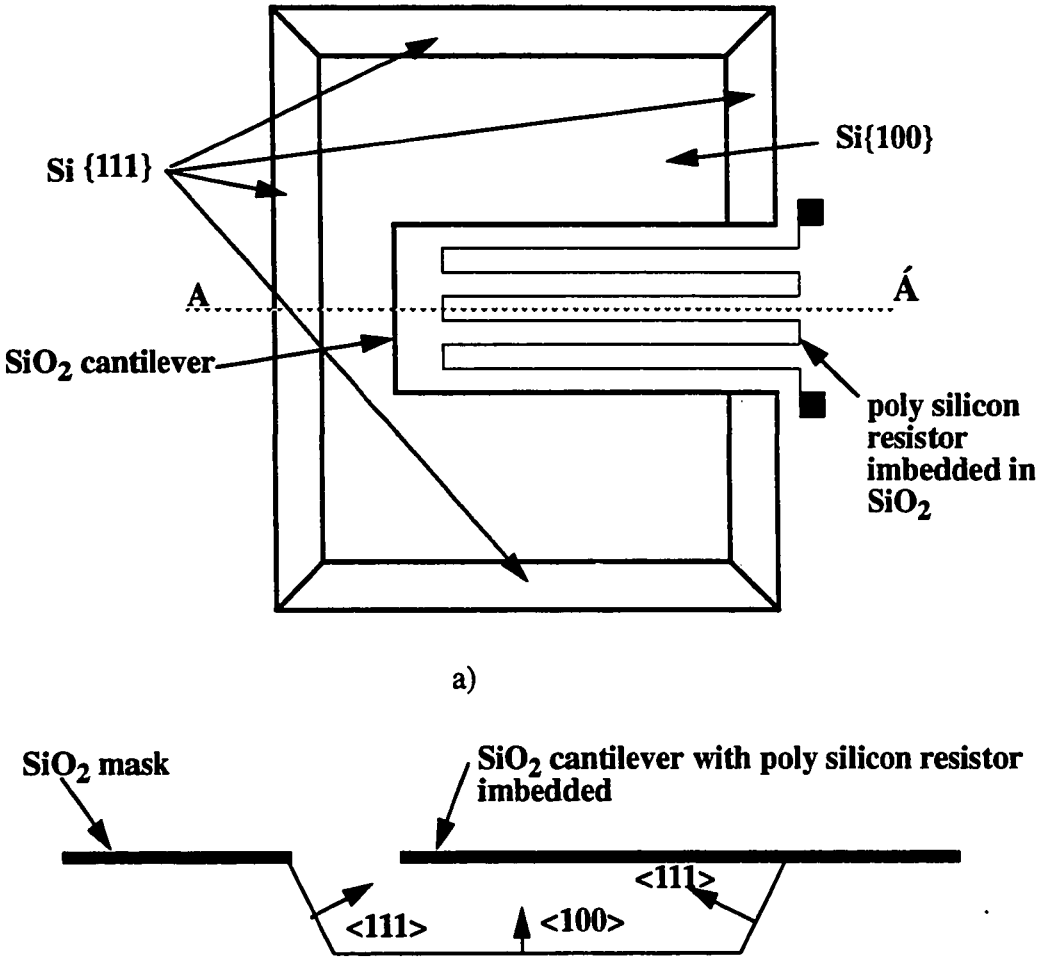

Fig. 7.1: (a)Top view and (b) view of the A-Á cross section of the oxide cantilever fabricated on a Si {100} wafer and released using anisotropic etching.

can be used to detect forces applied to the surface, or can be used as an accelerometer for measuring acceleration in the direction perpendicular to the cantilever surface [20].

However, in actuality there is a problem in releasing this simple cantilever structure. This problem was caused by the residual stress in the cantilever structures, inherent to the layers fabricated by the host process (Mitel 1.5 μm process). Fig.7.2 shows some intermediate stages which are attained during silicon etching. The underetch of the cantilever starts by the etching of convex corners, where fast etching planes emerge as are shown in the Fig.7.2. By continuation of etching the silicon beneath the oxide becomes a triangular structure which has a sharp corner. At this stage of etching, the released part of cantilever bends upward because of internal stress in the field oxide. The special shape of the silicon under the oxide causes that this bending happens in a nonuniform way which can cause a catastrophic device failure during the release process. It has been observed that in the course of etching some cracks appear in the oxide through which TMAH penetrates and attacks the poly silicon resistance in the cantilever. These cracks appear at the points which sharp corner of silicon appears underneath the oxide and with progress of etching they develop through the length of the cantilever. This is shown in the Fig.7.3 which is a SEM picture of simple cantilever structure. The white area close to the edge of the cantilever is a metal strip which was placed to strengthen the structure and keep the cantilever from bending upward. The white area at the center of the cantilever is because of cracks which have appeared during etching time.

Due to the above problem, the "cantlers" structure was developed as described below.

7.2.1 "Cantlers" Structure: Cantilever with "Antlers"

As it was explained above, bending of the thermal oxide during the anisotropic etching process is the reason for the cracks in the oxide. One way to avoid this problem, would be to keep the cantilever flat and unbent until all the silicon under the cantilever is etched. If the releasing of the cantilever were to happen after this, it would again bend upward

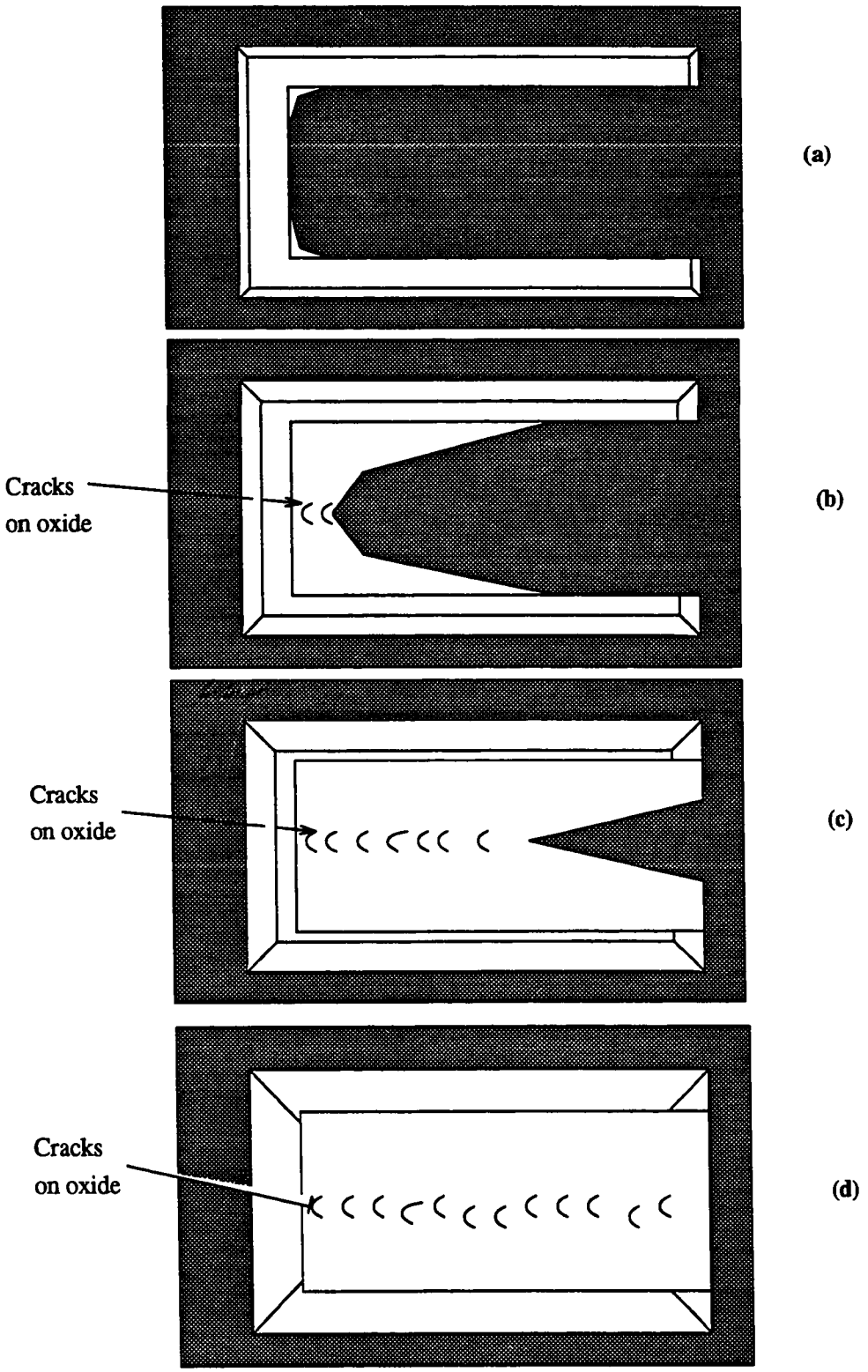

Fig. 7.2: Top view of a simple structure cantilever after: a) short time of etching, b) after an intermediate length of etching, c) after a long time of etching, d) after cantilever is released.

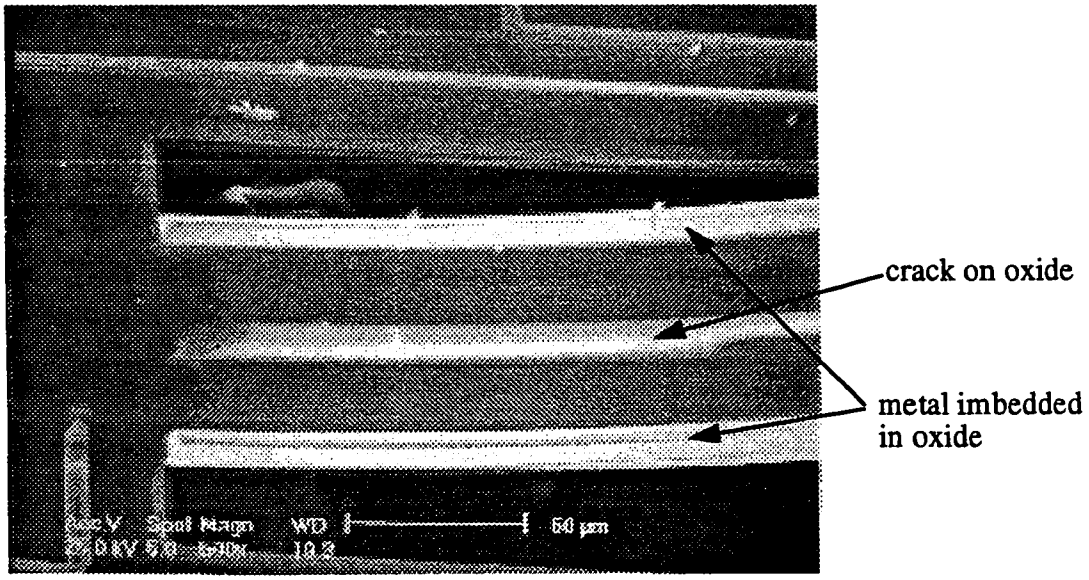

Fig. 7.3: SEM photograph of a released oxide cantilever. The white area at the middle is due to the cracks on the oxide. The white area around the cantilever is the effect of a strip of metal layers embedded in oxide.

because of internal stress in the oxide but since there would not be any mesa shape of silicon beneath the oxide, the bending would be uniform across the width of the cantilever and no crack would be created. The structures shown in Fig.7.4 are two different alternatives[1] designed to keep the cantilever flat and horizontal during the etch. The extra sections of oxide are called "antlers" due to their appearance. The antlers are designed to not be released until the main cantilever has been completely underetched (released). Therefore the cantilevers stay flat until after they are released. By then continuing etching the antlers will become released and for the reason explained earlier the whole structure will bend upward, at line $A - A'$ indicated in the diagram.

In order for this to work, the sizes of the antlers and cantilevers must be such that, given the etch rates of emerging planes, the cantilever release takes place after antler release. Therefore knowing the underetch rates of silicon for different directions, as

1. The original "cantlers" design was done by Dr. L. M. Landsberger and Dr. M. Paranjape.

described in Chapter 4, is critical. To determine the correct dimensions for cantilevers and antlers some calculations are required. Since there are some convex corners etched in the anisotropic etching of silicon it is necessary to know which planes emerge at convex

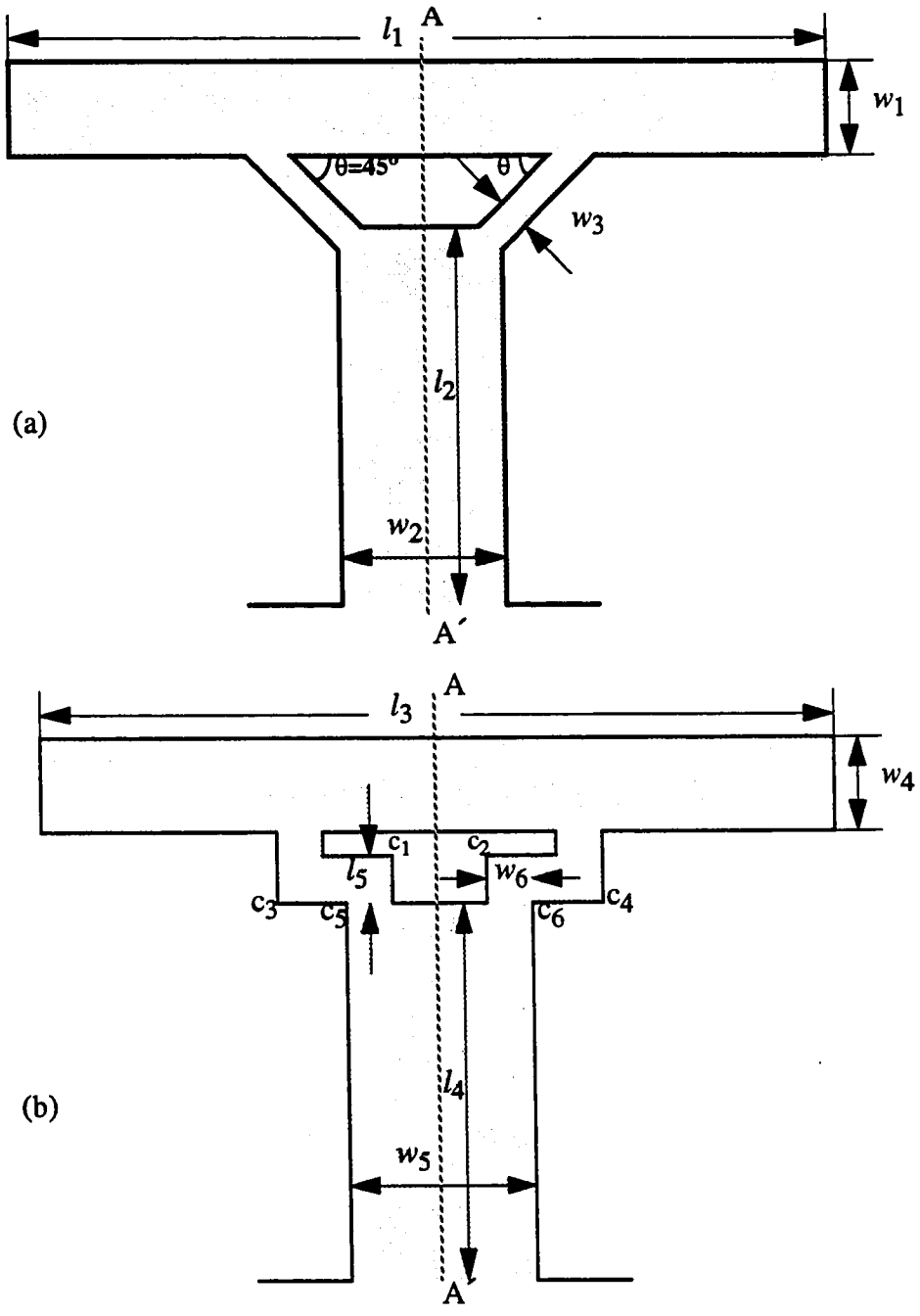

Fig. 7.4: Two different cantilever structure designed to solve the problem of cracking. Hatched area is silicon dioxide and area around it is bare silicon.

corners (which are the fastest etching planes) and what their etch rate is. In the cantilever shown in Fig.7.4 (a) it is also required to know what angle the connectors between cantilever and antler make with intersection of {111} and {100} planes and what underetch rate they have.

For calculating the time necessary for releasing a structure like antler, Fig.7.5 can

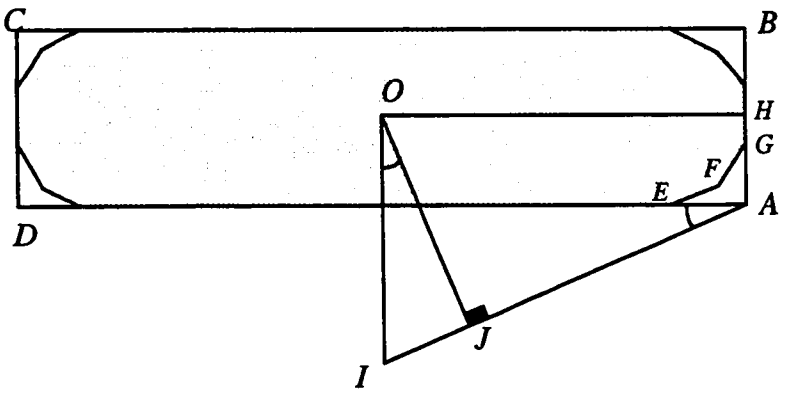

Fig. 7.5: Demonstration of derivation of time required for releasing a cantler.

be considered. Rectangle *ABCD* (made of oxide) is aligned with intersections of {111} and wafer surface therefore underetching happens only at the convex corners of *A*, *B*, *C* and *D*. In this figure four corners are shown after a short time of etching. Considering the corner *A*, lines *EF* and *FG* indicate the emerging planes at that corner. The etch front *FG* will disappear after some time of etching and only etch front *EF* will be left. This is shown in Fig.7.2 (b) and (c). Line *AI* has been drawn parallel to *EF*. The time required to completely etch underneath the rectangle *ABCD*, it is necessary that etch front *EF* should develop from corner *A* to the point *O*. This means that the distance $\overline{JO}$ should be etched completely. Value of $\overline{JO}$ is calculated as:

$$\overline{JO} = (\frac{\overline{AD}}{2}\tan(\angle IAD) + \frac{\overline{AB}}{2})\cos(\angle JOI) \tag{7.1}$$

and since $\angle IAD = \angle JOI$ next relation can be obtained:

$$\overline{JO} = \frac{\overline{AD}\sin(\angle IAD) + \overline{AB}\cos(\angle IAD)}{2} \tag{7.2}$$

By using the notations used in Fig.7.4 (a) it can be seen that the time needed for the antler release is:

$$t_1 = \frac{w_1\cos\phi + l_1\sin\phi}{2E_\phi} \tag{7.3}$$

in which t_1 is the time required for the antlers to be released, ϕ is the angle the fastest etching planes in {100} surfaces make with the intersection of wafer surface and {111} planes, and E_ϕ is the underetch rate of the fastest etching plane. By using the graph shown in Fig.4.8 it can be seen that $\phi \cong 24^o$ and $E_\phi \cong 58$ μm/hr. For calculating the required time for releasing the cantilever it can be seen readily that first, the silicon underneath the connectors must be etched completely and then convex corners of cantilever start being etched. Therefore the time required to release cantilever is addition of the time required to release the connectors and the time required to release the cantilever itself. The first part of the time can be calculated readily by looking at Fig.7.4 (a) and supposing that etch rate of undercut of the connectors is E_θ (it is called E_θ because rate of undercut is a function of θ as described in Chapter 4). Angle θ is shown in Fig.7.4 (a). Therefore the time required for releasing the connectors is:

$$t_2 = \frac{w_3}{2E_\theta} \tag{7.4}$$

Using Eq.(7.3) and Fig.7.4 (a), the time required for releasing the cantilever is calculated:

$$t_3 = \frac{w_2 \cos\phi + 2l_2 \sin\phi}{2E_\phi} \tag{7.5}$$

in which t_3 is the time required to etch the silicon underneath the cantilever entirely, w_2 and w_3 and l_2 are values of dimensions shown in Fig.7.4 (a), angle ϕ and E_ϕ are the same parameters as in Eq.(7.3). As was said earlier t_2+t_3 should be smaller than t_1 in order for release of the cantilever to happen before release of cantler.

Similar formulas can be written for the structure shown in Fig.7.4 (b). The only difference between the calculations for the two structures is in the calculation of the time required for the releasing of the bridges between cantilevers and antlers. Therefore the Eq.(7.3) changes to the following formula:

$$t_1 = \frac{w_3 \cos\phi + l_4 \sin\phi}{2E_\phi} \tag{7.6}$$

To calculate the time required to release the connectors, it can be seen from Fig.7.4 (b) that there are two convex corners in each connector (identified as c_1,c_3 and c_2,c_4 in Fig.7.4 (b)) but in this case the corners c_1 and c_2 (which have the distances w_6 and l_5 from the edges of the cantilever) are important, because after etching starts these two corners reach the two concave corners c_5 and c_6 before c_3 and c_4. Therefore the time required for corners c_1 and c_2 to be etched to expose corners c_5 and c_6 to etching is:

$$t_2 = \frac{l_5 \sin\phi + w_6 \cos\phi}{E_\phi} \tag{7.7}$$

The time for releasing the cantilever is:

$$t_3 = \frac{2l_4 \sin\phi + w_5 \cos\phi}{2E_\phi} \tag{7.8}$$

in which ϕ and E_ϕ are same as in Eq.(7.3) and other parameters are dimensions shown in Fig.7.4 (b). Same as the case of the previous cantilever, t_2+t_3 should be smaller than t_1 in order for release of cantilever to happen before antler.

In the derivation of Eq.(7.3)-Eq.(7.8) it is supposed that {111} planes have a negligible etch rate (confirmed by data in Chapter 3,4).

At first, the designs sent to CMC for fabrication in Mitel-1.5 μm process, the underetch rate of silicon in TMAH was not yet available and the dimensions of the structure were not designed precisely, and the result of etching the chips in TMAH was not successful (all cantilevers had crack in them after etching was finished).Therfore for the next run of fabrication, the dimensions of structures were modified based on the underetch rate data (It was assumed that TMAH used in the releasing the structures is 25 wt.% at 80^o C). Dimensions of structure shown in Fig.7.4 (a) are: w_1=70 μm, l_1=670 μm, w_3=32 μm, l_2=200 μm and w_2=100 μm. Substituting these values in Eq.(7.3) to Eq.(7.5) gives the times of t_1=174 minutes, t_2=40 minutes and t_3=131 minutes, which indicates that cantilever is released 3 minutes before antler. This time interval is too short and if there is any tolerance in the dimensions of structure or in the underetch rate data it is possible that releasing of the cantilever happens before releasing of the antler. After etching of the cantilevers with dimensions mentioned above, it was observed that there are some cracks on the cantilever. This observation most probably means that the antler has been released before cantilever. This also means that t_2+t_3 is greater than t_1. The time interval by which antlers were released before cantilevers could not be measured accurately but it is believed that most probably it was less than 10 minutes.

To solve this problem the possibility of using different etch conditions was consid-

ered, to give somewhat different underetch rates so as to solve the timing problem in releasing the cantilever. By checking Eq.(7.3) to Eq.(7.5) it can be seen that if the angle ϕ does not change in two different etchants, it is possible that by changing the ratio of $\frac{E_\phi}{E_\theta}$ change the difference t_1-(t_2+t_3) to a positive value. In Chapter 4 different underetch rate curves for different concentrations were given. It can be seen that for the concentration of TMAH 15 wt.% and temperature 80° C (Fig.4.13) the underetch rate curve has a $\frac{E_\phi}{E_\theta}$ smaller than that of the TMAH 25 wt.% at 80° C and has almost same angle ϕ=24° as in the TMAH 25 wt.% at 80° C. The values of E_ϕ=50 μm/hr and E_θ=35 μm/hr are obtained from graph shown in Fig.4.13. Using Eq.(7.3) and Eq.(7.5) values of t_1=202 minutes, t_2=8 minutes and t_3=152 minutes are determined. These data show that cantilever is released 40 minutes before antler. This structure was etched in TMAH 15 wt.% at 80° C for 5 hours so that connectors are underetched completely and then etching is continued. In this case the time distance between releasing of antler and cantilever is longer and most of the releasing of cantilevers are successful. In Fig.7.6 picture of a released cantilever without crack is shown.

For improving the design shown in Fig.7.4 (a) it can be seen from figure that by changing the angle θ shown in the figure, to a value which has a higher rate of undercut it is possible to etch the silicon underneath the connectors faster than in the present case with θ=45°. Again by looking at the curve shown in Fig.4.8, it is clear that by choosing the angle θ≅68° the time t_2 in Eq.(7.4) is decreased because E_θ has increased. This point was considered in the new design of cantler structure sent to CMC for fabrication (die not yet received from CMC at this writing.)

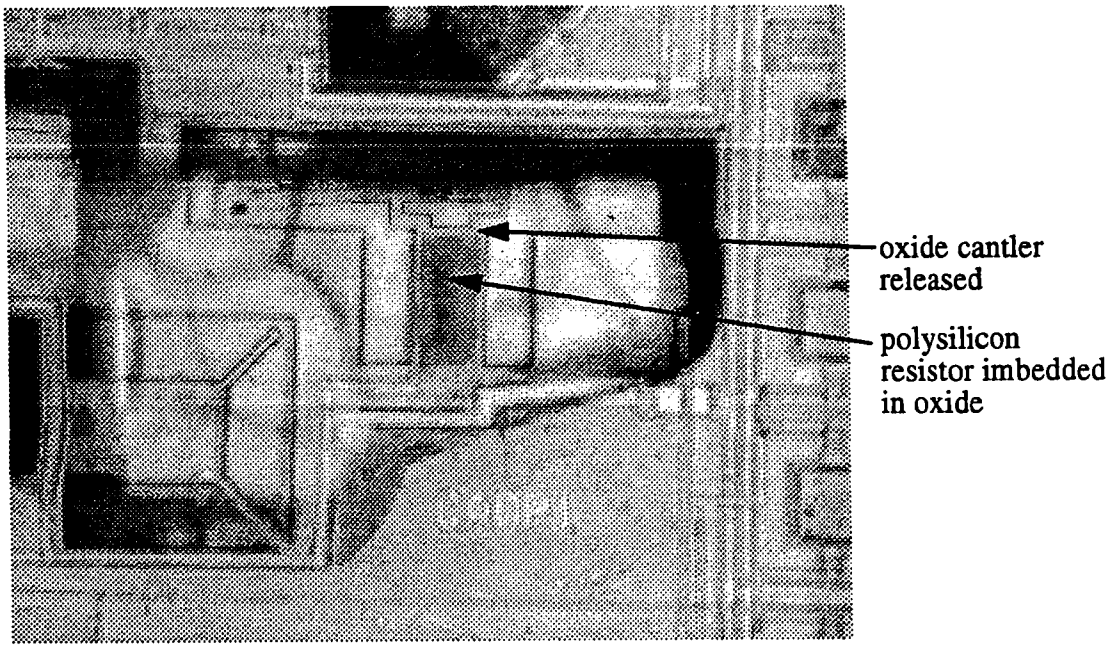

Fig. 7.6: Photograph of an intact cantilever.

7.3 The Behavior of Aluminum in TMAH

7.3.1 General

One important problem in the fabrication of devices such as what explained above is that during anisotropic etching of silicon all exposed aluminium is attacked by the TMAH [55,56]. The pads which connect all circuitry to the outside world are an example of this.

To solve this problem either an etchant should be used which does not attack aluminum, like hydrazine, or an extra process should be carried out on the wafer so that all area which require protection are covered with some layer resistant to etchant. For this purpose an alloy of chrome-gold is suggested to be deposited on the aluminum pads.

While this causes problem in that it makes the above structure impossible to test with-

out protecting the pads during etch, it suggests the possibility of surface micromachining using sacrificial metal instead of usual sacrificial oxide.

In the next sections behavior of aluminum and a potential application of aluminum as sacrificial layer is explained.

7.3.2 Characteristics of Aluminum Etching

To see how fast aluminum is etched when it is sandwiched between two layers of oxide, a structure which consists of a long metal 1 (Appendix B) tube with a width of 30 μm and a length of 1165 μm embedded between deposited oxide layers has bee designed and an inlet was placed at on end of this long strip of metal 1. In Fig.7.7 the cross section view and side view section of this structure is shown. TMAH used at 80° C with a concentration of 25 wt.% attacks aluminum through the inlet and creates an empty space which can be compared to a long narrow tube. The aluminum was etched with a rather uniform rate along the length of the tube as shown in Fig.7.8. Gas evolution during the dissolving aluminium in TMAH is considered as a cause of stirring of TMAH which makes the supply of etchant stay fresh during most of the etching and therefore etching is done with uniform etch rate.

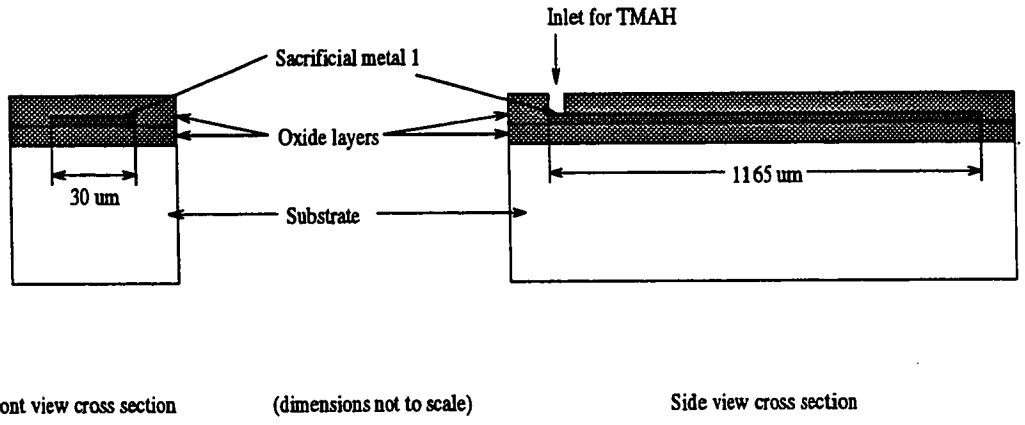

Fig. 7.7: Structure used to determine aluminum etch rate in Mitel 1.5 μm process.

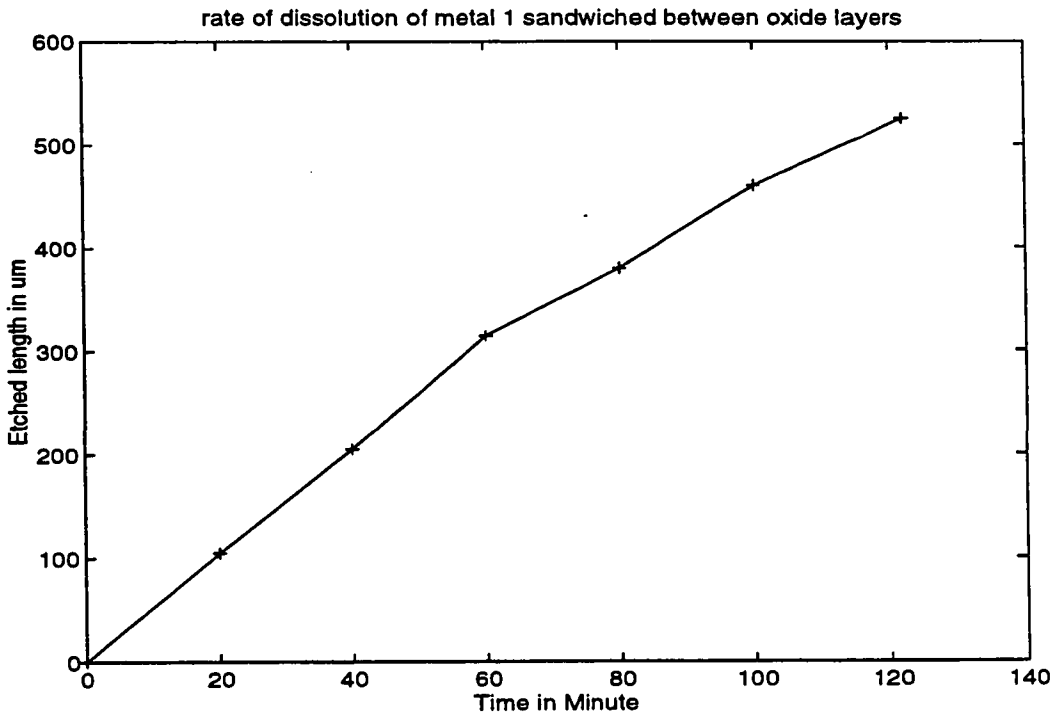

Fig. 7.8: Characteristics of aluminium etch rate in TMAH 25 wt.% at 78° C.

From the curve shown in Fig.7.8 it is reasonable to estimate the etch rate of the sputtered aluminium is equal to 5 μm/min. in TMAH 25 wt.% at 80° C. This experiment indicates that sacrificial metal processes using TMAH to release oxide structures may be promising.

CHAPTER 8

Conclusions

8.1 Overview

This work attempts to provide experimental data in the study of anisotropic etching of silicon in TMAH solutions. Important motivations for this study were:

- Anisotropic etching is a critical process and post-process step in micromachining devices such as microsensors and microactuators.
- Other anisotropic etchants for silicon have been studied at length by other researchers, and have been found to have problems: either serious toxicity issues or incompatibility with CMOS processes. On the other hand, TMAH is relatively non-toxic, and is only recently beginning to be reported in the research community.

The aim of this research was to investigate TMAH, both for practical use in micromachining applications, and to provide data to better understand the fundamental mechanisms of anisotropic etching of silicon.

In this regard, a variety of experiments were conducted. Data regarding the etch rate and parameters affecting the etch rate were collected and compared, in certain cases, with results from other etchants reported in the literature. Measurements of underetch rate were executed to observe the variation of etch anisotropy with crystal orientation. The appearance of hillocks, which is a common phenomenon in all of the anisotropic etchants of silicon, was studied in detail. The effect of bending stress on the etching of silicon in TMAH was studied. The etch information gathered was used in post-processing devices made in Mitel's 1.5 μm CMOS technology.

8.2 Contributions

In Chapter 3, basic etch rate experiments were reported on Si{100} and Si{110}, as well as various masking materials, in TMAH at 5, 15, and 25 wt.% and at 50-90° C. It was found that:

- Results of basic etch rate measurements of Si {100} and Si {110} in TMAH 25 wt.% and 15 wt.% in almost all cases were in good agreement with other reported results.
- Stirring had no effect on the etch rate in 15 wt.% and 25 wt.%, suggesting that the etch reaction is surface-reaction-limited rather than reactant-diffusion-limited.
- However, etching at 5 wt.% was found to be accelerated by stirring, indicating that at this concentration diffusion of reactive species in the etchant to the etching surface becomes an important rate-limiter.
- The etch rates of thermally grown SiO_2 (57 Å/hr) and Si_3N_4 (7 Å/hr for LPCVD nitride and 15 Å/hr for PECVD nitride) in TMAH were found to be in agreement with other reports.
- The etch rate of spin-on glass (SOG) in TMAH 25 wt.% at 80° C was measured (440 Å/hr).
- Titanium nitride (TiN) was found to be very resistant to etching in TMAH.

In Chapter 4, underetch rates and underetched inclined planes of Si{100} as a function of mask-edge deviation angle were measured for TMAH 25 wt.% at 80° and 50° C, and for TMAH 15 wt.% at 80° and 50° C.

- A mask was designed consisting of group of aligned right angled triangles which exposes bare silicon to etchant with different mask edge deviation from 0-40° in steps of 1°.
- Using the triangles mask, underetch rates of Si in TMAH were measured and it was observed that they are a strong function of TMAH concentration.
- Underetch rate of Si{100} in TMAH 25 wt.% at 50 and 80° C were measured and emerging planes were examined. Underetch rate curves in these two cases are similar and the difference is basically a scaling factor. SEM pictures showed that the emerging planes are also similar in these two cases.
- At a deviation angle of 0° from the intersection of (100)-(001) in the cases of TMAH 25 wt.% at 50 and 80° C, the emerged plane consists of a vertical Si{100} with a very smooth surface, and another sloped plane with a rough surface at the bottom of the etched pit.

- Si{100} plane is a local minimum in the underetch rate at these two conditions. The pronounced nature of this minimum explains the smoothness of etched surfaces, both vertical and horizontal.
- The underetch rate curve in Si {100}, TMAH 25 wt.% at 80° C was compared with that of KOH and EDP type "T". Qualitatively, these curves are very similar but quantitatively there are some differences among them (Fig.4.10).
- The fastest underetching planes in TMAH appear at a deviation angle of about 22° and were identified as {252} planes in TMAH 25 wt.% at 80° C. Si {111} planes have the minimum underetch rate and have a very smooth surfaces.
- Underetch rate of Si{100} in TMAH 15 wt.% at 80° C and 50° C were measured. The emerged planes in these cases are totally different from the case of TMAH 25 wt.%. At 0° deviation, the emerged planes are a Si{110} which is a local minimum underetch rate in the curve.
- In the case of TMAH 15 wt.%, 80° C, the fastest underetch planes appear at same deviation angle as 25 wt.% (δ=22°). These planes were identified as Si{525}.
- In the case of TMAH 15 wt.% at 50° C the underetch rate curve of Si{100} was found to have a similar shape to the case of Si{100} in TMAH 15 wt.% at 80° C but scaled down.
- dissolved silicon in the TMAH 15 wt.% at 50° C can have considerable effect on the anisotropy of silicon etch rates.
- A simple model for predicting the emerging plane in the case of TMAH 15 wt.% with a silicon content of 0.6 gr./liter at 50° C was suggested.
- As opposed to more typically-found anisotropy, the {110} plane was found to be etching at a slower rate than {100} under certain conditions.
- For Si{110}, it was found that the underetch rates of Si {110} in TMAH 25 wt.% at 80° C are qualitatively similar to those found in other etchants. The local minima in the underetch curves are {100} and {111} planes.

In Chapter 5, the evolution of hillocks during anisotropic etching of silicon in TMAH was studied. It was found that:

- Typical near-pyramidal hillocks were found to occur in high densities when etching at concentrations less than 20 wt.%.
- They were observed to reach sizes of up to > 20 μm after etching for 2 hours in 15 wt.% at 80° C.
- Each hillock face is made up of two sub-faces, near to made up of {332} planes, slightly deviated from {111} planes.

- It is found that the normal life cycle of a hillock is disturbed by interrupting the etch. After brief re-etch, essentially all of the larger hillocks change shape dramatically to become more regularly octagonal, and are quickly attacked from the apex.
- It was observed that hillock formation is affected by stirring of the etch solution. The area which is more exposed to agitation of solution has more hillocks than the areas which are protected from agitation.
- At higher etch temperatures, the hillocks formed are distinct and their aerial density of hillocks is uniform. At lower etch temperatures, the hillocks mostly overlap each other and they are distributed non-uniformly on the etched surface.
- Contamination was found to be a possible source of hillocks formation.

In Chapter 6, the effect of applied bending stress on silicon pieces during etching is studied. It was found that:

- Compressive or tensile bending stresses were applied to strips of Si with patterned SiO_2 on one side and un-patterned SiO_2 on the other side, such that the bending and stress varied from 0 at the ends to a maximum ~ 10^9 pascals at the center. The etch rate of Si{100} in open squares was not found to vary with stress, neither in the compressive nor in the tensile case.
- The underetch rate variation with mask deviation angle is unaffected by bending during etching in TMAH 25 wt.% and at 80^o C.
- These results suggest that the etch mechanism is mostly determined by more robust phenomena (such as the number of back-bonds or density of kink sites) and not by sensitive variation in bond energies.
- Nevertheless, subtle stress-induced ridges are observed on etched surfaces near to mask edges perpendicular to the bending axis. The distance of these ridges from the mask edges was found to vary with the stress.

In Chapter 7, the use of TMAH in post-processing of a standard CMOS process (CMC-Mitel's 1.5 μm process) was demonstrated. A particular issue was addressed: the creation of cracks and damage in a bulk-micromachined cantilever during post-process release, due to structural deformations during the release. In this part of the work:

- Two different cantlers structures were devised, to keep the main cantilever flat, in spite of intrinsic stresses, until it was completely released. This was accomplished by the addition of "antlers" which held the main cantilever down until it was completely underetched.

- The underetch results of Chapter 4 were successfully used to design a post-process release etch to successfully release a cantlers structure without incurring stress-induced damage to the imbedded polysilicon lines. Also, for improving the fabricated designs some modifications were suggested and incorporated in later designs.
- Also, the etch rate of sputtered aluminium in TMAH 25 wt.% at 80^{o} C was measured (5 μm/min.). This suggests the use of TMAH for surface micromachining, releasing SiO_2 structures by etching Al.

8.3 The Importance of Future Study of Anisotropic Etching

The study of anisotropic etching for bulk micromachining of Si is quite important and is becoming increasingly involved. Further experimental and theoretical study are required. Careful study of underetch rates and emerging planes of silicon as a function of a broader range of concentrations and temperatures of TMAH is warranted. Also, different doping types in the silicon and different silicon content in the TMAH should be studied.

In particular, the mechanism of hillock creation is not yet understood. More theoretical and experimental work is necessary to understand how to control and eliminate them, for example if a silicon trench is intended to hold an optical fiber.

There is great potential for sculpting special-purpose shapes in Si, for example in the fields of microsensors and opto-electronics. At present, only a limited set of shapes are available, usually constrained by {111} planes. Detailed study of etch anisotropy as a function of etch chemistry has the potential for enabling a much wider variety of etched shapes.

Appendix A

RCA cleaning procedure

Cleaning of the wafers is one of the most important steps in the VLSI fabrication process and all the samples, if there is no metal exposed, one should go through this process before any high temperature step. Following procedure which has been developed in RCA has been used very successfully from the time it was devised [68,69]. It consists of the following steps:

1-Dipping the samples in boiling solution of (H_2SO_4: H_2O_2, 1:1) for 5 minutes. This step removes the gross residues of photoresist and other organic contamination. The solution mentioned is also called piranha solution. After this step samples should be rinsed with DI water for enough long time.

2-Dipping the samples in the (NH_4OH:H_2O_2:H_2O, 1:1:5) at temperature 75^o-80^o C for 5 minutes. This step removes the organic contaminations on the surface of the samples and also some kinds of metal like group IB,IIB metals and some other metals like gold,silver,copper,nickel,cadmium,zink,cobalt and chromium are dissolved and removed.

3-Dipping the samples in (HF:H_2O,1:50) for 15 seconds. This step removes the thin layer of oxide created at the previous step. samples should be rinsed with DI water.

4-Dipping the wafers in the solution of (HCl: H_2O_2:H_2O, 1:1:5) for 5 minutes at the temperature 75^o-80^o C. This step removes the alkali ions from the surface of the samples. After this samples should be rinsed with DI water and dried using blow of nitrogen.

Appendix B

Mitel 1.5 μm CMOS technology description

Fabrication of integrated circuit design is based on deposition of thin films and photo-lithography. For designing a circuit with a particular technology it is necessary to know different layers and their electrical parameters like resistivity and distributed capacitance. For designing micromachining devices using standard technologies, again same type of information about technology which is used for design is required. Following figure shows different layers of materials and their thickness which is used in Mitel 1.5 μm CMOS technology which was used for designing some devices in this work.

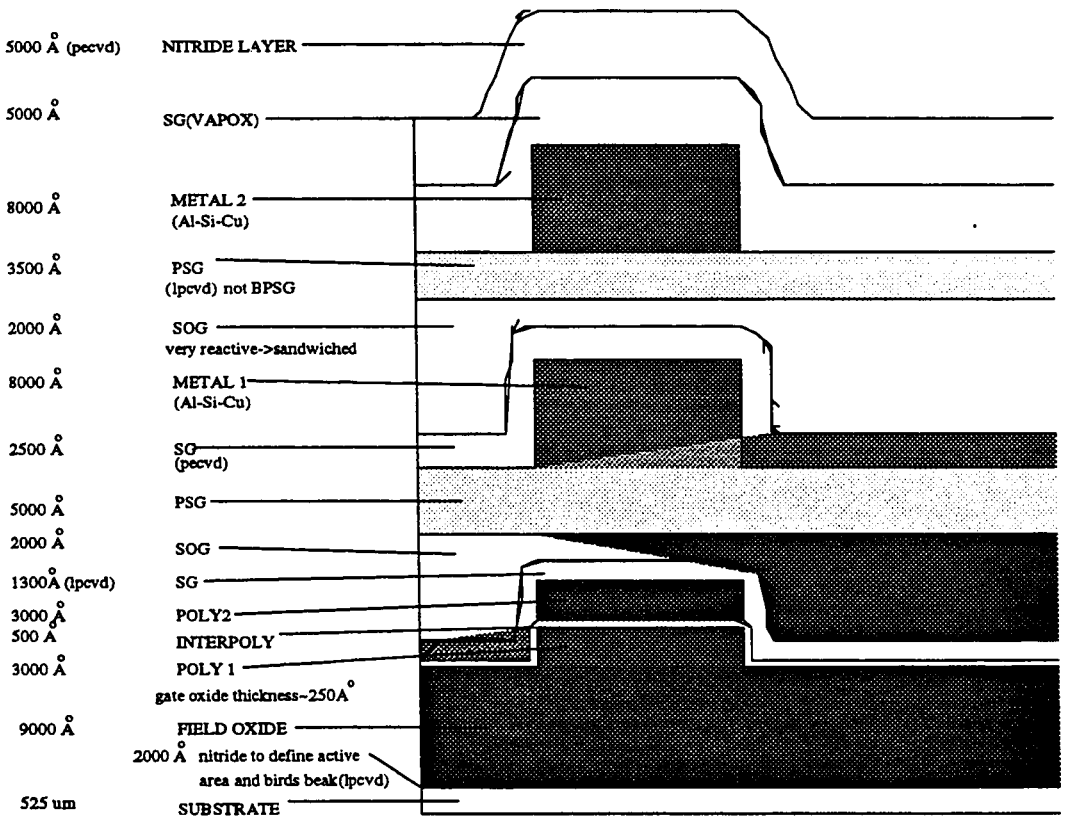

Fig. B.1: Cross section of Mitel 1.5 μm CMOS technology.

References

[1] K. E. Peterson, "Silicon as a Mechanical Material," *Proc. of IEEE Electron Devices,* 70 (1982), p. 420.

[2] *"Transducers' 93. The 7th International Conference on Solid-Sate Sensors and Actuators,"* Digest of Technical Papers. June 7-10, 1993, Pacifico, Yokohama, Japan.

[3] L. Ristic, *Sensor Technology and Devices*, Artech House, Inc., Boston, MA (1994), Chapter 1.

[4] L. Ristic, *Sensor Technology and Devices*, Artech House, Inc. Boston, MA (1994), p. 50.

[5] W. K. Zwicker and S. K. Kurtz, "Anisotropic Etching of Silicon Using Electrochemical Displacement Reaction," *Semiconductor Silicon*, The Electrochemical Society Softbound Symposium Series, The electrochemical Society, Inc., Princeton, NJ, U.S.A. (1973), p.315.

[6] M. Asano, T. Cho and H. Muraoka, "Application of Choline in Semiconductor Technology," *Electrochemical Society Extended Abstracts*, (1976), p. 911.

[7] J. B. Price, "Anisotropic Etching of Silicon with KOH-H_2O-Isopropyl Alcohol," *Semiconductor Silicon*, The Electrochemical Society Softbound Symposium Series, The electrochemical Society, Inc., Princeton, NJ, U.S.A. (1973), p. 339.

[8] L. D. Clark, Jr. and D. J. Edell, "KOH:H_2O Etching of (110) Si, (111) Si, SiO_2 and Ta: an Experimental study," *Micro-Robots and Teleoperator Workshop,* Proceedings of IEEE, Hyannis, MA, (1987).

[9] J. W. Faust, *The Surface Chemistry of Metals and Semiconductors*, ed. H. C. Gatos, Wiley, New York (1959), p. 151.

[10] I. J. Pugacz-Muraszkiewicz, "Detection of Discontinuities in Passivating Layers on Silicon by NaOH Anisotropic Etch," *IBM J. Res. & Dev.*, 16 (1972), p. 523.

[11] D. B. Lee, "Anisotropic Etching of Silicon," *J. Appl. Phys.*, 40 (1969), p. 4569.

[12] M. J. Declerq, L. Gerzberg, J. D. Meindl, "Optimization of Hydrazine-Water Solution for Anisotropic Etching of Silicon in Integrated Circuit Technology," *J. Electrochem. Soc.*, 122 (1975), p. 545.

[13] M. Mehregany and S. Senturia, "Anisotropic Etching of Silicon in Hydrazine," *Sensors and Actuators*, 13 (1988), p. 375.

[14] R. M. Finne and D. L. Klein, "A Water-Amine-Complexing Agent System for Etching Silicon," *J. Electrochem. Soc.*, 114 (1967), p. 965.

[15] U. Schnakenberg, W. Benecke and B. Lochel, "NH_4OH-Based Etchants for Silicon Micromachining," *Sensors and Actuators,* A21-23, (1990), p. 1031.

[16] U. Schnakenberg, W. Benecke, B. Lochel, S. Ullerich and P. Lange, "NH_4OH-Based Etchant for Silicon Micromachining: Influence of Additives and Stability of Passivation Layers," *Sensors and Actuators*, A25-27 (1991), p. 1.

[17] TMAH Material Safety Data Sheet (MSDS). Moses Lake Industries, Inc., 8249 Randolph Rd. NE, Moses Lake, WA 98837.

[18] E. Bassous and E. F. Baran, "The Fabrication of High Precision Nozzles by the Anisotropic Etching of (100) Silicon," *J. Electrochem. Soc.*, 125 (1978), p. 1321.

[19] S. C. Terrry, J. H. Jerman and J. B. Angell, "A Gas Chromatographic Air Analyzer Fabricated on a Silicon Wafer," *IEEE Transactions on Electron Devices,* ED-26, (1979), p. 1880.

[20] L. M. Roylance and J. B. Angell, "A Batch Fabricated Silicon Accelerometer," *IEEE Transactions on Electron Devices,* ED-26 (1979), p. 1911.

[21] G. Kaminsky, "Micromachining of Silicon Mechanical Structures," *Journal of*

Vacuum Science and Technology, B 3 (1985), p. 1015.

[22] T. A. Kwa, P. J. French, and R. F. Wolffenbuttel, "Anisotropically Etched Silicon Mirrors for Optical Sensor Application," *J. Electrochem. Soc.*, 142 (1995), p. 1226.

[23] K. E. Bean and W. R. Runyan, "Dielectric Isolation: Comprehensive, Current and Future," *J. Electrochem. Soc.*, 124 (1977), p. 5C.

[24] M. J. Declerq, "A New C-MOS Technology Using Anisotropic Etching of Silicon," *IEEE Journal of Solid State Circuits*, SC-10 (1975), p. 191.

[25] E. S. Ammar and T. J. Rodgers, "UMOS Transistors on (110) Silicon," *IEEE Transactions on Electron Devices*, ED-27 (1980), p. 907.

[26] D. A. Neamen, *Semiconductor Physics and Devices, Basic Principles*, Irwin, Boston, MA (1992), p. 552.

[27] R. K. Smeltzer, D. L. Kendall and G. L. Varnell, "Vertical Multijunction Solar Cell Fabrication," *10th IEEE Photovoltaic Spec. Conf.*, Palo Alto, CA. 1973, p. 194.

[28] Kenneth E. Bean, "Anisotropic Etching of Silicon," *IEEE Transactions on Electron Devices*, ED-25 (1978), p. 1185.

[29] M. M. Abu-Zeid, "Corner Undercutting in Anisotropically Etched Isolation Contours," *J. Electrochem. Soc.*, 131 (1984), p. 2138.

[30] L. Offereins, K. Kuhl and H. Sandmaier, "Methods for the Fabrication of Convex Corner in Anisotropic Etching of (100) Silicon in Aqueous KOH," *Sensors and Actuators*, 21 (1990), p. 1036.

[31] Don L. Kendall, "Vertical Etching of Silicon at Very High Aspect Ratios," *Ann. Rev. of Mater. Sci.*, 9 (1979), p. 373.

[32] J. C. Greenwood, "Ethylene Diamine-Catechol-Water Mixture Shows Preferential Etching of p-n Junctions," *J. Electrochem. Soc.*, 116 (1969), p. 1325.

[33] A. Bogh, "Ethylene Diamine-Pyrocatechol-Water Shows Etching Anomaly in Boron Doped Silicon," *J. Electrochem. Soc.*, 118 (1971), p. 401.

[34] N. F. Raley, Y. Sugiyama and T. Van Duzer, "(100) Silicon Etch Rate Dependence on Boron Concentration in Ethylene Diamine-Pyrocatechol-Water Solutions," *J. Electrochem. Soc.*, 131 (1984), p. 161.

[35] E. D. Palik, J. W. Faust, Jr., H. F. Gray, R. F. Greene, "Study of Etch Stop in Silicon," *J. Electrochem. Soc.*, 129 (1982), p. 2051.

[36] E.D. Palik, V. M. Bermudez and O. J. Glembocki, "Ellipsometric Study of the Etch-Stop Mechanism in Heavily Doped Silicon," *J. Electrochem. Soc.*, 132 (1985), p. 135.

[37] H. Seidel, L. Csepregi, A. Heuberger and H. Baumgartel, "Anisotropic Etching of Crystalline Silicon in Alkaline Solutions, II. Influence of Dopants," *J. Electrochem. Soc.*, 137 (1990), p. 3626.

[38] O.J. Glembocki and R. E. Stahlbush, "Bias-Dependent Etching of Silicon in Aqueous KOH," *J. Electrochem. Soc.*, 132 (1985), p.145.

[39] T. J. Rodgers and J. D. Meindl, *IEEE Transactions on Electron. Devices.*, ED-20 (1973), p. 226.

[40] H. A. Waggener, R. C. Kragness and A. L. Tyler, Technical Abstract, *Electronics*, 4 (November 1967), p. 274.

[41] A. I. Stoller, "The Etching of Deep Vertical-Walled Patterns In Silicon," *RCA Review*, 31 (1970), p. 271.

[42] D. L. Kendall, Abstract 25, *IEEE Transactions on Electron Devices*, ED-20 (1973), p. 1177.

[43] D. L. Kendall, "On Etching Very Narrow Grooves in Silicon," *Applied Physics Letters*, 26, 15 February (1975), p. 195.

[44] D. L. Kendall and G. R. de Guel, "Orientations of the Third Kind: The Coming of Age of (110) Silicon," C. D. Fung, P. W. Cheung, W. H. Ko and D. G. Fleming, *Micromachining and Micropackaging of Transducers*, Elsevier, Amsterdam, (1985), p. 107.

[45] H. Seidel, L. Csepregi, A. Heuberger and H. Baumgartel, "Anisotropic Etching of Crystalline Silicon in Alkaline Solutions, I. Orientation Dependence and Behavior of Passivation Layers," *J. Electrochem. Soc.*, 137 (1990), p. 3616.

[46] S.Tan, H. Han, R. Boudreau and M. L. Reed, "Process Induced Hillocks Defects on Anisotropic Etched Silicon," *Proceedings IEEE Micro Electro Mechanical Systems Workshop,*" Oiso Japan, 25-28 Jan. (1994), p. 229.

[47] Y. K. Bhatnagar and A. Nathan, "On Pyramidal Protrusions in Anisotropic Etching of <100> Silicon," *Sensors and Actuators*, A36 (1993), p. 233.

[48] K. P. Wu and W. H. Ko, "Compensating Corner Undercutting in Anisotropic Etching of (100) Silicon," *Sensors and Actuators,* 18 (1989), p. 207.

[49] A. Reisman, M. Berkenblit, S. A. Chan, F. B. Kaufman and D. C. Green, "The Controlled Etching of Silicon in Catalyzed Ethylenediamine-Pyrocatechol-Water Solutions," *J. Electrochem. Soc.*, 126 (1979), p. 1406.

[50] M. M. Abu-Zeid, D. L. Kendall, G. R. de Guel and R. Galeazzi, *Electrochemical Society Extended Abstracts,* 85-1, Toronto, Canada, May 12-17 (1985), p. 400.

[51] N. F. Raley, Y. Sugiyama and T. Van Duzer, "(100) Silicon Etch Rate Dependence on Boron Concentration in Ethylene Diamine-Pyrocatechol-Water Solutions," *J. Electrochem. Soc.*, 131 (1984), p. 161.

[52] J. G. Hooley, "The Kinetics of the Reaction of Silica with Group I Hydroxide," *Canadian Journal of Chemistry,* 39 (1961), p. 1221.

[53] L. D. Clark, Jr. and Jennifer L. Lund, and D. J. Edell, "Cesium Hydroxide (CsOH):

A Useful Etchant for Micromachining Silicon," *Digest of Technical Papers, IEEE Solid State Sensors and Actuators Workshop,* Hilton Head Island, SC, 1988, p. 5.

[54] Osamu Tabata, R. Asahi and S. Sugiyama, "Anisotropic Etching of Silicon with Quaternary Ammonium Hydroxide Solutions," *Technical Digest of the 9th Sensor Symposium,* (1990), p. 15.

[55] U. Schnakenberg, W. Benecke and P. Lange, "TMAHW Etchant for Silicon Micromachining," *6th Int. Conf. Solid-State Sensors and Actuators, Tech. Digest, (transducers 91)* San Francisco, CA, USA, June 24-28 (1991), p. 815.

[56] O. Tabata, R. Asahi, H. Funabashi, K. Shimaoka and S. Sugiyama, "Anisotropic Etching of Silicon in TMAH Solutions," *Sensors and Actuators,* A34 (1992), p. 51.

[57] E. Steinsland, M. Nese, A. Hanneborg, R. W. Bernstein, H. Sandmo and G. Kittilsland, "Boron Etch-Stop in TMAH Solutions," *The 8th International Conference on Solid-State Sensors and Actuators, and Eurosensors IX,* Stockholm, Sweden, June 25-29 (1995), p. 190.

[58] A. Merlos, M. Acero, M. H. Bao, J. Bausells and J. Esteve, "TMAH/IPA Anisotropic Etching Characteristics," *Sensors and Actuators,* A37-38 (1993), p. 737.

[59] H. Robbins and B. Schwartz, "Chemical Etching of Silicon I. The System HF, HNO_3 and H_2O," *J. Electrochem. Soc.,* 106 (1959), p. 505.

[60] H. Robbins and B. Schwartz, "Chemical Etching of Silicon II. The System HF, HNO_3 and $HC_2H_3O_2$," *J. Electrochem. Soc.,* 107 (1960), p.108.

[61] A. I. Stoller, R. F. Speers and S. Opresko," A New Technique for Etch Thinning of Silicon," *RCA Review,* 31 (1970), p. 265.

[62] S. M. Sze, *VLSI Technology,* McGraw-Hill, Newyork (1988), p. 35.

[63] H. E. Avery, *Basic Reaction Kinetics and Mechanisms,* Macmillan, London

(1974).

[64] Alliedsignal, Inc., 3500 Garrett Drive, Santa Clara, CA 95054-2827.

[65] S. Tan, M. Reed, H. Han and R. Boudreau, "Morphology of Etch Hillock Defects Created During Anisotropic Etching of Silicon," *J. Micromechanics and Microengineering*, 4 (1994), p. 147.

[66] I. Stiharu, R. B. Bhat, M. Kahrizi and L. M. Landsberger, *proceedings # 2045 of SPIE 93*, Quebec City, August, 254 (1993).

[67] G. A. Olsen, "*Elements of Mechanics of Materials,*" fourth edition, Prentice-Hall, (1982), Chapter 7.

[68] W. Kern and D. A. Puotinen, "Cleaning Solution Based on Hydrogen Peroxide for Use in Silicon Semiconductor Technology," *RCA Review*, 31 (June 1970), p. 187.

[69] W. Kern, "The Evolution of Silicon Wafer Cleaning Technology," *J. Electrochem. Soc.*, 137 (1990), p. 1887.